Natural Gas and Methane Hydrates

Report Number PH3/27
July 2000

Title: **Natural Gas and Methane Hydrates**
Reference number: **PH3/27**
Date issued: **July 2000**

Other remarks:

Background to the Study

The IEA Greenhouse Gas R&D programme (IEA GHG) is systematically evaluating the cost and potential of measures for reducing emissions of greenhouse gases arising from anthropogenic activities, especially the use of carbon dioxide capture and storage. Captured CO_2 can be stored in geological reservoirs instead of being emitted to the atmosphere. Geological reservoirs that can be considered include: deep saline aquifers and depleted oil and gas fields. CO_2 can also be injected into oil fields to enhance oil recovery (CO_2-EOR) and into coal seams to enhance the release of methane (CO_2-ECBM). In these the costs of storage are offset by product sales, making these storage options more attractive commercially.

Another option that can be considered is the formation of CO_2 hydrates. Analogous compounds, methane hydrates, are known to have existed for thousands of years in many parts of the world. Initial scientific evidence suggests that, under the appropriate conditions of temperature and pressure, CO_2 hydrates form stable molecules, similar to methane hydrates. If CO_2 can be stored in a similar manner, considerable quantities of CO_2 could be sequestered. There are two options for CO_2 storage as hydrates. The first is the direct formation of CO_2 hydrates, perhaps on the ocean floor, whilst the second, and possibly more attractive, option is to combine CO_2 storage with release of methane from hydrate deposits. If this approach could be achieved in practice, the storage option could be more attractive, in the same way as CO_2-EOR or CO_2-ECBM are more attractive than simple storage.

Compared to the other storage options, knowledge on hydrate chemistry and the potential for storage of CO_2 as hydrates is at an early stage of development. Hydrates are attracting considerable interest internationally and studies on the fundamental science of hydrates are now underway in many research laboratories throughout the world. To assist the international community in assessing this potential CO_2 storage option, IEA GHG commissioned a small study to review the current state of knowledge about hydrates and determine where further information about CO_2 storage as hydrates is needed (for example, information which could be obtained by appropriate research). This study entitled "Issues underlying the feasibility of storing CO_2 as hydrate deposits" has been reported (Ph3/25) previously.

A second, more extensive study to investigate the practicalities and potential for combining methane extraction from natural gas hydrates with CO_2 storage has now been completed. This second study also focused on natural gas hydrate deposits in permafrost regions rather than sub sea hydrate deposits. Prof. Dendy Sloan of the Colorado School of Mines, USA, undertook this study.

Results and Discussion

The following areas are described in the report

- A comparison of natural gas and methane hydrate reserves and resources
- The composition of CO_2 in natural gas reserves
- The potential for exploitation of the methane hydrate resource
- The potential for CO_2 injection combined with methane extraction from natural gas hydrates
- Costs of CO_2 storage in methane hydrates

- Steps to be taken before CO_2 enhanced methane hydrate extraction can be considered further.

Comparison of natural gas and methane hydrate reserves and resources

One of the initial objectives of the study was to compare natural gas and hydrates reserves[1] and resources[2] Natural gas current reserves are some 147 Trillion Cubic Metres (TCM) whilst the potential future natural gas resource could be as high as 137 TCM approximately twice the proven reserves. Estimates of the ultimate[3] natural gas reserves vary between 300 and 450 TCM[4]. The estimated methane hydrate resource is about 21,000 TCM[5]. Putting this in perspective the estimated natural gas hydrate resource is about 75 times greater than current natural gas reserves and resources and some 50 times greater than ultimate natural gas resource estimates. It must, however, be noted that the estimates of methane hydrate resource are highly uncertain.

Methane hydrates are widely dispersed throughout the world. Over 90% of the methane hydrates exist as finely dispersed particles on the ocean floor. The concentration of methane hydrates in the ocean sediments is typically as low as 3%. The remainder (<10%) occur in permafrost regions as hydrate capped gas reservoirs. These permafrost deposits are much more concentrated than the ocean hydrate resource. The consultant concluded that exploitation of the sea floor hydrate resource is not practical with current technology and the best option is exploitation of the permafrost hydrate resource. These findings were consistent with the conclusions in report Ph3/25.

The composition of CO_2 in natural gas reserves

The composition of natural gas hydrates can be considered to be essentially methane. However, natural gas fields can have significant concentrations of CO_2 present along with the natural gas. The average concentration of CO_2 in natural gas reserves in different parts of the world is given in Table 1 below; it should be noted there can be considerable range about the mean.

[1] Reserves are considered to be technically and economically recoverable with current technology and current gas prices.
[2] Resources are less certain, but can be considered potentially recoverable with foreseeable technological and economic developments.
[3] The ultimate resource is an estimated figure and reflects expert judgement on hydrocarbon reservoirs yet to be found and allowances for future changes in economic and operating conditions.
[4] Survey of Energy Resources 1998, World Energy Council.
[5] Natural gas hydrate resource figure given is on a gas equivalent basis

Region	Average CO_2 content (%)
North America	2.65
Latin Am. & Caribbean	2.43
Western Europe	2.20
Central & East. Europe	10.7
Former Soviet Union	9.39
Mid. East & N. Africa	5.48
Sub-Saharan Africa	5.93
Central Asia & China	17.5
Pacific OECD	9.20
Other Pacific Asia	12.68
South Asia	21.2

Table 1. CO_2 concentration of known natural gas reserves.

The data on CO_2 concentration in conventional natural gas were considered to be approximate. The consultant identified that more accurate data will be available from a four-year US Geological Survey in mid-2000. It is worth noting that there are a few very large Malaysian reservoirs with very high CO_2 content, such as Natuna[6], which contains 71% CO_2. The Natuna field has gas reserves of 6.3 Tm^3, equivalent to 4.47 Tm^3 of CO_2 and 1.83 Tm^3 of CH_4. Burning the natural gas will therefore generate some 1.83 Tm^3 of CO_2. Production of natural gas from the Natuna field will generate nearly 2.5 times more CO_2 than will be produced from the utilisation of the natural gas. Bringing such gas fields into production will significantly increase CO_2 emissions from this sector unless the CO_2 is captured and stored.

Exploitation of methane hydrate resource

In order to determine the best exploitation route for the methane hydrate resource, a case study was examined of a permafrost hydrate resource. Of the options examined depressurisation was considered to be the most practical and economical method for dissociation of the hydrate. Gas production rates from the field were estimated by modelling the depressurisation technique in a hydrate dissociation model. . These gas production rates were used in an economic assessment of methane hydrate extraction. This economic analysis concluded that the cost of gas extraction from permafrost methane hydrate reservoirs using depressurisation were comparable with the cost of extracting free gas from an as-yet-unexploited Arctic field.

However, there is currently no exploitation of this permafrost hydrate resource, because there are natural gas reserves are available which are more technically and economically viable. For permafrost exploitation to take place a gas pipeline infrastructure will need to be installed in the permafrost regions, which will require a significant capital investment. Exploitation of the permafrost methane hydrate resource is not expected to begin before 2010 at the earliest.

Potential for CO_2 injection combined with methane extraction from natural gas hydrates

The study investigated in depth the potential for methane extraction from a permafrost reservoir combined with CO_2 injection and storage. The study examined the experimental work undertaken in four Japanese laboratories and concluded that the kinetics and thermodynamics for the displacement mechanism are, at best, on the margin of being sufficient for this application.

[6] Barriers to overcome in the implementation of CO_2 capture and storage (1), storage in disused oil and gas fields. Ph3/22, February 2000.

It has been found that injecting CO_2 would not extract all the methane from the methane hydrate. At best some 29% of the methane will remain in the hydrate phase[7]. The gas produced would, therefore, contain significant quantities of CO_2, as soon as the injected gas had filled the void space. Early breakthrough of CO_2 to the gas producing wells could, therefore, be expected. This would add to the field capital and operating costs because CO_2 separation plant would be required for treating the produced gas.

Costs of CO_2 storage as methane hydrates.

An initial economic analysis of CO_2 storage combined with methane extraction was performed. The cost of storage was found to be extremely sensitive to the amount of methane that can be extracted. The theoretical maximum extraction potential was determined as 71%. However, in practise actual recovery rates were expected to be significantly lower, possibly as low as 5-10%. Storage costs were estimated for a range of extraction rates. The storage cost estimates are given in Table 2 overleaf for a range of displacement efficiencies.

Displacement Efficiency	Cost (thousands, US$)	Cost per tonne CO_2 Sequestered (US$)
10%	33 291	1,360
25%	28 169	1,115
50%	19 631	800
71%	11 094	510

Table 2 Calcuated costs of storing CO_2 combined with methane extraction from methane hydrates.

At 10% extraction the cost of storage was estimated at \$1 360/t CO_2, whilst at the theoretical maximum extraction (71%) the cost was some \$510/t CO_2. These costs are substantially higher than those determined in other studies for storage in depleted oil and gas fields[8].

Steps to be taken before CO_2 enhanced methane hydrate extracted can be further.

The consultant identified that, before CO_2 enhanced methane hydrate extraction can be considered seriously, a number of key issues must be addressed. The steps identified were;

1. The planned laboratory and pilot scale tests in Japan and the USA must clearly demonstrate the technical viability of this method. These tests are likely to be completed by 2001/2002.

2. Commercial exploitation of permafrost hydrate deposits must be proven to be technically and economically viable. Exploitation of the permafrost methane hydrate resource is not expected to begin before 2010 at the earliest.

[7] When CO_2 displaces methane in a hydrate not all the methane is displaced, rather both molecules compete for available sites in the hydrate lattice. Laboratory results from Japan indicate that CO_2 is taken into the hydrate lattice at 2.5 times the concentration of methane, leaving a minimum (equilibrium) concentration of 29% methane in the hydrate phase.

[8] In a recent study (PH3/22) the costs for storage in depleted gas fields were found to vary from \$7 to \$17/t CO_2 whilst in depleted oil fields up to 120 GT CO_2 could be stored at no net cost.

Hydrate deposits as a storage option

An alternative option could be merely to use the permafrost hydrate fields as CO_2 storage sites, without exploitation of methane. In this case, CO_2 storage costs would still be at least \$250-300/t CO_2 in this case, because of the remoteness of permafrost regions (high transportation costs) and the high costs of drilling and infrastructure establishment in these regions. Again, these costs are extremely high compared to storage in depleted oil and gas fields near to sources of CO_2. In addition, it is noted that storage of CO_2 storage in hydrate fields could only be considered as an abatement measure in reservoirs that will never be exploited for gas production. Whilst currently exploitation of this resource is not underway, methane hydrate resources are increasingly being considered as the natural gas resource of the future. Industry experts suggest exploitation may well begin by 2020.

Expert Group Comments

The comments drawn from the experts were generally complimentary of the study. Most of the reviewers agreed with the general conclusions of the report. Many of the comments received were editorial. Several experts commented that the economic model used gave an optimistic picture of the costs of extraction; also that the extraction efficiencies used in the storage cost estimates were optimistic; and that, conceivably, recovery efficiencies as low as 1-2% could be expected in practice.

Major Conclusions

Regarding methane hydrate resources the study has shown the following main conclusions:

1. The methane hydrate resource is 21 000 TCM, which is about 75 times greater than current natural gas reserves and resources and some 50 times greater than ultimate natural gas resource estimates.

2. The natural gas hydrate resource is widely dispersed throughout the world. Over 90% of the methane hydrates exist as finely dispersed particles on the ocean floor.

3. The concentration of hydrates in the ocean sediments is typically as low as 3% whilst the remainder (<10%) occur in permafrost regions as hydrate capped gas reservoirs. These permafrost deposits are much more concentrated than the ocean hydrate resource.

Exploitation of the sea floor hydrate resource is not practical with current technology and the best option is exploitation of the permafrost hydrate resource.

The extraction of methane from permafrost natural gas hydrate deposits is questionable on technical grounds and economically unrealistic at this stage.

Recommendations

It is clear from the study that the option of methane hydrate extraction combined with CO_2 storage does not warrant further consideration at this time. Once the key steps identified by the consultant have been successfully completed then the topic can be reassessed.

The distribution of CO_2 in natural gas reserves has been approximately estimated in this study, indicating something of the impact that exploitation of high CO_2 natural gas reserves could have on climate change. Once the USGS report identified by the consultant becomes available this aspect of the study should be considered again.

Methane Hydrate Recovery and Mitigation of Greenhouse Gases

A Report to the

IEA Greenhouse Gas R&D Programme

by

E. Dendy Sloan, Jr.
Center For Hydrate Research
Colorado School of Mines
Golden, Colorado 80401
U.S.A.
Email: esloan@gashydrate.mines.edu
Webpage: http://www.mines.edu.research/chs

Assisted in Production by Douglas Turner and John Kosanovich

April 1, 2000

Executive Summary

When water contacts small molecules such as carbon dioxide or methane at low temperature and high pressure, solid ice-like compounds called hydrates form. The amount of hydrated methane in deep oceans and permafrost is twice the methane equivalent of all other fossil fuels combined, with energy and environmental implications. The methane amount in ocean hydrates surpasses that in permafrost by two orders of magnitude. In addition hydrates will play a role in CO_2 ocean-sequestration.

The report objectives were to: (1) assess the amount and location of *in situ* methane hydrates, compared to conventional natural gases, (2) determine the most likely means of methane recovery, (3) evaluate the potential for hydrate fugitive emissions and geohazards, (4) estimate the hydrate impact on carbon dioxide ocean sequestration, and (5) appraise carbon dioxide displacement of methane from hydrate reserves.

In situ methane hydrates are widely distributed in the earth. Economic recovery of methane from hydrates is confounded by both the remote locations (in deep oceans or in permafrost) and the concentration in sediment (< 6% in the ocean and < 30% in permafrost) of the resource.

Due to access and concentration, permafrost hydrates associated with a free gas reservoir will likely be produced in the next decade as a pilot demonstration. Recovery is most economical when the pressure is lowered to dissociate the hydrate, with energy supplied from the earth. It is debatable whether such a demonstration took place in one Siberian field during the decade of the 1970's; however, it was reported that hydrate decomposition contributed as much as 36% to that field's total gas field production.

The estimated uncertainty in climate change due to fugitive gas emission from *in situ* hydrates is less than the climate change due to uncertainty in predicted hydrocarbon usage by man. The region of highest hydrate jeopardy is the Arctic shelves, where hydrate associated with permafrost may be degrading in the near shore environment; preliminary Russian models indicate such emissions are small. Hydrate dissociation can cause ocean geohazards, with magnitudes similar to that of climate change.

Experiments with CO_2 ocean sequestration have gone beyond modeling and laboratory studies, to pilot injections in the ocean. CO_2 liquid droplets injected at depths less than 2650 m form a thin hydrate shell which slow CO_2 dissolution until the droplet rises to shallow water, where rapid vaporization and dispersion occur. CO_2 injected at large depths (>3600m) shows more promise for long-term sequestration.

The CO_2 displacement of CH_4 from hydrates is a concept with four major technical challenges: (1) large-scale laboratory validation, (2) a hydrate depressurization production base for improvement, (3) an inexpensive CO_2 supply, and (4) a gas-gathering, separation, and distribution infrastructure. This concept (called EHBM) is an analogue to enhanced coal bed methane (ECBM); similarities and differences are shown.

Table of Contents

Introduction

Hydrate phenomena are related to global energy and climate change concerns in two ways: (1) methane hydrates can be destabilized in the permafrost or sea floor, and (2) carbon dioxide may be sequestered in hydrates for long-term storage. This report provides a state-of-the-art evaluation of both possibilities.

The amount of *in situ* hydrated methane is estimated at twice the methane equivalent of all other fossil fuels combined. However, there is a major concern for the viability of methane (CH_4) recovery. A second concern relates to the CH_4 hydrate stability and the greenhouse gas consequences. A recent conference raised significant questions regarding climate change and margin stability (Henriet and Mienert, 1998) due to CH_4 evolution from ocean hydrates.

One thing is certain about interactions of CH_4 and CO_2 with the ocean – hydrates will have a significant role at deep ocean temperatures, pressures, and high CH_4/CO_2 concentrations. Yet many technical and economical questions arise. At the end of the first national five-year project on methane hydrates, the Japanese concluding workshop had a question mark at the end of its title - "Methane Hydrates: Resources in the Near Future?" (Japan National Oil Corporation, 1998). Also the role of CO_2 ocean hydrates previously was considered mixed: on one hand, they were thought to provide additional disposal and to protect liquid CO_2 from dissolution; on the other, hydrates can interfere with rapid dissolution process necessary when injecting CO_2 at shallow depths (Adams et al., 1994).

Along with the ideas of CO_2 sequestration and CH_4 evolution, is the possibility of combining the two, by displacing CH_4 from hydrates with CO_2, thereby disposing of a greenhouse gas and recovering an energy source. This concept has been explored with only a few laboratories, mostly in Japan via preliminary experiments on a small scale.

There are five objectives of this report:

1. Compare *in situ* hydrate amounts and locations to conventional natural gases,
2. Determine the most likely means of methane recovery,
3. Evaluate the potential for fugitive emissions and geohazards from hydrates,
4. Summarize new data which show the hydrate impact on CO_2 ocean sequestration, and
5. Appraise the potential for methane displacement from hydrates by carbon dioxide.

The body of the report is devoted to each of the above objectives, with a section for each, save objectives 2 and 3, which are combined. Details of hydrate structure and properties, likely recovery sites, a case study, and a summary of ocean sequestration and climate effects are left to appendices.

I. Comparison of Hydrated Gas and Conventional Gas

The amount of methane in hydrates is uncertain and speculative, centering around $21x10^{15}$ m^3, or 21,000 trillion cubic meters (TCM), within a range from 10^{15} to less than $10^{17}m^3$. The estimates in Table 1 were based upon local measurements or parameters considered to be proxies for hydrate concentration (e.g. 18 actual sample recoveries and multiple acoustic reflections) extrapolated to estimate world reserves. The extremes, serving as an approximate error estimation, differ from $21x10^{15}$ m^3 by a factor of about 50 (Kvenvolden, 1998).

Table 1. Estimates of *In Situ* Methane Hydrates

Permafrost Hydrates m^3 (STP)	Deep Sea Hydrates m^3 (STP)	Reference
$5.7xl0^{13}$	$5\text{-}25xl0^{15}$	Trofimuk et al. (1977)
$3.lxl0^{13}$	$3.lxl0^{15}$	McIver (1981)
$3.4xl0^{16}$	$7.6xl0^{18}$	Dobrynin et al. (1981)
$1.4xl0^{13}$		Meyer (1981)
$l.0x10^{14}$	$l.0Xl0^{l6}$	Makogon (1988b)
	$2.1xl0^{16}$	Kvenvolden (1988a)
$7.4x10^{14}$	$2.1x10^{16}$	MacDonald (1990b)
	$2.6\text{-}13.9x10^{16}$	Gornitz and Fung (1994)
	10^{15}	Ginsburg and Soloviev (1995)
	$7x10^{15}$	Holbrook et al. (1996)
	$1.5x10^{15}$	Makogon (1997)

The early resource estimates by Dobrynin (1981) assumed that hydrates existed at any place in their stability field, but without regard for sufficient carbon to produce methane; consequently the estimates were too much high. Later, with the realization that significant sources of methane were required, the ocean abyssal plains were ruled out as viable hydrate sources. The most authoritative estimate was obtained from MacDonald (1990b) who considered both carbon content of sediments and the hydrate stability field. Kvenvolden's (1988a) estimate was based upon a worldwide extrapolation of a careful estimation of hydrate resource in the Alakan continental margin. The numbers of Kvenvolden and MacDonald coincide to one decimal place and serve as a mean for subsequent estimations; both investigators agree that their estimates should be accurate to an order of magnitude.

The worldwide total recoverable conventional methane reserve is estimated at 164 trillion cubic meters (Masters et al., 1994). This estimate is likely to be revised upward in the near future (Ahlbrandt, 1999), because it did not include gases associated with liquids.

Table 2 presents the worldwide distribution of the conventional gas reserves and resources compared to the methane in hydrate reserves, modified from Rogner (1997). It

may be argued that, due to recovery feasibility reasons listed later in this report, hydrates should be considered a resource, rather than a reserve and thus compared to conventional gas resources. Reserves are economically and technically recoverable at current technology and prices, while resources are less certain, but considered potentially recoverable with foreseeable technological and economic developments. While the above estimates of hydrated gas are highly uncertain, if only 1% of the 21,000 TCM of the hydrated gas estimate is recovered, that amount will exceed the conventional methane reserve. About 2.4% of the hydrated methane is equivalent to the world gas resource.

Also listed in Table 2 is the CO_2 content of conventional gases (Petroleum Consultants, Inc., 1999), while the gas in hydrates is essentially all methane. The conventional gas CO_2 concentrations in Table 2, while they are the best currently available, are still very approximate. The CO_2 gas content for each country was weighted by reservoir capacities, before country averages were obtained for the world regions. For countries with small numbers of high CO_2 concentration fields in the database, undue weight is given to the CO_2 content of that country. For example, a few very large Malaysian reservoirs with high CO_2 content, may cause high averages in the Pacific Asian region in Table 2. More accurate world CO_2 gas concentrations will be available from a four-year US Geological Survey report in mid-2000 (Ahlbrandt, 1999).

Methane and carbon dioxide fugitive emissions are detailed in Section II.F.1, which identifies the key areas in need of technology for reducing CO_2 from natural gas extraction. Table 2 compares the worldwide distribution of conventional gas reserves and resources (Masters et al., 1994) to hydrates and other unconventional gas e.g. coalbed methane (24.5% of total), fractured shales (43.3%), tight formations(20%), modified from Rogner (1997). Also listed in Table 2 is the CO_2 content of conventional gases, (Petroleum Consultants, Inc., 1999), while hydrated gas is essentially all methane.

Table 2. Conventional, Unconventional, and Hydrated Gas Reserve

Region	Convent Gas (TCM)			Methane Hydrate	Other Unconv
	% CO_2	Reserve	Resource	(TCM)	(TCM)
North America	2.65	9.29	32.82	6853	258.9
Latin Am. & Caribbean	2.43	5.98	21.1	5139	106.9
Western Europe	2.20	5.75	15.27	856	37.1
Central & East. Europe	10.7	0.55	2.05	0	7.9
Former Soviet Union	9.39	30.8	117	4711	203.7
Mid. East & N. Africa	5.48	37.9	77.2	214	126.1
Sub-Saharan Africa	5.93	3.07	13.9	429	36.0
Central Asia & China	17.5	0.87	10.07	429	149.7
Pacific OECD	9.20	1.65	2.68	1713	101.2
Other Pacific Asia	12.68	4.25	11.18	214	30.4
South Asia	21.2	1.26	4.72	429	9.0
Total		101.4	310.3	20,987	1,066.9

Gas estimates in Tables 1 and 2, respectively, call our attention to three facts:

1. the amount of deep sea hydrated gas is also two orders of magnitude greater than that in the permafrost; more than 97% of the hydrated methane is offshore,
2. the mean amount of hydrated methane is about two orders of magnitude greater than the conventional gas reserve or resource, and
3. several locations around the world (notably the Pacific Rim and Asian countries and Eastern Europe and former Soviet Union) have very high CO_2 contents in gases and should be closely monitored for fugitive green house gas emission associated with normal gas production.

Figure 1 is a map and Table 3 is a listing of evidence of 56 hydrate locations, in the world (Sloan, 1998). Gas hydrates in nature occur so commonly that recent discoveries cause such maps to rapidly become dated, and it may not serve long as an accurate detailed record of hydrate sites, but rather an overview of their pervasiveness. The map does provide visual confirmation that ocean hydrates occur much more frequently than permafrost hydrates on a global basis. Table 3 indicates that while hydrate samples have been obtained at 18 locations, most of the evidence is indirect and from seismic means, without detailed analysis of amount of methane in each deposit.

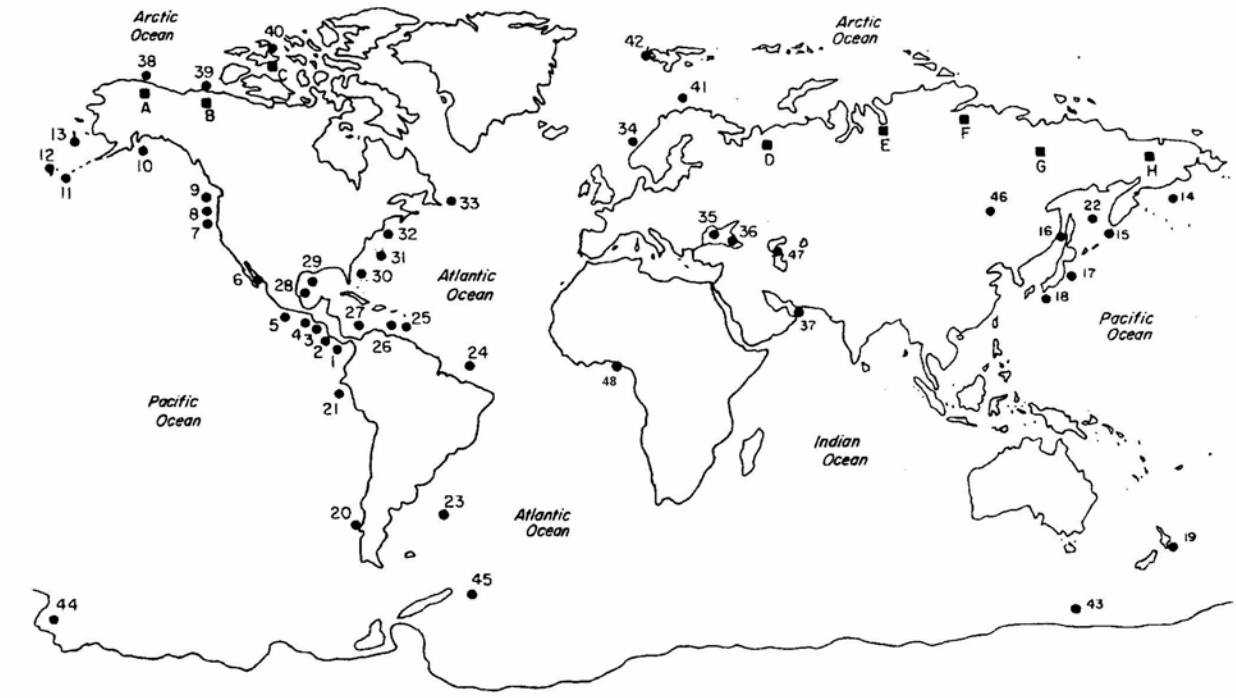

Figure 1. World Map Showing Locations of Known and Inferred Hydrate Deposits in Oceans (●) and in Permafrost (■). See text for nomenclature. (modified from Kvenvolden et al., 1993a)

Table 3. Natural Gas Hydrate Locations (modified from Kvenvolden, et al. 1993a)
(due to document size constraints, complete references are in Sloan, 1998)

Number in Figure 1	Location	Evidence	Reference
1	Pacific Ocean off Panama	BSR	Shipley et al. (1979)
		Lit Rvw	Krason & Ciesnik (1986a)
2	Middle America Trench (MAT) off Costa Rica	BSR	Shipley et al. (1979)
		Samples	Kvenvolden & McDonald (1985)
		Lit Rvw	Finley & Krason (1986a)
3	MAT off Nicaragua	BSR	Shipley et al. (1979)
		Lit Rvw	Finley & Krason (1986a)
4	MAT off Guatemala	BSR	Shipley et al. (1979)
		Samples	Harrison & Curiale (1982)
		Samples	Kvenvolden & McDonald (1985)
		Chlorinity	Hesse and Harrison (1981)
		Chlorinity	Harrison and Curiale (1982)
		Lit Rvw	Finley & Krason (1986a)
5	MAT off Mexico	BSR	Shipley et al. (1979)
		Samples	Shipley and Didyk (1982)
		Lit Rvw	Finley & Krason (1986a)
6	Mexico (Gulf of California, Guaymas Basin)	BSR	Lonsdale (1985)
7	Eel River Basin off California	BSR	Field & Kvenvolden (1985)
		Samples	Brooks et al. (1991)
		Lit Rvw	Krason & Ciesnik (1986b)
8	Oregon USA (Cascadia Basin)	BSR	Moore et al. (1992); Yuan et al. (1996)
		Samples	Westbrook et al. (1994)
9	Vancouver Island (Cascadia Basin)	BSR	Davis et al. (1990)
			Hyndman and Spence (1992)
10	E. Aleutian Trench off Alaska	BSR	Kvenvolden & von Heune (1985)
11	Mid Aleutian Trench	BSR	McCarthy et al. (1984)
		Chlorinity	Hesse and Harrison (1981)
		Lit Rvw	Krason & Ciesnik (1987)
12	Bering Sea Alaska	VAMPS	Scholl and Cooper (1978)
13	Beringian Margin off Alaska	BSR	Carlson et al. (1985)
		Lit Rvw	Krason & Ciesnik (1987)
14	Shirshov Ridge (Russia)	BSR	Saltykova et al. (1987)
15	Paramushir Island (Okhotsk Sea)	Samples	Zonenshayn et al. (1987)
16	Japan (Japan Sea)	Sample	Tamake et al. (1990)

17	Japan (Japan Trench)	Chlorinity	Moore and Gieskes (1980)
18	Nankai Trough off Japan	BSR	Aoki et al. (1983) Tamano et al. (1984), Ashi and Taira (1993), Kastner et al. (1993)
19	Hikurangi Trough off New Zealand	BSR	Katz (1981)
20	Peru-Chile Trench off Chile	BSR	Cande et al. (1987)
21	Peru-Chile Trench off Peru	BSR	Miller et al. (1991)
		Samples	Kvenvolden & Kastner (1990)
22	Sahkalin Island (Russia) (Okhotsk Sea)	Samples	Ginsburg et al. (1993)
23	Argentina (Central Argentine Basin)	BSR	Manley and Flood (1988)
24	Brazil (Amazon Fan)	BSR	Manley and Flood (1988)
25	Barbados Ridge Complex off Barbados	BSR	Ladd et al. (1982)
26	S. Caribbean Sea	BSR	Ladd et al. (1984)
27	Colombia Basin off Panama & Colombia	BSR	Shipley et al. (1979)
		Lit Rvw	Finley & Krason (1986b) Minshull et al. (1994)
28	W. Gulf of Mexico off Mexico	BSR	Shipley et al. (1979) Hedberg (1980)
		Lit Rvw	Krason et al. (1985)
29	Gulf of Mexico off S. USA	Samples	Brooks et al. (1984, 1986) Pflaum et al. (1986)
		Lit Rvw	Brooks & Bryant (1985)
30	Blake Outer Ridge off SE USA	BSR	Markl et al. (1970) Shipley et al. (1979) Dillon et al. (1980)
		Samples	Kvenvolden & Barnard (1983)
		Chlorinity	Jenden and Gieskes (1983)
		Lit Rvw	Krason & Ridley (1985a)
	Leg 164	All 3 Above	Paull et al. (1997)
31	Carolina Rise	BSR	Dillon et al. (1983)
32	Continental Rise off E. USA	BSR	Tucholke et al. (1977)
		Lit Rvw	Krason & Ridley (1985b)
33	Labrador Shelf off Newfoundland	BSR	Taylor et al. (1979)
		Lit Rvw	Krason & Rudloff (1985)
34	Norway (Cont. Slope)	BSR	Bugge et al. (1987)
		Chlorinity	Hesse and Harrison (1981)
35	Crimea, Ukraine	Samples	Yefremova and Zhizhchenko (1972)

	Black Sea (Russia)		Kremlev and Ginsburg (1989)
			Konyukhov et al. (1990)
		Lit Rvw	Ciesnik & Krason (1987)
36	Caucasus, Russia	BSR	Nomokonov and Stupak (1988)
	Black Sea		Gorchilin and Lebedev (1991)
37	Makran Margin,		
	Gulf of Oman	BSR	White (1979)
38	Beaufort Sea	BSR	Grantz and Dinter (1980)
	off Alaska		Andreassen et al. (1995)
39	Beaufort Sea		
	off Canada	Logs	Weaver & Stewart (1982)
40	Svedrup Basin		
	off Canada	Logs	Judge (1982)
41	Norway (Barents Sea)	BSR	Andreassen et al. (1990)
42	Svalbard (Fram Strait)	BSR	Eiken and Hinz (1989)
			Andreassen and Hansen (1995)
43	Wilkes Land Margin		
	off Antarctica	BSR	Kvenvolden et al. (1987)
44	W. Ross Sea	Gas	McIver (1975)
	off Antarctica)	Chlorinity	Lonsdale (1990)
45	Weddell Sea		
	off Antarctica	BSR	Lonsdale (1990)
46	Caspian Sea,	Samples	Yefremova and Gritchina (1981)
	Azerbaijan		Ginsburg et al. (1992)
47.	Lake Baikal, Russia	BSR	Hutchinson et al. (1991)
48.	Niger Delta Front	BSR	Hovland et al., (1997)

Continental Hydrates

A	North Slope, Alaska	Logs	Collett (1983)
		Sample	Collett & Kvenvolden (1987)
		Lit Rvw	Collett et al. (1988)
B	Mackenzie Delta,	Logs	Bily & Dick (1974)
	Canada Well L-38	Samples	Dallimore et al. (1996)
	Well 2L-38	Logs	Dallimore, Uchida, and
		Samples	` (1999)
C	Arctic Islands,	Logs	Davidson et al. (1978)
	Canada		Judge (1982)
D	Timan-Pechora		
	Province,USSR	Gas	Cherskiy et al. (1985)
E	Messokayha, USSR	Sample	Makogon et al. (1972)
F	E. Siberian Craton,		
	USSR	Gas	Cherskiy et al. (1985)
G	NE Siberia, USSR	Gas	Cherskiy et al. (1985)
H	Kamchatka, USSR	Gas	Cherskiy et al. (1985)

In Table 3 and Figure 1, a surprising number of occurrences are situated in oceans around the equator, where one might not anticipate ice-like compounds. This is due to the phase equilibrium property of hydrates which enable their stability at temperatures both below and above the ice point, when the pressure is elevated. The deep bottom waters are at temperatures ranging between 275 and 278 K, with 277K being a typical world-wide number at water depths greater than 500m.

Figures 2a,b are arbitrary examples of the depths of hydrate phase stability in permafrost and in oceans, respectively, as shown in the shaded regions. In each figure the dashed lines represent the thermal gradients as a function of depth. The slopes of the dashed lines change at the base of the permafrost and at the water/sediment interface, where new thermal gradients are caused by new sediment thermal conductivities, densities, and heat capacities. The solid lines were drawn from the methane hydrate phase equilibria data, with the pressure converted to depth assuming hydrostatic conditions in both the water and sediment. In each diagram the intersections of the solid and dashed lines bound the depths of the hydrate stability fields.

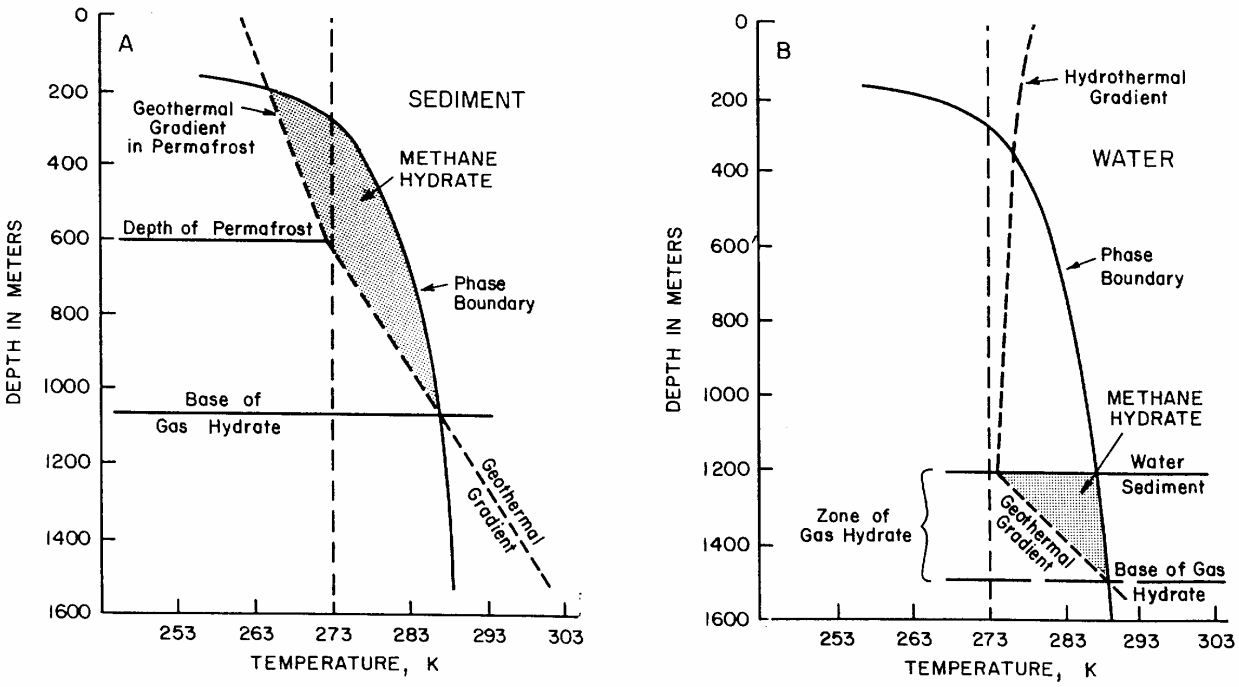

Figure 2. Envelope of Methane Hydrate Stability (a) in Permafrost, and (b) in Ocean Sediment (from Kvenvolden, 1988)

In Figure 2b one would not expect hydrates to be stable in the region above the sediment due to an absence of means to concentrate gas in water and a means of retaining the hydrates, because their density (0.9g/cc) is less than that of water. Kvenvolden

(1988a) notes that sub-sediment hydrates depths are 130-2,000m in the permafrost, and 100-1,100m below the seafloor, at typical ocean depths greater than 500m (Anderson et al., 1992). In atypical cases, anecdotal hydrates outcroppings have been found from thermogenic gases in the Gulf of Mexico and the Caspian Sea (Ginsburg and Solviev, 1994), where migration of thermogenic gases typically occurs along salt diapirs or faults. In no case however, have hydrates been found at depths below the surface greater than about 2000 m, due to the high temperatures resulting from the geothermal gradient.

With a very few exceptions, such as the Gulf of Mexico and Caspian sea, all the hydrated gas is almost pure methane of biogenic origin, as determined by $\delta^{13}C$ analysis and very high (>1000) ratios of CH_4 to (C_2H_6 +C_3H_8). Most of the gases present are composed of > 99% methane, with very small amounts of ethane and propane. In Figure 2 the methane hydrate phase stability line is appropriate, with corrections for salinity and porous media.

The substantial *in situ* hydrate reservoirs provide three major motivations for evaluation of methane extraction: (1) an energy resource, (2) potential for climate change by evolving methane, and (3) geohazards for stability and safety imposed by hydrate decomposition.

II. Methane Extraction, Fugitive Emissions and Geohazards from *in situ* Hydrates

While the amounts of methane hydrate reserves are very large, they are also highly dispersed in sediments. The best characterized hydrate reservoirs have bulk volume fractions in ocean sediment and in permafrost of 0.03 (Blake Bahama Ridge) and 0.30 (Mallik 2L-38), respectively. A smaller difficulty is that hydrate reservoirs are in hostile environments which are hard to access. Such environments are becoming more commonplace in the exploration and production industry, as the easily recoverable hydrocarbon reservoirs become depleted.

The second section of this report is organized to evaluate the methane extraction, fugitive emissions, and geohazards from hydrates. In Section II.A, the need for both resource estimation and characterization is stated, before the specification of two case study sites at the Blake Bahama Ridge and at Mallik 2L-38 in Section II.B. Section II.C provides an extraction technique overview, with a detailed examination of the three most promising techniques in Section II.D, including a model of depressurization in the permafrost. Comparative economics of the two most likely recovery techniques are presented in Section II.E. The final section (II.F) evaluates the possibility for fugitive emissions of methane and geohazards from hydrates.

II.A. Resource Estimation and Characterization.

The first step in all hydrate multi-year plans for the future (e.g. USDOE 1998, 1999a), must be resource characterization, before anything can be said about applications in production, global climate change, or geohazards. Hydrate contributions to world energy will depend upon the availability and production of methane from the hydrate phase. Yet the overall size and production at any one site are still very much in question.

Which sites have highly concentrated hydrates? Ocean hydrates are the subject of the largest debate since they contain more than 97% of the gas. Hovland (1998) indicates that the two best-known deepsea hydrate deposits (from ODP Leg 146 in the Cascadia Margin, and Leg 164 in the Blake Bahama Ridge) may be characteristic of all ocean hydrates, but their bulk hydrate volume contents are below 6%, much less than that needed for commercial extraction of a metal ore (e.g. copper) on land. This is partly due to the expected deepsea host sediment conditions (Clennell et al., 1999). A consensus has grown to support Hovland's suggestion that mud volcanoes are likely sites to search for ocean hydrates.

At a recent workshop, seven senior U.S. hydrate researchers reached consensus about the future of hydrates in the natural environment (Sloan, et al., 1999). To date few dedicated surveys have been conducted to identify hydrate deposits, and better methods to identify and survey gas hydrates need to be developed, particularly to define the zones of high concentrations. Our understanding of processes that control hydrate accumulation is primitive.

To formulate a productive hydrate program, it is essential to:
(a) identify the best sites appropriate to hydrates as either a potential resource, an agent in global climate change, or a factor in seafloor hazards,
(b) assess any targeted sites in terms of cross-cutting scientific needs, and
(c) evaluate experiments to be performed at these sites, along with laboratory experiments which are supportive of field observations.

As projects progress toward commercialization, they usually undergo several stages - from conceptualization and preliminary calculation, to bench-scale experimentation, to pilot/field experimentation, and finally to commercialization. At the current time, the technology is moving beyond conceptual and laboratory studies, to pilot plant and field work to define the needs before commercialization is contemplated.

II.B. Selection of Case Studies for Ocean and for Permafrost Hydrates.

Thus far, this report might have convinced the reader that (1) there is a very large amount of gas in the hydrated resource, and (2) we do not know very much about the details of many *in situ* locations. With such a complicated ocean or permafrost system involving all the geosciences and engineering fields, it is not feasible to perform a comprehensive, meaningful global study because there are too many unknowns.

Instead, the focus will be on two field cases for which the hydrate reserve is best characterized, namely a permafrost hydrate reserve and an ocean hydrate reserve. Results will give the best case for gas recovery from each type of hydrate reservoir. While the permafrost reserve has advantages of being more accessible and more concentrated, the ocean total hydrated reserve is greater by at least two orders of magnitude.

The “best case” study sites were determined by reservoir characterization reliability and thoroughness, by reservoir size and hydrate concentration, and by information accessibility and documentation. The best reservoirs for permafrost and for seafloor hydrates, respectively, are the Mallik 2L-38 well in the Mackenzie Delta, completed in 1998, and the three subsea hydrate wells completed in late 1995 along the Blake-Bahama Ridge off Charleston, S.C.

In choosing the case studies, it was noted that results from the 1999 Japanese offshore hydrate well in the Nankai Trough were not available at the completion of this report. An alternative case study candidate was the Siberian Messoyakha field, which was produced during the decade of the 1970’s (see Appendix B.3). However, the Messoyakha field had two detractions: (1) there is some question whether the gas produced was from hydrates or from normal gas production (Collett and Ginsburg, 1998) and (2) there is a paucity of reliable data, by Western hemisphere standards, upon which to base the evaluation.

II.B.1. Permafrost Hydrate Recovery Site. The Mallik 2L-38 well in the Mackenzie Delta of Canada was drilled specifically for hydrates and thoroughly characterized by the Japan National Oil Corporation (JNOC) and the Canadian Geological Survey (GSC), with completion on March 30, 1998 at a cost of $6,600,000. This well represents one of the richest hydrate deposits known in the world, with as much as 30% bulk volume hydrates in strata. It represents the best candidate for a permafrost recovery case study.

The location of the Mallik 2L-38 well is on Richards Island in the Mackenzie Delta, just east of the Canadian-Alaskan Border, as shown in Figures 3a,b. The Mallik 2L-38 reservoir is summarized in Appendix B. A detailed description (well logs, sample cores analyses, etc.) is given in the monograph Scientific Results from JAPEX/JNOC/ GSC Mallik 2L-38 gas Hydrate Research Well, MacKenzie Delta, Northwest Territories, Canada, Dallimore, S.R., Uchida, T., and T.S. Collett, Eds., Geological Survey of Canada Bulletin 544, (1999)

The Mallik 2L-38 hydrate reserve differs slightly from that diagrammed in Figure 2a. In that figure the shaded hydrate stability region extends both above and below the permafost. However, in the Mallik well, the permafrost extended to 640m, while hydrate occurrences were observed at 10 intervals between 896 and 1106m depth (Uchida et al., 1999). Thus no ice-bearing sediments were involved in the hydrated sediments. A second distinguishing feature of Mallik 2L-38 is that the free gas layer is only 1.5 m underlying the 10 hydrate zones which are distributed over 200 m. However, the thin free-gas layer may broaden away from the well.

The hydrates sampled in the Mallik well represent an estimated reserve total of 0.19 TCM of gas. As a reference, the US annual consumption is 0.71 TCM of gas. Principally due to such high concentrations and ease of access, it is likely that methane production will first be demonstrated from permafrost hydrate reservoirs in the Mallik region. An alternative permafrost site is in the Prudhoe Bay region, although that region has not been proven for hydrate recovery, as in the Makenzie Delta.

II.B.2. Seafloor Hydrate Recovery Site. The Blake-Bahama Ridge represents a seafloor hydrate resource with 38-80 TCM of gas in hydrates dispersed (3% of bulk volume) over a large area (24,000 km^2). If completely recovered, this one resource has the potential of providing the current USA energy requirement for over 100 years. On Leg 164 three hydrate wells (Sites 994, 995, and 997) were completed in December 1995 with thorough geoscience and core analyses. This is the best characterized seafloor hydrate resource.

Maps of the three ODP well sites are provided in Figures 4a,b, with a summary of the reservoir in Appendix B. The geological, geochemical, and geophysical details of this reservoir are recorded in a monograph, Proceedings from Ocean Drilling Program (ODP) Volume 164 (Paull, Matsumoto, Wallace, et al., 1996)

3a

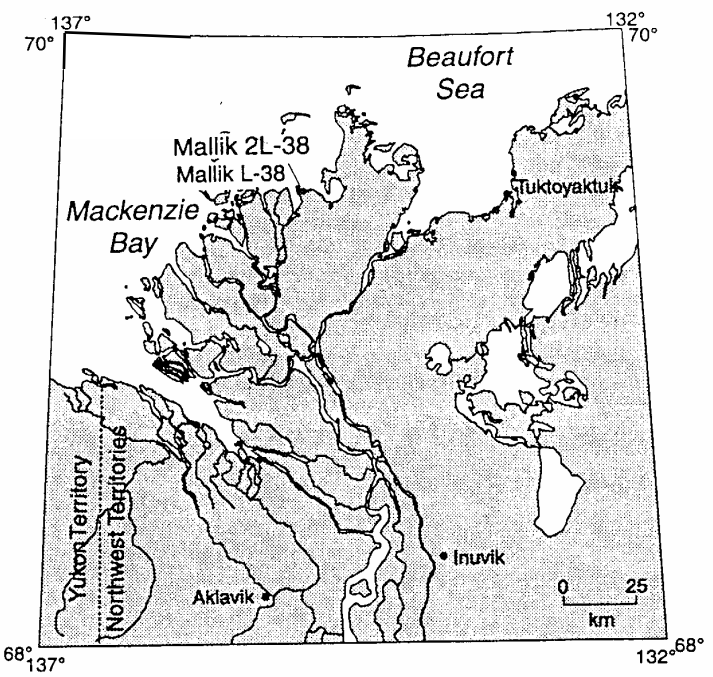

3b

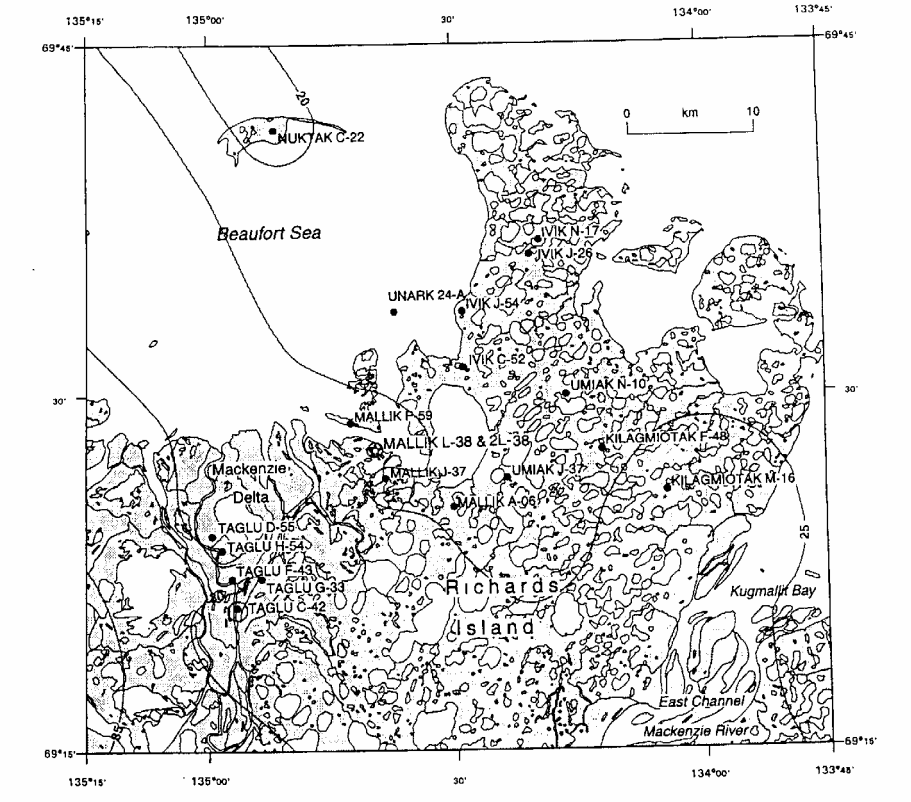

Figure 3. Location of Mallik L-38 and 2L-38 (from Dallimore et al., 1999)

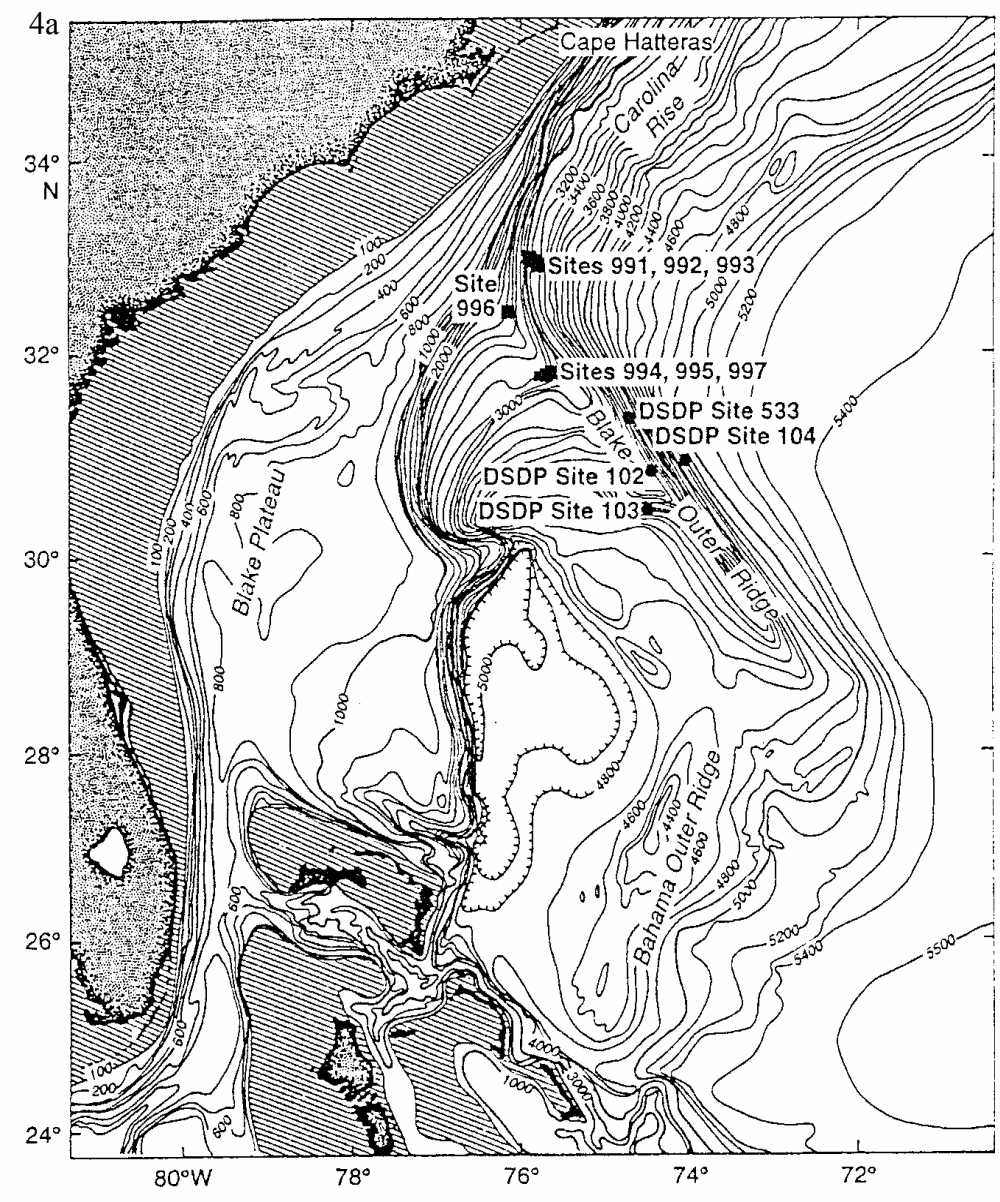

Figure 4a. Location of Sites 994, 995, and 997 on ODP Leg 164 (from Paull et al., 1996)

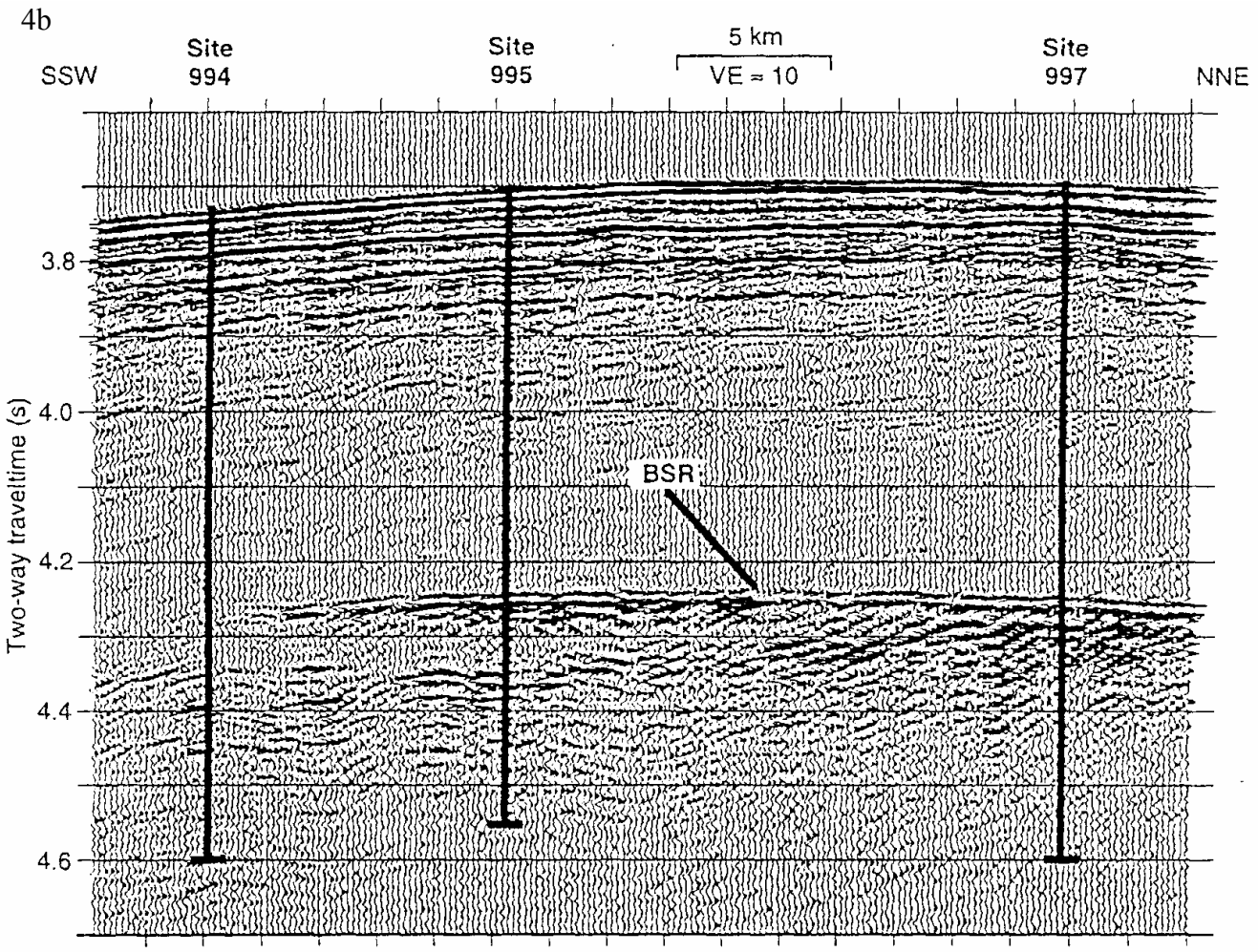

Figure 4b. Positions of Sites 994, 995, and 997 Relative to Bottom Simulating Reflector (from Paull et al., 1996)

The disperse nature of the seafloor resource poses an engineering challenge for recovery. A 3 bulk volume % hydrate concentration, as was found in the Blake-Bahama Ridge, is typical of seafloor hydrates, except in anecdotal instances of hydrates filling a fault, such as the massive (3m) hydrate sample found on ODP Leg 84 in the Mid-American Trench. A dispersed resource means that substantial energy must be applied to the sediments surrounding the hydrates, thereby reducing the process thermal efficiency. Nevertheless, the seafloor resource deserves careful consideration because it represents the largest methane resource. The total permafrost hydrate resource is well within the error margin of seafloor hydrate estimation.

The remaining portion of this section evaluates recovery techniques for the above two cases, since the most information is known about them. By showing the recovery

feasibility for the best known individual reserves, we hope to provide a first estimate, and to enable a later extrapolation on a broader scale to worldwide resources.

II.C. A Preliminary Look at Recovery Techniques.

Every hydrate recovery scheme requires energy input to the hydrates – even those like depressurization or inhibitor injection (discussed below) for which energy is not explicitly considered. Because the un-combusted hydrate products contain more energy than the solid phase, energy must flow from the environment to dissociate the hydrate.

The first question in any energy recovery scheme concerns the energy balance, "Is more energy obtained than input to the process?" For pure methane hydrate without sediment at the ice point dissociation temperature the answer is clearly favorable: 54.2 kJ/mol methane is required to dissociate the hydrate, while the recovered methane can be combusted to provide 834 kJ/mol methane. Only 6.5% of the recovered energy is needed for dissociation, yielding a maximum energy efficiency ratio (E_{out}/E_{in}) of 15.

However, for hydrates in sediment, the energy efficiency is always lower than for pure hydrates. Consider the cases illustrated in Figure 2a,b, iterated below. The hydrate in sediment exists along the geothermal gradient at the left boundary of the shaded regions. In order to decompose the hydrates: (1) sensible heat must be input to the hydrate and associated sediment until the temperature reaches the right phase boundary of the shaded region in Figures 2a,b, and (2) the heat of hydrate dissociation must be input at the phase boundary, where dissociation occurs.

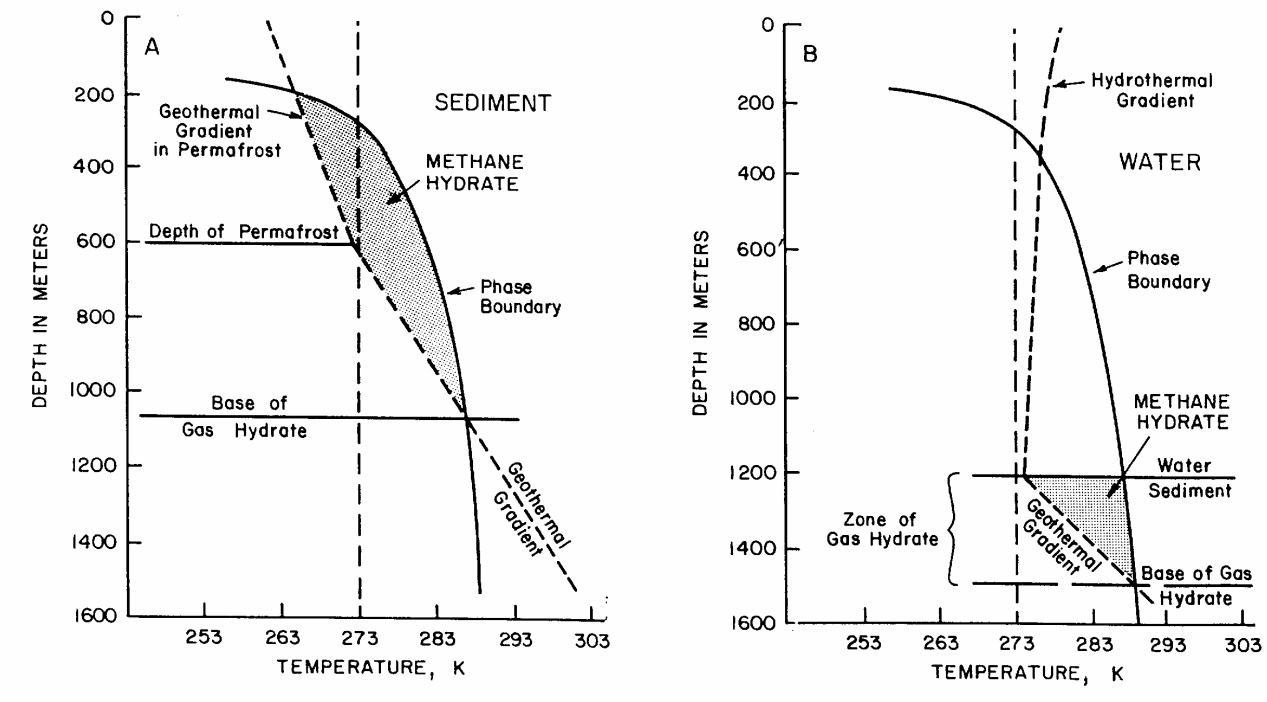

Figure 2a,b. Envelope of Methane Hydrate Stability in (a) Permafrost and (b) Ocean

When the hydrate is mixed with sediment, as it is in both the Mallik 2L-38 well and the Blake Bahama Ridge, significant energy is spent to increase the sediment temperature from the geothermal gradient line to the phase boundary. A substantial portion of the input energy is absorbed by the surrounding sediments and other phases. Hydrates in Mallik 2L-38 were below the permafrost layer, so that ice dissociation need not be considered.

In words, a simple energy balance assumes only hydrate and sediment are present:

Energy Input to Dissociate Hydrates	=	Energy to Heat Sediment to Phase Boundary	+	Energy to Heat Hydrate to the Phase Boundary	+	Dissociation Energy for Hydrate Decomposition	(1)

Figure 5a,b show energy balances for the Blake-Bahama Ridge and for Mallik 2L-38. The net recovery of energy is plotted against the percentage hydrate recovery with parameters on each line for the fraction of hydrate in the reservoir. The two figures show that in order to make the process energy efficient, only a small percentage of the total hydrate requires recovery, and that the amount of hydrate is the most important variable in the energy balance. This emphasizes the necessity to accurately estimate the amount of hydrate in each reservoir. The negative values in each figure shows that in many cases a minimum of 10% recovery must be performed in order to be economical.

Such energy balance calculations confirm that there is significant potential for energy recovery from hydrate reserves. That is, more energy is frequently obtained than is input. As a result, the hydrate recovery process poses challenges to engineering creativity and execution.

5a

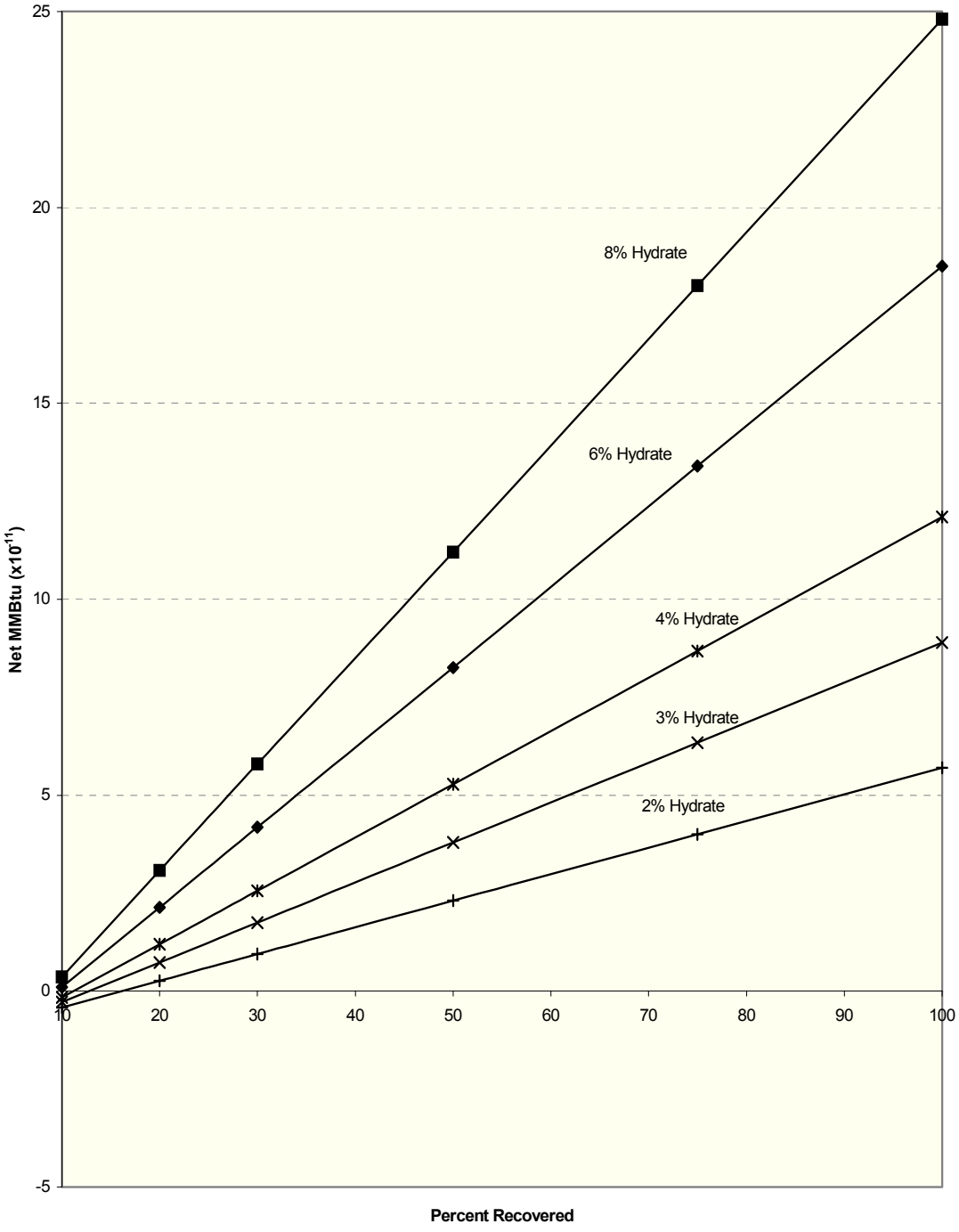

Figure 5. Approximate Energy Balances for (a) Blake Bahama Ridge, (b) Mallik 2L-38 Well

5b

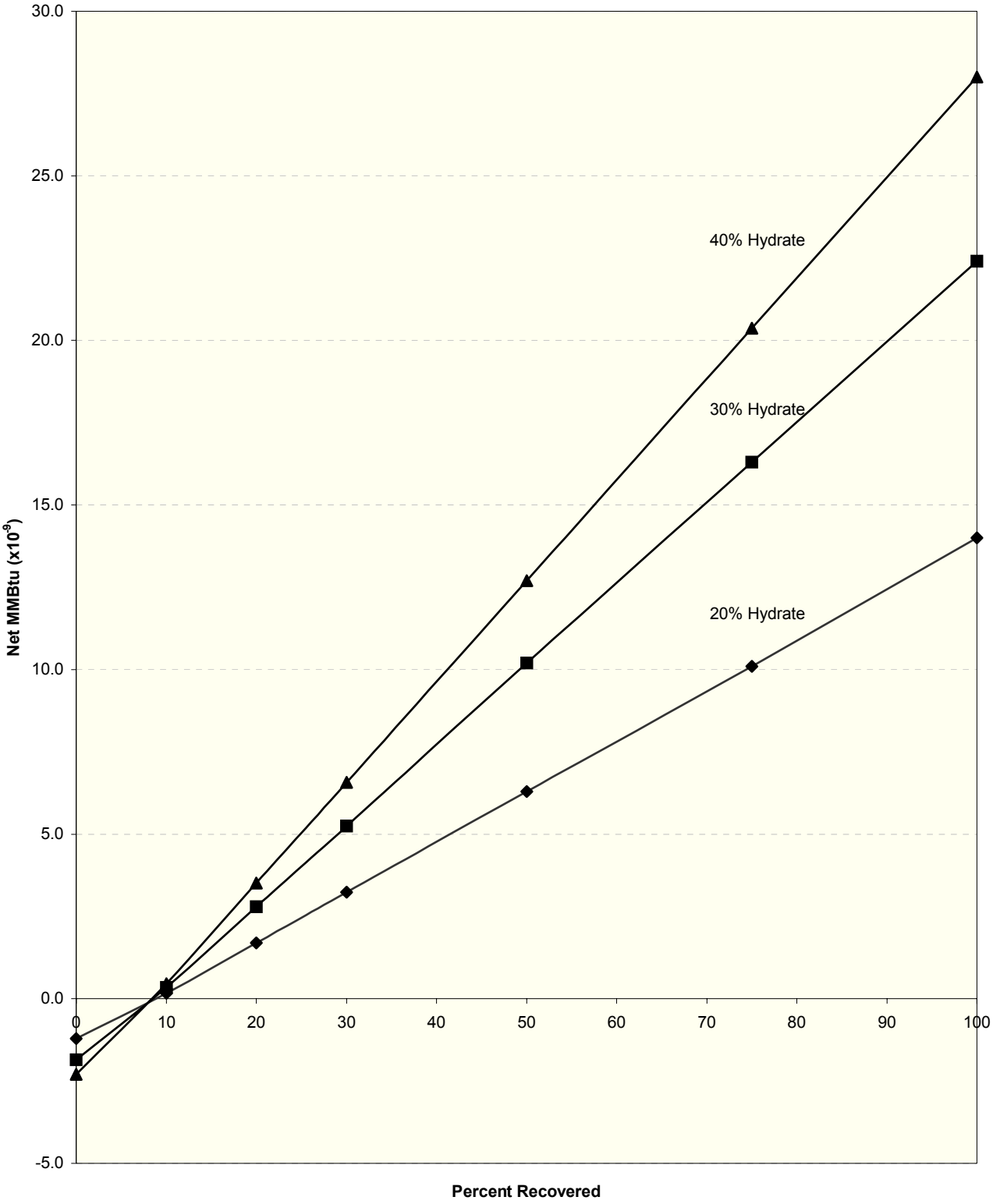
30.0
25.0
20.0
15.0
10.0
5.0
0.0
-5.0
Net MMBtu (x10-9)
40% Hydrate
30% Hydrate
20% Hydrate
0
10
20
30
40
50
60
70
80
90
100
Percent Recovered

Table 4 represents a listing of some hydrate recovery schemes. In the table, the developmental stage for each recovery scheme is denoted as (1) conceptual study, (2) lab experiments, (3) field trial. Only seven of the seventeen schemes have been conceptually developed, four have received laboratory study, and only two have had field trials (depressurization and inhibitor injection).

Table 4. Development of Recovery Schemes for Gas from *In Situ* Hydrates

Scheme	Description	Cncpt Stdy	Lab Stdy	Field Trial
1	Depressurization	✓	✓	✓
2	Inhibitor Injection	✓	✓	✓
3	Thermal Stimulation	✓	✓	
4	Displacement by Forming CO_2 Hydrates	✓	✓	
5	*In Situ* Combustion	✓		
6	EM Wave Decomposition	✓		
7	Microwave Decomposition	✓		
8	Geothermal Heating			
9	Mining from Above or Below Hydrates			
10	Low Grade Radioactive Waste			
11	Warm Ocean Currents			
12	Microbes that Consume Hydrated CH_4			
13	Resistance Heating			
14	Earthquake with Collection System			
15	Sediment Vacuum Hose Recovery			
16	Displace Hydrated Methane with Air			
17	Impact Dissociation			

Many recovery schemes have been considered; however, all are constrained by one (or a combination of) five techniques:

1. Depressurization –In this production scheme, pressure drop acts as a driving force for decomposition. As shown in Figure 6a, the hydrate usually contacts or overlies a free gas reservoir, so that regular production of the gas causes the reservoir pressure to be reduced below the hydrate dissociation pressure. Using either continuous or cyclical production, hydrates dissociate to replenish the gas produced from the normal reservoir. The heat to dissociate the hydrate (Equation 1) is provided through the heat reservoir of the earth. Neither external heating nor inhibitor media need be inserted in the reservoir. Due to this "free" heat input, depressurization is the most economical process to date, and serves as a standard for comparison.

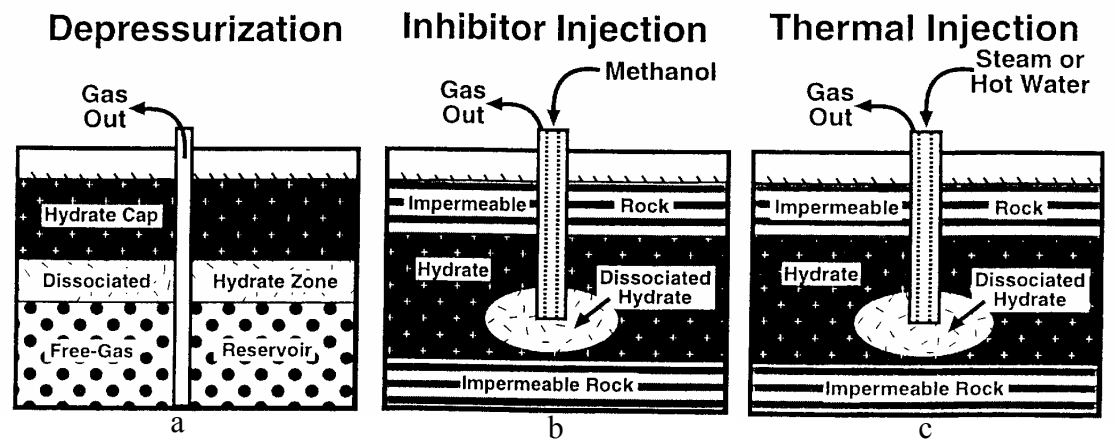

Figure 6. Schematic of Hydrate Production Methods (a) Depressurization, (b) Inhibitor Injection and (c) Thermal Simulation (from Collett, 1998)

2. Inhibitor Injection – As shown in Figure 6b, methanol, ethylene glycol, or calcium chloride brine may be injected down a well, to shift the hydrate equilibrium line so that at reservoir conditions hydrates are not stable. This is usually done in a cyclical process, to dissociate hydrates around the well. However, the high cost of unrecoverable inhibitors mandate careful economic justification. Inhibitors may be used with another recovery technique, to prevent hydrates from re-forming in the well bore or in the reservoir once dissociation has occurred through depressurization or thermal stimulation.
3. Thermal Stimulation – In this process temperature difference is the driving force for hydrate decomposition. Thermal stimulation, shown in Figure 6c, requires that an external source provide the energy to dissociate hydrates. The energy source can dissociate the hydrates at the surface (e.g. hot water, brine, controlled oxidation, warm ocean currents or geothermal heating) or in the hydrate interior (e.g. microwave, electromagnetic, ultrasonic stimulation, low grade radioactive waste, resistance heating). The expense appears to be high, relative to depressurization.
4. Displacement or Microbial Consumption – Four Japanese laboratories have made measurements on carbon dioxide displacement of methane from *in situ* hydrates; as much as 45% of methane has been displaced. Large scale pilot experiments will begin for this process over the next two years in Osaka. The CO_2 displacement technique is detailed further in Section IV. Another technique proposes sweeping air or water past hydrates to cause hydrate dissociation without re-formation. Finally, it has been discovered that microbes live adjacent to hydrate reserves and possibly consume them; it may be possible to harvest such microbes as an energy source.
5. Mechanical Disruption – These techniques are still in the early conceptual stages, and they include mining the hydrates (from above or below), exchanging kinetic energy for dissociation through creating artificial earthquakes, or impact dissociation. These appear to be relatively inefficient from an energy perspective.

Using Table 4 as a guide, let us examine in some depth the first seven recovery schemes, which are distinguished by calculations as a minimum certification of

engineering feasibility. Below we examine the general techniques of depressurization, which forms a base case, as well as inhibitor injection, and thermal stimulation (including schemes 5,6, and 7). The examination of the fourth case, displacement of methane by carbon dioxide, will be deferred until Section IV.

II.D. Details of Depressurization, Inhibitor Injection, and Thermal Stimulation

Much of the information in this section has been extracted from three recent reviews of *in situ* hydrate production methods by Kamath (1998), by Bishnoi and co-workers (Khairkhah, et al., 1999) and by Sloan (1998),

II. D.1. Depressurization. Depressurization is the most practical and economical hydrate dissociation method; consequently, it provides a base case for comparison of all other methods. It is the only technique which has been proven via commercial field gas production for over a decade (see the Messoyakha Field Production, Appendix B.3) but the gas volume production from hydrates is uncertain (Collett and Ginsburg, 1998). The details of depressurization relative to phase equilibria are given in Appendix B.3.

In depressurization, free gas is normally adjacent to the hydrate reservoir, so that free gas production can lower the reservoir pressure below that required for hydrate dissociation. Without free gas, the well may be in danger of producing extreme amounts of water.

Hydrate depressurization relies upon obtaining the heat of hydrate dissociation from the sensible heat of the rock matrix, the hydrate phase itself, or gas and water from the dissociated hydrate. Because the thermal conductivity of other condensed phases is much greater than that of the gas or hydrate phase, there is the danger of ice formation (or hydrate reformation). When pipelines are depressurized to dissociate hydrates (Peters, 1999) water forms ice from dissociated hydrate. However, the depressurization of pipelines is much more rapid than that of reservoirs, so individual cases should be considered, particularly when the hydrated reservoir is below or close to the ice point.

The possibility of hydrate and ice hindering flow paths suggests that fracturing may provide an increased surface area and better flow paths. The large water production rates compound the reservoir flow problems and may require surface facilities for handing water and gas lift.

McGuire (1981) simulated depressurization, proposing that fracturing be used to increase the depressurization area. Holder et al. (1982) assumed a free gas zone in communication with the hydrates and provided a three dimensional depressurization simulation of heat and mass transfer in a reservoir. Burshears et al.,(1986) extended the Holder model to incorporate hydrate composition, to provide a reservoir simulator. Kamath et al., (1989) studied contribution of gas from hydrate depressurization to the total gas produced. Sloan and co-workers (Selim and Sloan, 1990; Yousif et al., 1990,1991) used a moving boundary model to fit their data for depressurization of gas in

a hydrate zone, but with single phase flow through porous media. Most recently groups at Laurence Livermore Laboratory (Moridis et al., 1998), at University of Tokyo and JNOC (Masuda et al., 1998), and at Royal Dutch Shell, (Drenth and Swinkels, 1998) have incorporated hydrate dissociation models into modern reservoir simulators.

In the most recent review of potential gas production models for the Mallik 2L-38 reservoir, Khairkhah, et al. (1999) indicated a need for a three mechanism model for gas production by depressurization, to include:

a) two-phase flow (gas and liquid) through porous media,
b) kinetics of gas hydrate dissociation, and
c) heat transfer rates.

Such a hydrate depressurization model is yet to be completed and added to a reservoir production model. However, a simple depressurization production model by Omenihu (1995) for hydrates below the permafrost, is summarized in Section II.D.4.

II. D.2. Inhibitor Injection. Hydrate inhibitors can be injected down a well into a hydrate reservoir to shift the equilibrium line so that hydrates will dissociate at reservoir conditions which are in contact with inhibitor. As indicated for the Messoyahka field (Appendix B.3), inhibitor injections result in very high flows in the short term, decreasing as the inhibitor becomes diluted by the water produced when hydrate dissociates. Short term, reservoirs flows can be increased by a factor of from 1.25 to 10 by inhibitor injection.

Laboratory work by Sira et al., (1990) extended the data of Kamath et al., (1989) to provide a simple relationship for gas flow rate with inhibitor injection

$$Q/(\phi A) = a\Delta T^b \qquad (2)$$

where:

Q = gas production rate in presence of inhibitors, gmol/sec
ϕ = volume (or area) fraction of hydrates at the interface
A = cross sectional area of the core, cm^2
ΔT = true temperature driving force ($T_{inhib\ fluid} - T_{equil}$), ^oC
with parameters a and b given in Table 5.

A cyclical process is used with inhibitor injection to dissociate hydrates around the well, without communication between wells (i.e. an injection well and a production well). Kamath (1998) notes that application may be more suitable for treatment of small volumes near the well bore, rather than a large volume injection due to the high cost of unrecoverable inhibitors. Inhibitors may be used in conjunction with another recovery technique to prevent hydrates from re-forming once dissociation has occurred through depressurization or thermal stimulation.

Table 5. Parameters in Inhibitor Injection Equation (2)

Injection Fluid	constant "a"	constant "b"	Reference
15wt% brine	1.353×10^{-7}	2.195	Kamath et al. (1989)
30wt% methanol	4.577×10^{-7}	1.668	Sira et al. (1990)
30 wt% glycol	8.606×10^{-8}	2.578	Sira et al. (1990)

II. D.3. Thermal Stimulation. Thermal stimulation of hydrate reservoirs is technically feasible. The cost of thermal stimulation techniques, as shown in Section II.E, is considerably above that of depressurization; this fact alone has limited the study of thermal stimulation to conceptual and laboratory studies. The major cost disadvantages of thermal stimulation are twofold:

- Depressurization uses "free" heat from the earth to dissociate hydrates, and thus has an economic advantage over thermal methods, in which heat originating above ground is lost passing through permafrost or oceans before reaching the hydrate.
- Efficient thermal stimulation requires the establishment of flow paths for heating media between injection and production wells, which necessitates reservoir strength, and perhaps fracturing. The early stages of thermal stimulation processes are cyclical, and thus rely only on heat conduction, whereas latter stages with heating media communication between wells can use both conduction and convection.

Yet thermal stimulation may be feasible, and future developments are a function of engineering ingenuity. These techniques are bifurcated: (1) heating at the hydrate surface and (2) downhole *in situ* heating, each of which is discussed below.

II. D.3.a. Heating at Hydrate Surface via Hot Water/Brine/Steam. McGuire (1981) modeled cyclic steam injection from a single well, using steam for hydrate dissociation and brine injection to keep hydrate from reforming around the well-bores and fractures, once dissociation occurred. McGuire's "five-spot" placement with communication between wells, may be typical for thermal stimulation processes. As diagrammed in Figure 7 each single injection well has four production wells.

McGuire provided four summary observations based upon his model for hot water frontal sweeps and hot water fracture injection:

- The frontal sweep method is more efficient than the fracture-flow stimulation method.
- Gas production rate is high for temperatures below 120^{o}C in frontal sweep models.
- Steam with temperatures higher than 200^{o}C cannot act as an efficient injection fluid.
- With frontal sweeps, the hydrate thickness and sediment porosity should be greater than 5 m and 15%, respectively.

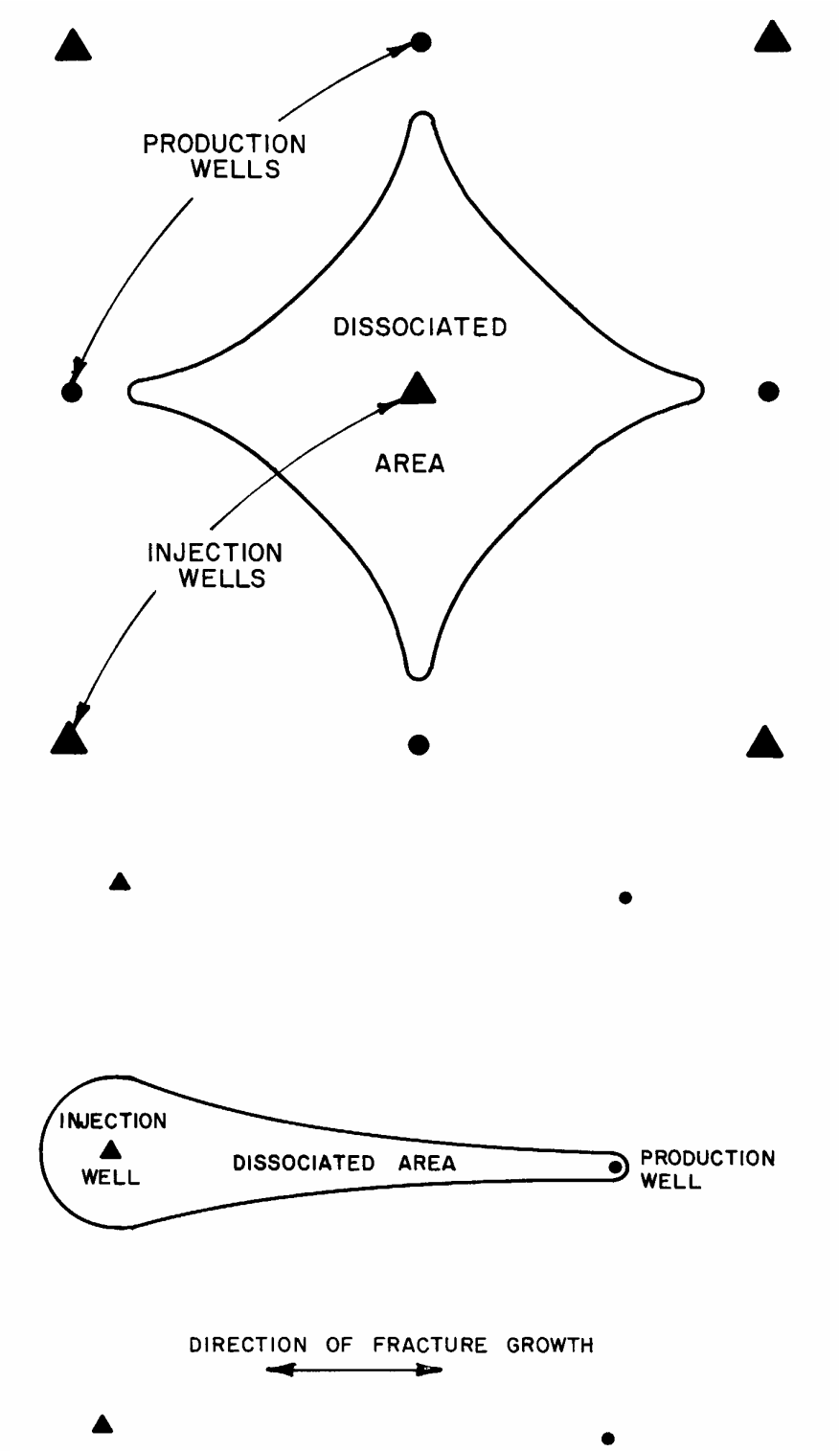

Figure 7. Schematic for Thermal Stimulation Well Placement (from McGuire, 1981)

Initially a cyclic process using hot media injection with an insulated tubular precedes continuous injection, when there is no communication between injection and production well(s). In the later stages of injection, a continuous brine injection and drive process may be used. However, with steam injection the energy losses appear to be substantial due to the long paths of cold water or permafrost traversed by the steam.

Kamath and Godbole (1985) reported energy efficiency ratios between 11 and 16 for cyclic hot brine injection methods, with thermal efficiency ranging from 70-85% for 177^{o}C hot brine injection. Hot brine injection may be the most promising thermal injection method due to two significant advantages:

- Brine acts as an inhibitor, reducing the equilibrium temperature, requiring a lower sensible heat increase to bring the reservoir to dissociation conditions,
- Heat losses are lower due to the lower brine temperature. This means better efficiency from a perspective of the both laws of thermodynamics – that is, energy conservation and lower entropy production.

The hot brine injection technique may be most applicable when geothermal reservoirs are close to the hydrate reservoir. Iseux (1990) extended the work of Kamath and Godbole with promising results to indicate fracturing can substantially increase the injection pathways as well as surface contact area.

It may be concluded that hot brine injection is better than either steam injection or hot water injection. However, production of water from hydrate may cause problems either by diluting the brine, in lifting gas to the surface, or water/ice plugging pores. Geothermal heating shows significant promise, using a thermal stimulation technique; however, no conceptual studies are published for this technique.

II. D.3.b. Downhole *In Situ* Heating for Hydrate Decomposition. Downhole thermal stimulation techniques are conceptual and speculative. These methods are appealing due to their advantage of limiting heat loss before reaching the hydrate reservoir. Yet they, and others like them, should only be considered as potential methods until experimental and modeling work are done for a proper assessment. To illustrate the breadth of ingenuity in hydrate recovery concepts, schemes 5, 6, and 7 in Table 4 are briefly outlined below: (1) *In Situ* Combustion, (2) EM Wave Decomposition, and (3) Microwave Decomposition.

II. D.3.b.1. *In Situ* Combustion. Chu (1983) reviews the current enhanced oil recovery processes using *in situ* combustion; this technique has been also used in recovery of hydrocarbons from coal and shale. With *in situ* combustion, a fire in the hydrate reservoir generates the heat to dissociate hydrates. The fire is controlled by input of oxygen (or air) which is compressed at the surface and injected downhole. Figure 7 can represent this case by a center well for injection of air, while the surrounding four wells provide production points.

In the hydrate reservoir, the sweep of the burning front will control the overall system economics; yet the sweep cannot be established until the cyclic stage can be

surpassed to achieve communication between wells. The propagation of a flame front is limited by the need to raise the surrounding sediment to the combustion temperature, which is highly energy intensive, particularly for sparsely distributed ocean hydrates.

In situ combustion of hydrates is composed of four steps, for a permafrost hydrate reservoir without sediments: (1) sensible heating to the dissociation boundary (typically 33.6 J/mol from the ice point), (2) dissociation of the hydrate (54,000 J/mol), (3) combustion of methane at standard conditions (-802,625 J/mol), and (4) product heating (172,105 J/mol) to adiabatic flame temperature. A significant amount of energy (-76,486 J/mol) is released by *in situ* combustion. However, a substantial amount of this energy may be absorbed by the surrounding sediments and other phases, which are not considered in the above calculation.

An adiabatic flame temperature of 1793^{o}C is calculated in the absence of phases other than hydrates, using the method of Smith and Van Ness (1987, p.127). This means that the hydrate surroundings must be raised to a very high temperature in order to support combustion. The extreme difficulty of raising the surrounding rock/sediment to this temperature is caused by substantial heat loss via conduction away from the flame front.

The process may be confounded by operational problems such as rig safety, control of flame front, high temperature cement failures, water handling, reservoir subsidence, and tubular corrosion. Due to the above problems, the recovery scheme of *in situ* combustion awaits a thorough engineering evaluation.

II. D.3.b.2. Electromagnetic and Radio Frequency Heating. Radio Frequency (RF) and electromagnetic (EM) heating methods have been used for shallow tar sands (Sresty et al., 1986), but not for hydrates to date. Kamath (1998) suggested the RF/EM method deserves consideration for hydrates application due to three reasons: 1) the waves can penetrate the hydrate interior without the initial need for fracturing, 2) the major part of the heating can be directed to the hydrate rather than the surrounding sediment, and 3) the waves can be used to penetrate the hydrate away from the well bore, perhaps as far as 3000 ft.

Special tubular electrodes are implanted in the well bore and EM energy is applied to heat large hydrate volumes by matching the frequency to the electrical characteristics of the hydrates for efficient operation. Leakage of currents into adjacent formations can induce potentials not only in the earth, but in metallic materials well away from the electrodes. This raises substantial safety and energy loss questions, which should be investigated further.

Islam (1994) reported that EM heating may recover as much as 70% of hydrate reserves, with an cyclic heating/production process. Islam used an existing thermal simulator for tar sand recovery solving the conduction and electrical charge balance equations. He evaluated 25 different reservoir scenarios with resulting energy efficient ratios ranging from five to forty, the latter surpassing the thermodynamic limit.

II. D.3.b.3. Microwave Heating. In the microwave heating scheme, an alternating wave which is tuned for the frequency of water (2450 MHz) causes a molecular dipole rotation, causing polarized molecules to align and relax. This alignment and relaxation occurs 4.9×10^9 times per second, which causes heating and breaks the hydrated water hydrogen bonds, thus freeing the encaged molecules in hydrates.

For hydrates, the microwave scheme has three advantages over many others: (1) it can be tuned for water molecules and thus avoid direct heating of other phases or molecules (however other phases such as sediments and gases may be indirectly heated by the water) (2) it penetrates the hydrate volume rather than relying upon heating the smaller exposed surface area, and (3) it does not rely upon a temperature gradient to transfer heat via conduction, but instead generates internal temperatures within the solid, and a reverse temperature gradient can be generated via radiation.

However microwave heating is hindered by a low efficiency compared to other schemes. Penetration of microwaves into the hydrate medium decreases exponentially with depth. In addition, 50% efficiency (Meredith, 1998) is typical for the most common means of microwave generation from electricity. Since the efficiency of electricity generation from hydrocarbons is about 35%, the total efficiency of generation of microwaves from hydrocarbons is about 17%; this number does not compare favorably with either direct thermal stimulation or the more stringent comparison with depressurization.

At the current time, microwave heating has only been considered in a preliminary manner. A comprehensive evaluation is yet to be done.

II.D.4. Modeling Results for Hydrate Depressurization Below the Permafrost

In summary it appears that depressurization, perhaps complemented via thermal or inhibitor stimulation, is the most likely method to produce methane from hydrates. Makogon (1988) indicated that depressurization was used during the decade of the 1970's to produce gas from the Messoyakha field in Siberia. However, that claim has recently been questioned by Collett and Ginsburg (1998). A detailed summary of the Messoyakha case study together with phase equilibrium boundaries is found in Appendix B.3.

In this section, results from a depressurization model are presented for the recovery of methane from a permafrost hydrate reservoir, which has many similar characteristics of the Mallik 2L-38 reservoir. To date, no such model has been made for sub-ocean hydrate recovery, because the recovery cost of ocean hydrated methane would be much more substantial than that on land for two major reasons:

1. As shown in the two reservoir case study comparisons in Appendix B.1 and B.2, ocean hydrates are at lower concentrations by an order of magnitude than those in the permafrost.
2. There are logistical difficulties in reaching and gathering gas from the oceanic hydrate reservoir, relative to those on land. In the Messoyakha field (Appendix B.3) gas underlying the hydrates enabled depressurization, and a gas gathering system was in place via normal production wells.

For the above two reasons, the initial depressurization model is presented for land hydrates, with the economic justification in the following section. It is generally accepted that economical production verification will be obtained first on land hydrates, before the ocean hydrates are seriously considered as a near-term energy resource.

There are two model types for hydrate dissociation by depressurization: the first is in which hydrate kinetics controls the process, and the second is a heat-transfer controlled process. The physics of the dissociation process dictate that neither mass transfer nor fluid flow control hydrate dissociation; therefore they are not considered.

1. The first type of model is that for which hydrate kinetics controls dissociation (Kim et al., 1987; Masuda et al, 1998, Moridis et al., 1998). For these models, it is assumed that energy flow to the hydrate dissociation front is sufficient to provide dissociation rates, and slow kinetics of hydrate decomposition are the rate limiting factor. These models usually rely upon kinetic data from Bishnoi's laboratory (Kim et al., 1987) and typically do not include an energy balance, simplifying the modeling process.
2. The second type of model has energy flow controlling dissociation, usually based upon a moving boundary (Ullerich et al., 1987; Selim and Sloan, 1989, 1990; Yousif et al., 1990). In these models, the low thermal conductivity of hydrate is assumed to limit the flow of heat to the hydrate dissociation front, and dissociation kinetics occur instantaneously when sufficient heat arrives at the front.

It has not been shown experimentally which of the two model types (if either) represent reality in the reservoir. In a few models from the laboratories of Bishnoi and Sloan (Jamaluddin, et al., 1989; Yousif et al., 1991, respectively), both kinetics and heat transfer are considered, so both extremes and intermediate cases can be achieved. However, as indicated by Bishnoi and coworkers (Khairkhah, et al., 1999) such models do not adequately account for other reservoir phenomena, and they provide results which are difficult to interpret simply.

This section considers results of the hydrate depressurization production model of the first type from Omenihu (1995) in Kamath's Alaskan laboratory, for three reasons:

1. The model results may be unambiguously interpreted and applied to economic modeling. At the end of this subsection, the model's deficiencies are listed, pointing toward future improvements. However, this fundamental model does allow an interpretation of qualitatively correct reservoir behavior, as shown below.

2. The model enables a sensitivity analysis to basic hydrate reservoir parameters. Again, suggestions for improvements at the end of this subsection indicate that the qualitatively correct model should be improved to enable engineering calculations for depressurization.

3. the model incorporates gas reservoir parameters for the Alaskan North Slope permafrost region close to the Mallik 2L-38 well; thus the results may apply to permafrost reservoir conditions for which hydrates will first be produced.

The results of the original work are given in SI units, however, the figures are given in both SI and U.S. oilfield engineering units to illustrate production principles. The model considers the production of gas (G_p) from a hydrate reservoir at several constant rates, typified by a deliverability constant (c) in the equation:

(3)

$$G_p = c \int_0^t \left(P^2 - P_{wf}^2 \right)^{n'} dt$$

where:

G_p = gas produced, SCM/day
c = deliverability constant (range from 14,375 – 114,996), SCM/day/MPa
n' = numerical exponent (range 0.5 to 0.7), dimensionless
P = reservoir pressure, MPa
P_{wf} = flowing bottomhole pressure, MPa
t = time, days

The deliverability constant, c, determines the flowability of the well – that is how rapidly a well can be produced. The higher the deliverability constant, the shorter time necessary to produce the well. The deliverability constant, a very common means for characterizing gas well production, has parameters determined from field production testing. Since the production rate changes over the life of a field, over time it may be necessary to use several deliverability constant curves.

To determine the reservoir pressure as the gas and hydrate are produced, a second equation is based solely upon a mass balance in the reservoir:

$$\frac{dP}{dt} = \frac{q_g B_g \left[1 + \frac{K_w}{K_g} \frac{\mu_g}{\mu_w} \right] - \left[B_g - B_{gH} + 8.33E-04 B_w \frac{dG_{eH}}{dt} \right]}{43560 A \phi (1\text{-}sw) h_g \left(\frac{1}{B_g} \frac{dB_g}{dP} \right)}$$

(4)

where:

q_g = gas production rate, (dG_p/dt from the previous equation)
B_g = gas formation volume factor

K_w = permeability of water
K_g = permeability of gas
μ_g = viscosity of gas, cp
μ_w = viscosity of water, cp
B_{gH} = hydrate formation volume factor
B_w = water formation volume factor
G_{eH} = gas influx from hydrates (scm)
A = area, acres
ϕ = porosity
sw = water saturation in the gas zone

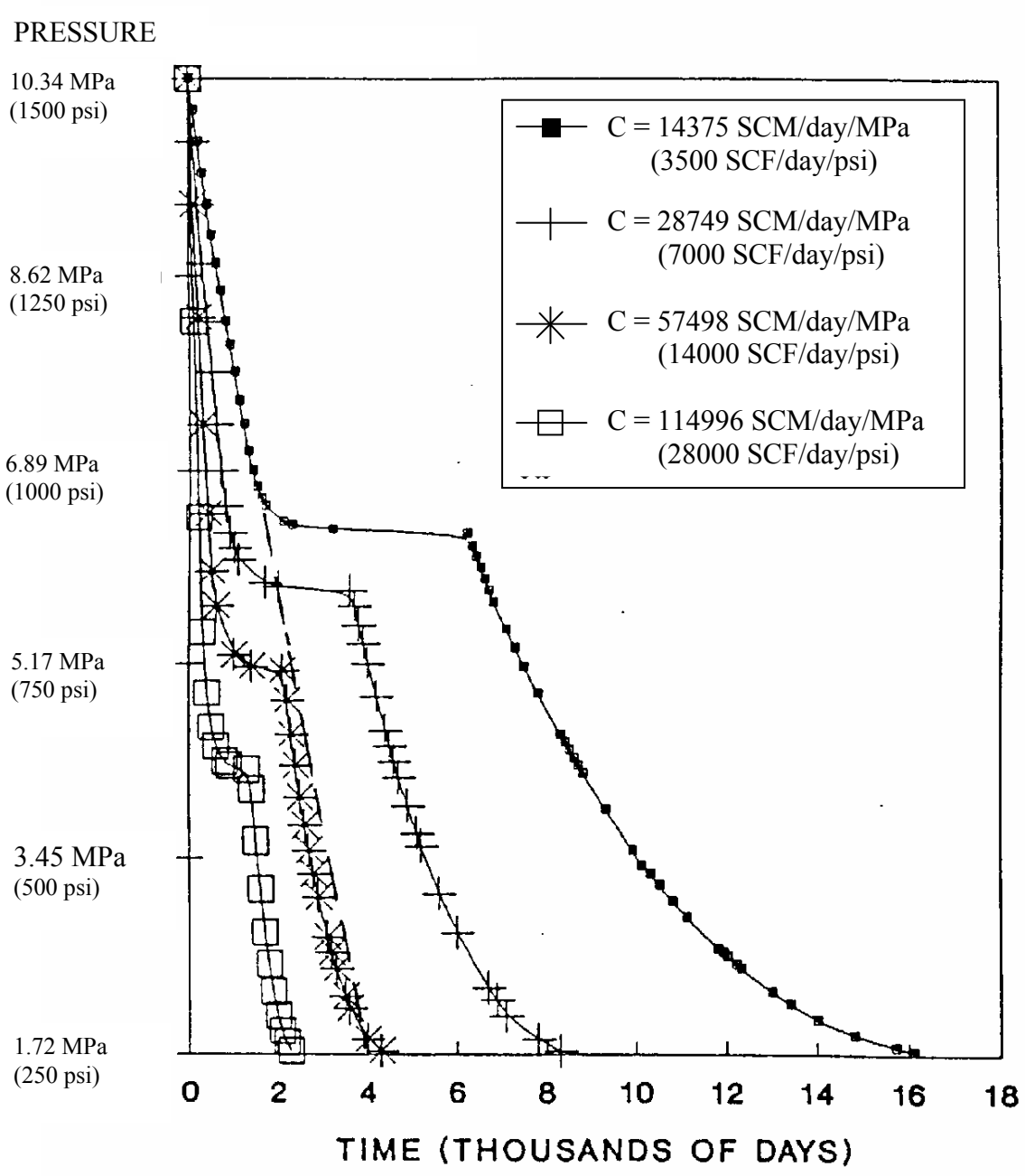

Figure 8. Pressure Drawdown with Time, as a Function of Deliverability Constant (from Omenihu, 1995)

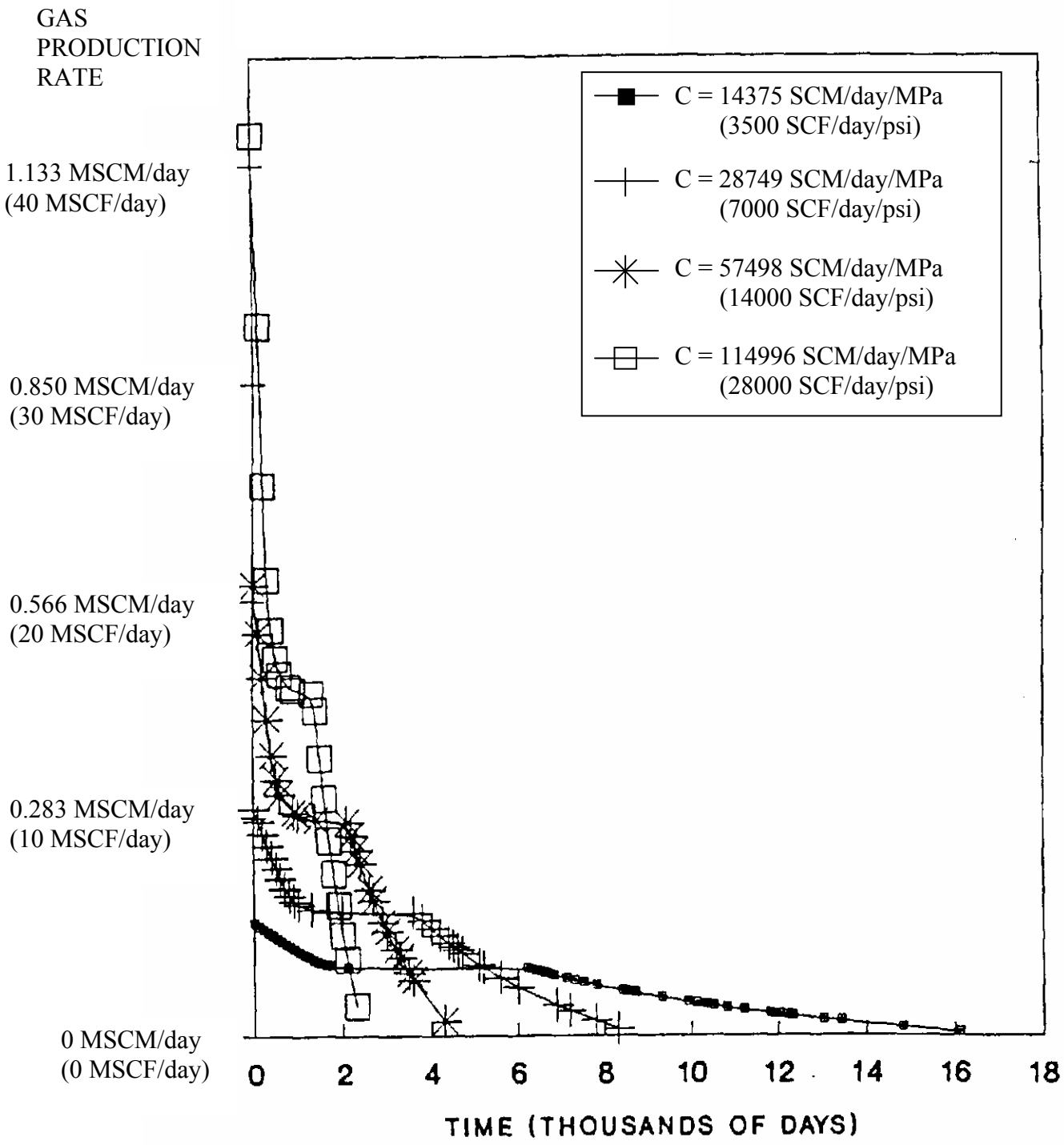

Figure 9. Gas Production with Time, as a Function of Deliverability Constant (from Omenihu, 1995)

Figures 8 and 9 give the basic model results. Figure 8 shows the pressure of the reservoir with time, and Figure 9 gives the well gas production rate with time. In both figures the parametric variable is the well deliverability constant. Other parameters for the model are given in Table 6.

In Figure 8, the top line (c= 14375 SCM/day/MPa) shows a rapid draw down of the gas reservoir from an initial value of 10.34 MPa to about 6.55 MPa after 2,000 days of production. At that reservoir temperature and pressure, hydrates begin to dissociate at a rate which equals the production rate, so that the pressure remain constant until 6,000 days. At 6,000 days the constant production rate exceeds the hydrate dissociation rate, so the pressure declines until the well is depleted at about 16,000 days. In Figure 8 higher deliverability constants cause briefer constant pressure periods, because the hydrated portion of the reservoir is depleted more rapidly.

Figure 8 clearly displays the effect of hydrate addition to the reservoir pressure. Without hydrates, the pressure would decrease approximately according to the dashed line for the case of c = 14,375 SCM/day/MPa. The difference between the c=14,375 SCM/day/MPa dashed and solid line, is the hydrate contribution to the reservoir pressure.

Table 6. Base Case Data for North Slope Hydrate Depressurization Model

Hydrate Reservoir Areal Extent	394.0 km^2
Initial Hydrated Gas in Place	0.368 TSCM
Initial Free Gas in Place	0.212 TSCM
Initial Average Reservoir Pressure	7.067 MPa
Hydrate Zone Average Thickness	17.1 m
Depth to Top of Hydrate Zone	762 m
Free Gas Zone Thickness	17.1 m
Average Reservoir Porosity	38% (both zones)
Average Initial Water Saturation	15% (both zones)
Initial. Avg. Reservoir Temperature	10 ^oC
Well Spacing	0.647 km^2
Number of Wells	608
Flowing Well Bottomhole Pressure	250
Well Gas Deliverability Exponent (n')	0.5
Hydrate Formation Volume Factor	0.0583 m^3/SCM
Water to Gas Ration in Hydrates	0.2942 bbl/SCM
Activation Energy of Hydrates (E/R)	9398.9 K
Hydrate Decomposition Equilibrium Constant (Ko)	2.3177E+17 SCM/day/MPa/km^2

Figure 9 shows the gas production rate as a function of time at various deliverability constants. The highest deliverability constant (114,996 SCM/day/MPa) has an initial production rate of 1.22 MSCM/day, rapid depletion of the reservoir, and only two slight changes in the slope of the depletion curve at around 1000 days while hydrates dissociate, before reservoir exhaustion at 2,500 days.

At the other extreme in Figure 9, the curve for c=14,375 SCM/day/MPa shows a constant slope until 2,000 days, at which time hydrates begin to dissociate at a rate to maintain constant production until 6,000 days, and a final decline to exhaustion at 16,000 days. It should be noted that all curves can be integrated to obtain similar total reservoir production in Figure 9, so the chosen production rate (or deliverability constant) is dictated by economics.

In Figure 9 the integrals of all curves will be equal because the total initial hydrate reservoir is assumed equal for all deliverability constants. This indicates that heat transfer effects do not restrict total reservoir production - only the rate of extraction.

The shortfalls of the Omenihu model are threefold:

(1) The model neglects the flow of energy to the hydrate dissociation front, which probably controls the dissociation process. This factor should be incorporated in the next generation of models for depressurization.
(2) Critical reservoir parameters (permeability, flow boundaries, re-hydration, etc.) are all incorporated in the deliverability constant "c" which is a gross representation of the reservoir properties.
(3) The model input data assumes a free gas layer of 17m, a factor of ten greater than that found in the Malik 2L-28 well. This was done for convenience, relying on the fact that a similar free gas volume will have to be found (perhaps up-reservoir of the previous Mallik well) before depressurization can be commenced.

Even with such shortfalls however, the Omenihu model is the best first-order approximation available to estimate the hydrate production effect on the reservoir as well as the economics of depressurization. It serves as the current best comprehensible approximation.

The above model has been extended to an economic evaluation by Kamath et al., (1998). The following section presents an economic evaluation of hydrate recovery by the two most likely means – namely depressurization and thermal injection. The other recovery methods in Table 4 await technical feasibility evaluation before an economic analysis.

II.E. The Economics of Depressurization and Thermal Stimulation

Several economic studies have been made for recovery of methane from permafrost hydrates, where the first recovery is likely to occur due to the comparatively high hydrate concentrations adjacent to conventional gas reserves. Table 7 compares the depressurization and thermal stimulation techniques to free gas production from an Alaskan permafrost reserve. In Table 7, the model of Kamath (1998) and Omenihu (1995) has been normalized to approximately the same costs per well for free gas production and depressurization, as the other models of Holder et al., (1984), Ehlig-Economides (1985), and MacDonald (1990).

Three things are apparent from the values in Table 7: (1) while there is not absolute agreement about the economics of gas production from hydrate, they are reasonably similar, (2) the cost of hydrate production by depressurization compares favorably to Alaska free gas production, but it is less expensive than thermal stimulation, compared to numbers by the same investigator, and (3) no matter how the gas is produced, transportation cost is currently a major expense in Alaska without a transportation system. It may be possible to insert the gas into the existing oil pipeline, but to date there has been reluctance to do so, to transport oil as a more energy dense fuel.

Table 7. Hydrate Depressurization and Thermal Stimulation Comparison to Free Gas Production in Alaska (in 1999 US$)

	Free Gas	Hydrate Production					
	Prdctn	Depressurization			Thermal Stimulation		
Reference	1	2	1	3	2	4	1
Total Investment (M$)	4.56	4.65	5.12	5.10	7.12	18.6	5.12
Total Operating Cost (M$)	1.77		4.75	5.45		4.10	5.73
Total Ann. Equiv. Cost (M$)	2.84	3.51	5.97	16.46	4.48	8.54	8.66
Total Production (MSCM/yr)	22.6	31.1	74.8	44.41	25.5	45.3	17.0
Production Cost ($/SCM)	0.114		0.080	0.371		0.188	0.509
Transportation ($/SCM)	0.216	0.210	0.216	0.216	0.210	0.224	0.216
Break Even Price ($/SCM)	0.331	0.351	0.297	0.587	0.432	0.412	0.726

References: 1 = Holder et al., (1984); 2 = MacDonald (1990); 3= Kamath (1998); 4 = Godbole and Ehlig-Economides (1985)

With such favorable economics, it seems that hydrates associated with a free permafrost gas reservoir will likely be produced by depressurization, when it is economical to produce free gas. While the North American permafrost only comprises 23% of the total, the Russian permafrost (74% of the total) is unlikely to have the technical or political infrastructure available for depressurization development in the near term. Because Alaskan gas transportation is so expensive, hydrate depressurization may be done in Alaska to resolve some production problem, such as the need to generate and re-inject gas to maintain reservoir pressure for oil production. For this reason, it is likely that hydrates in the Mackenzie Delta will be first produced by depressurization, due to previous success with the Mallik 2L-38 well, and an existing gathering and treating system.

II.F. Fugitive Methane Emissions from Hydrates and Geohazards

With such a large amount of methane in hydrates, the question naturally arises concerning the potential for evolution of methane from hydrates upon recovery. The 20 year atmospheric warming potential ascribed to methane by the IPCC assessment is 56 times that of CO_2 (Brewer, 1999). Section II.F.1 considers the potential for methane releases during hydrate recovery schemes, and Section II.F.2 discusses the potential for

geohazards. Because the potential for climate change via *in situ* hydrate dissociation is minimal, modern and ancient climate change scenarios are relegated to Appendix C.

II.F.1. The Potential for Fugitive Release During Hydrate Recovery. Fugitive methane emissions from the oil and gas industries are estimated as 47Mt/y (Riemer, 1999) with the natural gas industry contributing 73% of the total (Houghton, 1995) shown in Table 8. For non-associated gas, the fugitive emissions due to drilling and production are minor (8% of total). Methane emissions from the oil industry are due to venting or flaring of gas associated with the produced oil, when there is no infrastructure to support gas transport. Riemer (1999) estimates that 45% of all fugitive emissions could be avoided by measures financially benefiting the industry.

Table 8. Source of Fugitive Methane Emissions in the Oil and Gas Industry (Riemer, 1999)

Source of Fugitive Emissions	Percentage of Total
Associated Gas	27
Compressors	25
Distribution Leaks	18
Pneumatic Devices	14
Vents, Maintenance & Exploration	8
Other	8

Since the initial production of methane from gas hydrates will very probably be done in the permafrost by depressurization of free gas (see Sections II.D & E), the fugitive emissions of hydrate-produced methane will not increase beyond that of normal gas production system. The method for producing gas from hydrate will be through a typical well, used to produce the gas reservoir. The normal well cementing seals between the casing or tubing and reservoir will prevent fugitive emissions during production. The caprock and permafrost will serve to prevent methane emissions from the top of hydrates, just as conventional gas is prevented from escaping the reservoir.

A similar statement could be made for production of permafrost hydrates via thermal stimulation, the next most likely method of methane production from hydrates. Both injection and production wells shown in Figure 7 (page 25) will have similar seals to prevent methane escape from the wells.

However in ocean hydrate production, particularly where the hydrates lie close to the mudline, the caprock may be replaced with unconsolidated sediment and production facilities may have difficulty containing produced methane. With deeper ocean hydrates the containment problem is similar to that in permafrost hydrates. The containment of methane from ocean hydrates is a second order problem, yet to be addressed. The major problem for ocean hydrate production is the low concentration (< 6% by volume) which will cause methane production to be problematic until at least the latter half of the next century, when new technology may become available.

Fugitive emissions from conventional reservoirs (Riemer, 1999) are listed by region, along with the CO_2 concentrations (Petroleum Consultants, Inc., 1999) in Table 9. The high CO_2 concentration in some areas is due to a few dominant high CO_2 reservoirs; for example the giant Natuna Field in Indonesia contains up to 71% CO_2.

Table 9. Emissions and
CO_2 Concentrations by Region

Region	% of CH_4 Emissions	CO_2 Conc %
Former USSR	53	9.38
Middle East	12	5.48
North America	10	2.65
Africa	8	5.93
South America	6	2.43
Europe	6	6.43
Asia	4	10.9
China/Pacific	1	19.3

From Table 9 it appears that both methane and CO_2 emissions are of major concern in the former USSR, which contributes more than half of the fugitive emissions and has high concentrations of CO_2 in the normal gas reserve. As free gas production grows in Asia, China, and the Pacific, the CO_2 emissions will become of major concern in those regions.

Natural gas production also results in additional emissions of CO_2, which is stripped from the natural gas and released into the atmosphere. There is currently only one commercial facility in the world, the Sleipner West field project in the North Sea (see http://www.ieagreen.org.uk) that re-injects the CO_2 into a saline aquifer close to the original reservoir.

II.F.2. The Potential for Geohazards. When a hydrate dissociates, it changes from a solid to a fluid mixture. The resulting change in sediment physical properties and shear strength may encourage massive slope failure along low-angle detachment faults (Haq 1999).

In the past hydrates have been associated with significant movement of earth in deepwater ocean environments. Most notably Bugge et al. (1988) show the massive ancient Storegga slide of sediment (5600 km^3 - 290 km long and 450 km thick - traveled a distance of more than 800 km) off Norway, triggered by earthquake loading with friction reduction via gas evolving from hydrate decomposition. Paull et al. (1991) indicate slump features associated with numerous faults at or above BSR in the Carolina Trough in the Atlantic. MacDonald et al. (1994) have experimental evidence of hydrate dissociation over a short period in the Gulf of Mexico due to eddy warming.

With instances such as those above, concerns have been expressed (Campbell, 1991) about the effect of hydrates on foundations of platforms and pipelines. Typically a hydrate mound is 30 m high by 300-500 m across, and so could produce large volumes and instability. Campbell suggested that one crater found in more than 2,000 m of water resulted from rapid melting of a hydrate mound. In contrast, the doctoral work of Neurater (1988) on hydrate mounds in the Gulf of Mexico found no evidence of seafloor instability related to hydrates.

There has been some documentation of drillship operations in the Arctic (Hinkel and Thibodeau, 1988) related to hydrate instability. An additional article (Milgram and Erb, 1984) suggests that single hull vessels are fairly immune and double hull vessels are very immune to blowouts in deepwater.

It is clear that ocean gas and oil will become more important as easily accessed energy resources are depleted. The effect of hydrates on foundations of deepwater pipelines, platforms, and drilling will be of major importance in the future, but an insignificant amount of research has been done to date. This area represents a major future challenge.

III. Potential for CO_2 Sequestration as Ocean Hydrates

In the course of studying the issue of gas extraction from hydrates via CO_2, to fully cover the subject an additional exercise was completed – that of reviewing the most recent information on the potential for sub-sea storage of CO_2 as hydrates. Because hydrates will form when CO_2 contacts water at ocean temperatures (<10^oC) and pressures, hydrates will play a major part in any CO_2 ocean sequestration scheme. While a number of models and laboratory experiments have been done to predict the fate of ocean sequestered CO_2, results for actual sequestration experiments are just coming into the literature. In this section, very recent experimental results of small-scale ocean CO_2 injections are presented because they best predict large scale ocean CO_2 sequestration.

Appendix D provides a general background for CO_2 sequestration along with a summary of CO_2 sequestration models. The physical phenomena which control CO_2 sequestration in hydrates are also presented in Appendix D, to complement this section which summarizes the *in situ* CO_2 ocean injection data. With the data of the current section as a basis, Appendix D also provides a prediction for CO_2 injection at various depths in the ocean, along with a summary economic analysis.

In multiple deepwater experiments over the last three years, the Monterey Bay Aquarium Research Institute (MBARI) performed four types of *in situ* experiments on direct injection of CO_2 in sea water, using two remotely operated vehicles (ROVs): (a) experiments at depths of 300-1000 m, (b) experiments at depths of 3650 m, (c) experiments with varying injection rates and rising droplets of CO_2, and (d) experiments to examine the short-term effects on fish by pH and partial pressure of carbon dioxide. While many of the results presented here are published in very reputable journals (e.g. Science) some of the very recent data are in manuscript form or in press, made available through the courtesy of Dr. P.G. Brewer, Senior Scientist at MBARI.

III.A. Experiments at Depths from 300-1000m. In the first MBARI experiments (Brewer et al., 1998) ocean hydrates of CO_2, CH_4, and natural gas were formed by slowly bubbling gas into sediments in inverted cylinders in the deep ocean, using their shallow water ROV *Ventana*, equipped with subsea cameras. Liquid CO_2 was expelled into an inverted cylinder, and a hydrate skin formed around the droplets, within a few seconds. A time series experiment was done, in which the hydrate/CO_2 mass dissolved over several weeks, even though contact with the surrounding ocean water was limited. The CO_2/hydrate mass disappeared in only a few days from an inverted cylinder with open contact with the sea water.

The MBARI team concluded that CO_2 hydrate formed in the shallow ocean is capable of rapid dissolution. See Section III.C below for further experiments with shallow CO_2 injection. In contrast, the CH_4 hydrate formed simultaneously were stable over the period during which the CO_2 hydrate dissolved. Such effects may be attributed to the relative insolubility of methane in sea water.

III.B. Experiments at Depths of 3650 m. In preparation for the below deep ocean experiments, a small amount of CO_2 was injected as droplets from the deepwater ROV *Tiburon* at a depth of 2650 m (Brewer, personal communication, 1999), the critical depth at which the densities of CO_2 droplets and sea water are equal. The expelled droplets floated, neither rising nor falling, but were pushed about by ocean currents. When density gradients are absent, convective currents control the flow of particles.

At water depths of 3650m Brewer et al., (1999) carried out three experiments in the Monterey Bay Trench: (1) disposal of 2.5L of CO_2 into a 4L upright beaker, (2) disposal of 1.8L of CO_2 into an open-ended cylinder pushed into the sediment, and (3) free release of CO_2 on the sea floor. In contrast to shallower CO_2 droplet experiments, at these greater depths CO_2 hydrate particles formed at the surface and rapidly sank to the bottom of the container. Ohmura and Mori (1998) had previously shown that density differences can cause instability in a CO_2 film, using a surface chemistry and force balance analysis.

The sinking CO_2 hydrate ($\rho = 1.12$) also contained 6-8 molecules of water per molecule of CO_2. The hydrate had a larger volume in addition to being more dense than the surrounding liquid CO_2. As a result the hydrate due to its higher density sank to the bottom of the CO_2 liquid containers and due to the large hydrate volume, liquid CO_2 was displaced from the top of the container. Figure 10 shows overflow of some remaining liquid CO_2 from the top of the beaker.

For the freely released liquid CO_2 at 3650m, high interfacial tension of a hydrate film maintained a strong barrier between the liquid CO_2, the water, and the sediments. The hydrate-wrapped liquid CO_2 was highly mobile, and the density contrast was small, so that liquid CO_2 globules were easily disturbed by sea water motion. Several deep sea animals passed within a few centimeters of the CO_2 without apparent harm or distraction.

Figure 10. Overflow of Liquid CO_2 at 3650m (from Brewer, et al., 1999)

III.C. Experiments with Varying Injection Rates and Rising Droplets of CO_2. In experiments on November 17, 1998 an MBARI team (Brewer et al., submitted 1999) used the ROV *Ventura* to inject liquid CO_2 into an inverted beaker at 605m depth. A massive frothy hydrate floated when formed by rapid injection, accompanied by a rapid decrease of pH in the surrounding from 7.6 to 4.5, due to turbulent mixing. After a short while the frothy CO_2 hydrate bubbles compressed and the pH returned to normal in the water adjacent to the hydrate.

In similar experiments at the 605 m depth the MBARI team injected liquid CO_2 into an inverted beaker very slowly. A hydrate layer formed at the CO_2-sea water interface, with no change in the sea water pH below the interface. A flexible CO_2 hydrate film appeared below the CO_2 mass at the top of the inverted beaker, causing a very small mass transfer of CO_2 due to slow diffusion through the film. However, when the pH probe was inserted into the CO_2 mass, the pH decreased dramatically.

The vessel was then inverted and CO_2 liquid droplets were formed as the mass discharged in the ocean. The droplet diameter range was 0.25-2cm (typically 1cm). The ROV was flown upwards at the same rate (6 m/min) as the rising CO_2 droplets. Marine trash wrapped around CO_2 bubbles in one instance, but in most cases the bubbles were encapsulated with a thin hydrate film. At 250m, about 100 m above the CO_2 vaporization pressure, the hydrates decomposed, CO_2 vaporized, and the gas dissolved in water. A duplicate set of experiments was done on October 12, 13, 1999, with essentially the same results.

III.D. Experiments to Examine CO_2 Effects on Fish and the Environment. Finally, MBARI experiments have been done to examine the effect of CO_2 on the environment (Tamburri et al., submitted 1999). Finely ground fish food (tuna and clams) was injected from a point source in a beaker containing hydrates, attracting fish to the hydrate mass. The partial pressure of CO_2 in sea water displaced oxygen to the point that one fish lost consciousness on three separate occasions, reviving each time to be re-attracted to the fish food emanating from the CO_2 source. The scent of food was more attractive than the debilitating effects of the reduced oxygen. Other MBARI experiments (Hinrichs et al., Nature, in press, 1999) show compelling evidence for methane-consuming archaea, which may prevent climate change from methane evolving from hydrates.

The above MBARI experiments are important because they represent the best analogs for CO_2 injection in the ocean.

IV. CO_2 Displacement of CH_4 in Hydrates

The displacement of CH_4 from ocean hydrates via exchange with CO_2 hydrates is an appealing idea, because it provides storage for a greenhouse gas while recovering an energy gas. The idea is largely untested in either laboratory or field, but components of the idea are common in field technology. For example, the injection of CO_2 in a reservoir is very common in Enhanced Oil Recovery (EOR) technology. In another analogous process, adsorbed methane has been displaced from coal using CO_2 in a commercial pilot plant since July 1996 in Enhanced Coal Bed Methane (ECBM) recovery. Due to the similarities in CO_2 displacement from coal and hydrate processes, the abbreviation EHBM denotes Enhanced Hydrate Bed Methane, or CO_2 displacement of hydrated CH_4.

Figure 11 shows that the thermodynamics favor a transformation of CH_4 to CO_2 hydrates. At a seafloor temperature of 4-5^oC, if the pressure (or partial pressure) of CO_2 is greater than about 2 MPa but less than 4 MPa, CO_2 hydrates will be stable while methane hydrates will dissociate. The process transport phenomena and kinetics have only been studied in a preliminary way, yet they will control the displacement process.

In this portion of the report overviews of the transport phenomena and kinetics are discussed in Section IV.A, before summarizing the data from laboratory studies in Section IV.B. EHBM is compared with the still developing ECBM process in Section IV.C, to show the detailed similarities and differences, for evaluating the technical feasibility and economics of the EHBM process. Finally in Section IV.D, a prescription is given for future development needs of EHBM.

IV.A. Overview of Phenomena Affecting Displacement of CH_4 from Hydrates via CO_2

Because thermodynamics favor CO_2 hydrates over CH_4 formation at partial pressures between 2 and 4 MPa at a seafloor temperature of 4^oC, the question of this exchange becomes one of hydrate kinetics, and transport phenomena. In order for the CO_2/CH_4 hydrate exchange to occur, the three following steps must take place:

IV.A.1. The CO_2 must first reach the CH_4 hydrate particle surface and its interior. Macroscopic transport of CO_2 to the hydrate face determines reservoir fracturing requirements which provide gas migration pathways and large surface to volume ratios for gas transport and for hydrate exchange kinetics, respectively. Reservoir permeability, which will be lessened by produced water, will adversely affect transport. Secondly the CO_2 must microscopically penetrate the hydrate surface in order to displace the sub-surface layers of methane in the hydrate particle interior. As shown in Section IV.C, the microscopic diffusion step in the solid phase may be the rate-controlling step.

IV.A.2. The kinetics and energy exchange of CO_2 and CH_4 hydrates must occur. This requires (a) a fairly large surface to volume ratio, and (b) dissociation and reformation kinetics. The CO_2/CH_4 hydrate exchange kinetics have been measured in a very few laboratories (see Table 10). Hydrate dissociation and reformation are surface phenomena, and displacement within the hydrate volume may be very slow. The

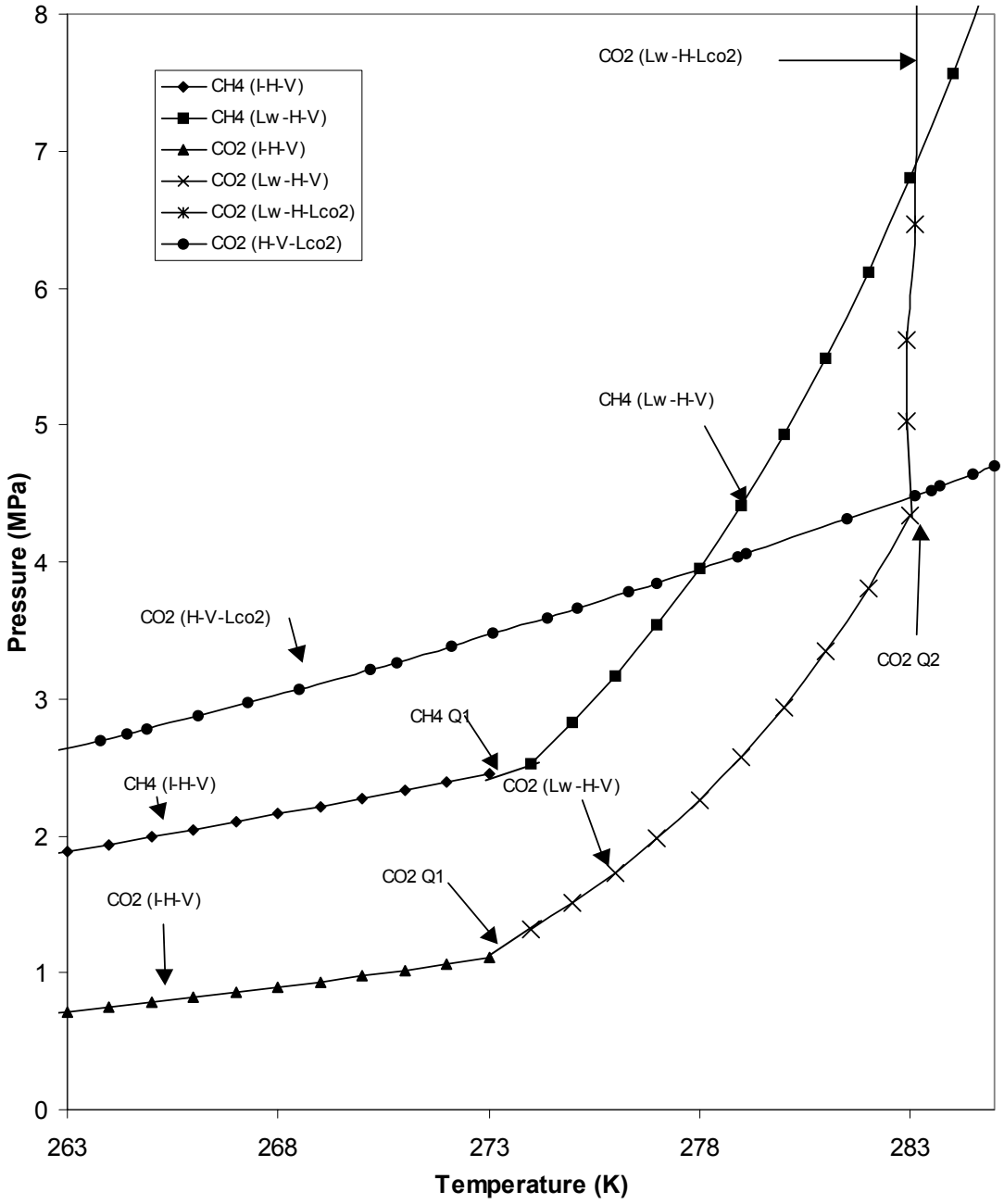

Figure 11. CH_4 and CO_2 Hydrate Phase Equilibrium

macroscopic laboratory experiments of Table 10 were designed to minimize experimental difficulties on the microscopic level.

In addition, the energy of melting of CH_4 hydrate has to be provided, and the energy of formation of CO_2 hydrates must be extracted. Fortunately these heats are very similar and should compensate, so that the process will not be limited by energy exchange.

IV.A.3. The freed methane must exit the system without reforming hydrates. Pathways and systems are needed to provide for the collection of methane and non-converted CO_2. Not only may reservoir fracturing be needed, but an efficient means of ensuring that the exiting methane and CO_2 do not reform hydrates at exiting conditions similar to those of the reservoir.

IV.B. CO_2 Displacement Experiments of CH_4 Hydrates

Only a very few experiments have been done to displace methane from hydrates via CO_2, in four Japanese laboratories, as shown in Table 10.

Table 10. Displacement Experiments for CH_4 by CO_2.

Laboratory	Results of Experiments
Osaka Univ. Ohgaki et al., 1994,1995, 1996,1997, 1999	1. The CH_4 hydrate is selectively replaced by CO_2, with an average distribution coefficient of 2.5. 2. The decomposition rate of CH_4 in the mixed hydrates is three times larger than that of pure CH_4 hydrate 3. There are optimum conditions (temperatures, zones, etc.) for the displacement
HNIRI Ebinuma et al., 1994,1995,1999	1. High pressures favor methane displacement 2. Displacement was found to occur over 100 hours
NIRE: Komai, et al., 1999	1. At 3.5MPa and 276K after 1 hour CH_4:CO_2 hydrate ratio was 45:40 2. Replacement may be achieved in as short a time as 12 hours.
Chiyoda Hirohama et al., 1996, 1997	1. CH_4 hydrate submerged 800 hours in liquid CO_2 2. At 4.5MPa & 281K CH_4 recovery was 16% after one month 3. At 4MPa and 274-276K CH_4 recovery was 10-30% after one month

As shown in Table 10, the initial studies indicate that thermodynamics and kinetics appear to be marginally favorable. Currently, the concept has shown sufficient promise to be considered for the next stage in development. Large scale laboratory experiments were initiated at Osaka University in late 1999, with funding by a major Japanese corporation. While the idea of CH_4 displacement from hydrates by CO_2 is innovative, it faces a number of technical challenges, illustrated by comparison with the developing enhanced coal bed methane process.

IV.C. Comparison: CO_2 Displacement of CH_4 from Hydrates and from Coal

On a continuous basis since July 1996 Burlington Resources, Inc. has injected a total of 85,000 SCM/day of CO_2 into four wells at the Allison pilot unit in the San Juan Basin in Northwestern New Mexico, USA. Methane has been produced from nine wells by CO_2 displacement from the Cretaceous Fruitland coal seem (Stevens et al., 1999a), using an injection/production layout of wells similar to Figure 7, page 24. The commercial pilot plant at Allison is the only existing process to demonstrate the feasibility of Enhanced Coal Bed Methane (ECBM) with CO_2. In January 1998 a second ECBM plant using nitrogen to displace coal bed methane was initiated by BP-Amoco at the Tiffany site in the Southwestern Colorado portion of the San Juan Basin.

Although Enhanced Oil Recovery (EOR) is a similar process which pumps CO_2 into energy reservoirs, a fundamental difference exists between EOR and the process of Enhanced Coal Bed Methane Recovery (ECBM). While EOR uses CO_2 to enable transportation, reducing the viscosity to produce reservoir oil, in ECBM CO_2 adsorbs strongly onto coal, displacing methane gas to a production well. An economic comparison of EOR and ECBM (Wong et al., 1999) showed that EOR produces US$14/tonne of CO_2 used while the value for ECBM is US$2/tonne of CO_2. As a result EOR is widely practiced in the field, compared to the single ECBM pilot at Allison.

In principle, Figure 12 (from Byrer and Guthrie, 1999) serves equally well as a schematic for CO_2 displacement of methane from coal or from hydrates, represented by the broad black horizontal lines in the figure. As CO_2 flows through the coal bed or hydrate reservoir, thermodynamic conditions may favor CO_2 incorporation onto the coal or hydrate more strongly, displacing and driving methane from the reservoir.

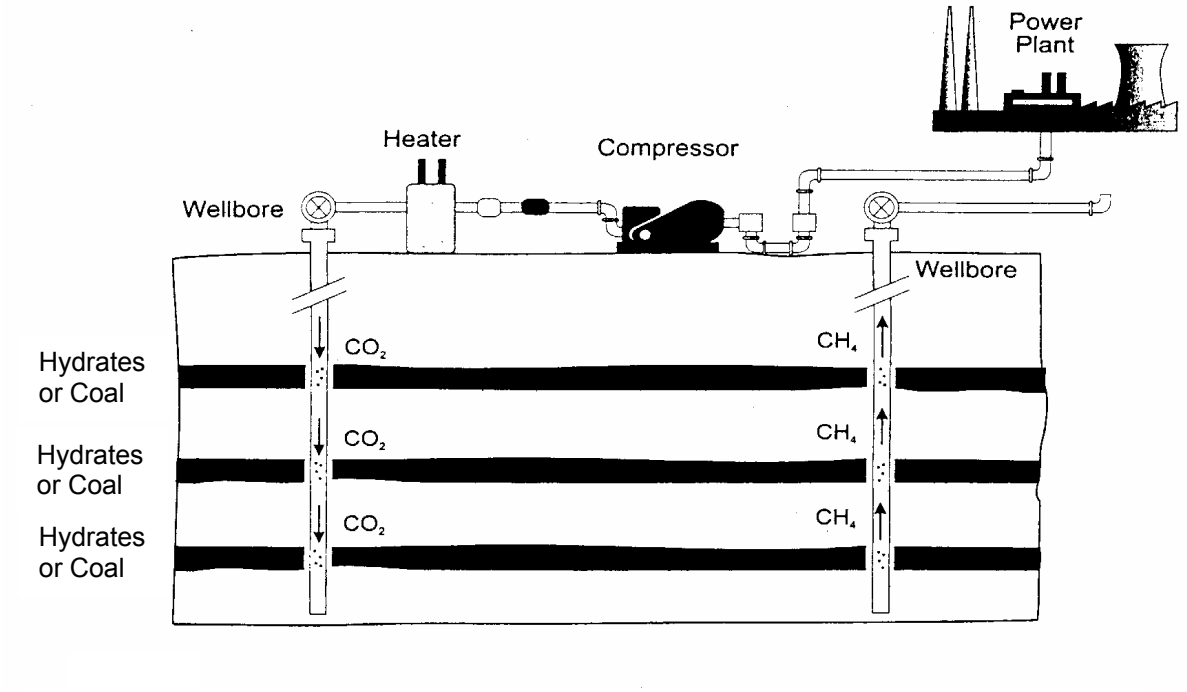

Figure 12. CH_4 Displacement by CO_2 (Byrer and Guthrie)

A brief summary of CO_2 ECBM as an established pilot and potential future commercial process is helpful for two reasons: (1) ECBM development provides a perspective on the technical feasibility of Enhanced Hydrate Bed Methane (EHBM) recovery and (2) as a newly-developing technology since 1995, ECBM enables a vision of a "best case" for the future development of EHBM.

IV.C.1. Enabling Factors for CO_2 Displacement of CH_4 from Coal. The enabling factors for economic production of ECBM were obtained in part from IEA GHG Programme Report PH3/3 (Advanced Resources International, August 1998). At the Allison pilot unit the CO_2 ECBM method produces methane at a cost of $0.06/SCM ($1.75/KCF) relative to a nominal methane wellhead price of $0.07/SCM ($2.00/KCF), while the economics for CO_2 ECBM projects outside the Southwestern U. S. locale require methane wellhead costs of $0.11/SCM ($3.00/KCF). The other enabling factors for ECBM are scientific considerations.

Three technical points enable ECBM.

1. The amount of methane in a coal bed can be five times the amount in a conventional sandstone reservoir of comparable size. The depth of a coal bed suitable for ECBM is 300- 1,500 m, in locations where mining of the coal is unlikely.

2. CO_2 displaces the methane very efficiently; at equivalent gas pressures in the laboratory, twice as much CO_2 is adsorbed per unit area as CH_4. In actual applications, the molecular replacement ratio of CO_2:CH_4 is 3:1. Before field application, coal bed adsorption isotherms were obtained for nitrogen (N_2) and CH_4 on coal (Puri and Yee, 1990) and a comparison was made for both N_2 and CO_2 adsorption, relative to CH_4 adsorption on coal (Arri et al., 1992).

   Even though N_2 adsorbs less strongly (by a factor of seven) on coal than does CO_2, BP-Amoco began the Tiffany pilot ECBM N_2 injection in the San Jual Basin in Southwestern Colorado (USA) in January 1998. The economics of ECBM displacement with N_2 are more favorable than using CO_2 (Stevenson, et al., 1993).

   Currently the nitrogen concentration is 16% in the recovered methane, and the N_2 concentration will increase with time, until separation is required. As shown below CO_2 displacement from hydrates (EHBM) will also require separation of CH_4 from the produced gas, due to early breakthrough of the non-combustible CO_2.

3. At the current nascent stage of ECBM, empirically based reservoir screening criteria do not yet exist (Stevens et al., 1999b). As a comparison, screening criteria for EOR required a decade to define and are still being perfected (Taber et al., 1997). Yet preliminary indicators of reservoir characteristics can be specified, as in the IEA GHG Programme Report PH3/3 (August 1998).

   For a good ECBM site, the coal surface area should be high (20-200 m^2/g), the permeability should be high (>1 millidarcies [mD]) and the coal should be methane-

saturated at 70-90% of maximum. Typically three hydraulic fractures per well are required and provide a reservoir permeability of up to 100 mD in the San Juan Basin. The reservoir should be laterally continuous, minimally faulted, with a coal rank of 0.6% to 1.2% on the vitrinite reflectance scale, with a low ash content to minimize CH_4 adsorption.

IV.C.2. Similarities and Differences: CH_4 Displacement via EHBM and ECBM. A comparison may be made between the two processes to show that while they are apparently similar, basic differences prevent a close analogy. First consider the fundamental phenomena of CO_2 displacement of methane in each substrate, in Figure 13. On the left in Figure 13, displacement of adsorbed CH_4 from the coal surface is fairly rapid and efficient, due to the surface availability and the strength of CO_2 adsorption. When CO_2 adsorbs on coal, about 3 SCM of CO_2 is required for every SCM of CH_4 produced at the Allison unit (Wong et al., 1999). This represents fairly efficient displacement because the adsorption isotherm specifies a theoretical minimum of two CO_2 molecules per molecule of CH_4 on the coal surface.

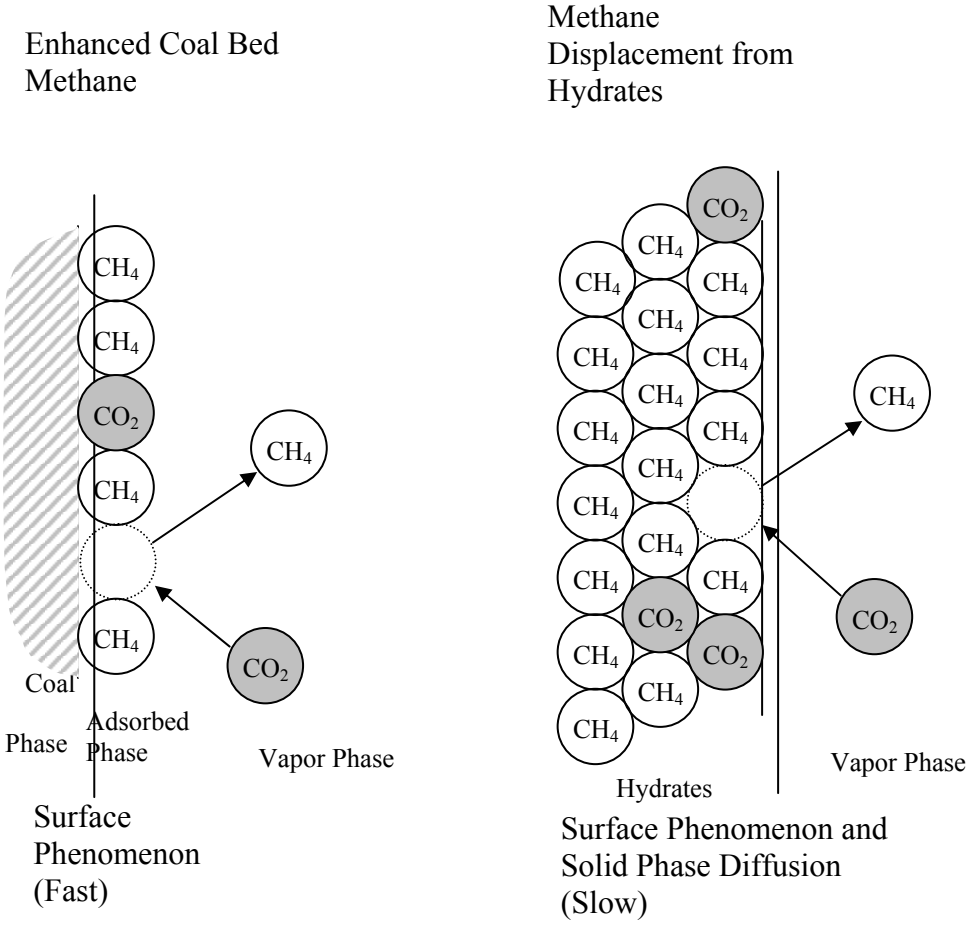

Figure 13. Comparison of Fundamental ECBM and EHBM Phenomena

On the right side of Figure 13, when CO_2 displaces CH_4 from hydrates, surface phenomena only account for a small amount of CH_4, namely the first layer of cavities. In order to exchange CO_2 for CH_4 in subsequent layers comprising the hydrate volume, solid phase diffusion must occur. While diffusion coefficients of neither CO_2 nor CH_4 have been measured through hydrates, typical solid phase diffusion coefficients are very low, on the order of 10^{-10} cm^2/s. In order for the CO_2 to reach deeply embedded CH_4 hydrate layers, very long (perhaps geologic) times will be required. These solid phase diffusion problems were circumvented by design in laboratory experiments of Table 10.

In IEA GHG Report PH3/25 entitled "Issues Underlying the Feasibility of Storing CO_2 as Hydrate Deposits," Rodger (2000) points out another fundamental difference. While CH_4 can occupy all eight hydrate cavities in a unit hydrate cell (see Appendix A for unit cell details), due to its larger size CO_2 usually occupies only the six large cavities. Rodger suggests that this size exclusion from small cages will cause mixed hydrates of CO_2 and CH_4 to co-exist rather than to provide complete methane displacement. In his report Rodger also indicates that marginal methane displacement is likely due to (1) the surface versus volume phenomena shown in Figure 13, (2) the slow kinetics shown by the Chiyoda data in Table 10, and (3) the mass transfer limitations to transport CO_2 to the CH_4 hydrate.

Since the commercial Allison pilot coal bed injection began continuously in 1996, the CO_2 concentration in the outlet gas has been less than 0.4%. Modeling suggests that very little of the CO_2 will appear at the production well(s) until a large fraction of the coal bed methane has been produced (Reznik et al., 1984). To accommodate the large amount of displaced water produced the reservoir permeability should be in the range of 1-10 mD. Some San Juan coal seams close to the Allison pilot unit have permeabilities in excess of 100 mD.

In contrast, the CO_2 displacing methane from hydrates does not dislocate all of the methane, but both molecules compete for the available hydrate sites. Laboratory results by Ohgaki et al. (Table 10), indicate that CO_2 may be taken into the hydrate structure at about 2.5 times the concentration of methane, leaving a minimum (equilibrium) concentration of 28.6% methane in the hydrate phase. This means that large amounts of CO_2 will be present in the produced gas as soon as the injected gas has filled the volume.

Table 11 provides a comparison summary of ECBM and EHBM using CO_2.

For worldwide CO_2 sequestration in coal beds, at small but significant amounts (5-15Gt), a net profit of US$15/tonne can be realized (Stevens et al., 1999a) for ECBM. Larger worldwide amounts of 60Gt may be sequestered at costs under US$50/t, and amounts of 150Gt can be sequestered at costs of US$100-120/t.

The ECBM economics represent an upper limit to EHBM for three reasons:
1. Microscopic transport phenomena and kinetics of replacement are slower for EHBM,

2. Residual CH_4 imposes a maximum of 71% theoretical CH_4 recovery in EHBM, versus 90+% theoretical maximum CH_4 recovery in ECBM, and
3. Rapid CO_2 breakthrough in EHBM will require separation of the product gases, while separation will not be required in ECBM. Breakthrough in EHBM may be almost immediate with concentrations of 50% CO_2 or greater. Surface facilities will have to be expanded to capture and recirculate large CO_2 volumes to the injection wells, adding substantially to surface capital and operating costs.

Table 11. Comparison of CO_2 Displacement of CH_4 from Coal and Hydrates

	Coal Displacement (ECBM)	Hydrate Displacement (EHBM)
Similarities		
Overall Phenomenon	CO_2 displacement of CH_4	CO_2 displacement of CH_4
CH_4 Normal Production by	Pressure depletion	Depressurization (in future)
Possibility of CH_4 Escape to Environment?	No: normal pressure depletion wells secure	No: depressurization with product wells secure
Reservoir Characteristics	Laterally homogeneous	Laterally homogeneous
Required Area/Volume	High	High
Water Displacement	High	High
Required Permeability, mD	1-10	>1-10
Depth for Replacement, m	300-1,500	100-2,000
Differences		
Fundamental Phenomena	Surface adsorption	Volume displacement
CH_4 Production Established	1970's	In future (2004?)
Enhanced Production Site	San Juan coal beds	Permafrost hydrate deposits
CO_2 Supply Available	McElmo Dome pipeline	None
Gas Distribution System	Normal for CBM gas	Not in all permafrost regions
Breakthrough Time Requiring CO_2 Separation?	Years from initial injection	Breakthrough from initiation
Proof of Concept	1 pilot plant (begun 1996)	Laboratory studies
Max % CH_4 Displacement	90^+%	71%
Typical Costs	\$1/tCO_2/Gt CO_2 sequestered	Uncertain

In summary, at first glance the Enhanced Coal Bed Methane process seems very similar to the Enhanced Hydrate Bed Methane process. However, the basic physico-chemical phenomena and application conditions of the two processes are substantially different. As a result the currently developing Enhanced Coal Bed Methane process

provides an upper limit for the best case of the Enhanced Hydrate Bed Methane future development, stated in Section IV.D.

IV.D. The Way Forward for Enhanced Hydate Bed Methane (EHBM) Production

The currently developing Enhanced Coal Bed Methane (ECBM) process discussed in the previous section suggests the requirements for process development of the EHBM concept. Four basic conditions should be fulfilled before EHBM can be realized. The failure of any of these four conditions would make EHBM production highly improbable.

1. Large scale laboratory experiments should indicate the viability of the method. The displacement of methane from hydrates by CO_2 is still in the conceptual stage, and only the few small-scale experiments indicated in Table 10 have been done. These experiments suggest that slow kinetics cause the process to be marginal technically, even when some mass transfer limitations are overcome by experimental design.

   In next two years pilot-scale EHBM laboratory experiments will be conducted at Osaka University, to show the feasibility of the process when mass transfer effects are considered. A reliable economic analysis cannot be done until pilot scale studies determine such vital components as, production rates with mass transfer, reservoir fracturing requirements, gas breakthrough concentrations, and gas separation requirements. In a similar way for ECBM development, laboratory studies by Puri and Yee (1990) and by Arri et al., (1992) indicated technical viability before a thorough economic analysis was done by Stevenson et al. (1993).

2. Permafrost depressurization development of hydrate bed methane should provide a basis for EHBM. Before the enhanced process can be considered, the most likely base case - methane hydrate depressurization - must be proved viable in the permafrost. There was an experience base of almost 25 years of coal bed methane pressure depletion production, which provided a foundation for improvement before continuous ECBM was initiated in 1996.

   Earlier in this report it was shown that hydrates will first be produced in the permafrost, probably with industrial partners (e.g. JNOC, or BP-Amoco) via depressurization sometime during the first decade of the new millennium. The most probable initiation site will be in North American permafrost, either in the Mackenzie Delta of Canada, or in the neighboring Prudhoe Bay of the U.S.A.

   Ocean hydrates are too dispersed and inaccessible to be viable for recovery in the near future. Until a standard production method can be established for permafrost hydrates, the foundation will not be available for enhanced methane production via CO_2 injection. With the depressurization of permafrost hydrates, basic knowledge of reservoir characteristics and potential sites will be identified for EHBM.

3. An inexpensive CO_2 source must be located for the EHBM Site. The ECBM pilot process was aided by an inexpensive ($0.018/SCM or $0.50/KCF) CO_2 pipeline supply within 50km of the site. In the North American permafrost, typical natural gases have low CO_2 contents. In order to prove the concept in permafrost regions CO_2 will most likely come from burning natural gas, with separation via a mono-ethanol amine absorption process. This process is relatively expensive, and will cause at least a doubling of the CO_2 supply cost in the ECBM process.

4. A gathering, and separation system should be available. Because such systems are available in the Mackenzie Delta, that region has the best potential for EHBM. In contrast, industry in the Prudhoe Bay region currently re-injects produced gas to maintain reservoir pressure. However, both regions have separation trains which are used for re-injection of gas.

With four such stringent technical restrictions to EHBM development, the future seems challenged, at best. Nevertheless issues of cost, monitoring and jurisdiction, and environmental impact can be estimated, assuming the technical hurdles can be overcome.

IV.D.1. Economic Estimates. Since there is so little data to use, economic estimates are at best tentative. Kinetic and mass transfer limitations may control the process and cause ECBM economics to be an upper limit which may not be attainable. The lowest possible cost of storing CO_2 using this option is found in the ECBM process at $1/t$CO_2$/Gt CO_2 sequestered. As noted earlier ECBM can afford to pay only US$2/tonne for CO_2 (Wong et al., 1999) while EOR can afford to pay US$14/tonne of CO_2. Best-case estimates were obtained for the cost of EHBM, assuming positive outcomes for the above four technical restrictions, which are incorporated in the following assumptions:

a. Only permafrost hydrates are likely to serve as a source for replacement, due to issues of hydrate concentration, accessibility, and natural gas infrastructure.
b. CO_2 is available for displacement at a cost of $0.018/SCM or ($0.50/KCF) and an existing gathering, separation, recycle, and marketing system is available.
c. As a maximum, CO_2 can displace 71% of CH_4 in hydrates; CH_4 costs are counted as income in the economics.
d. No CO_2 tax or carbon credit system is considered to reduce the basic cost.
e. No transportation costs are considered in EHBM economics.

In the absence of kinetic and mass transfer limitation data, three sensitivity case studies were run for the cases of 10%, 25%, and 50% displacement of the maximum CH_4 from the hydrate bed in Tables 12 through 14, respectively. These case studies were based upon similar economics from the base ECBM economics in the IEA GHG Programme Report PH3/3 (August 1998). ECBM economics were modified to account for a reduced total amount of CH_4 recovered, and the kinetics/mass transfer of CO_2/CH_4 exchange. With this modification, break-even costs between $1.34/SCM (for 10% displacement) and $0.16/SCM (for 100% efficiency) were obtained. These should be compared with free gas production cost of $0.32/SCM indicated in Table 7. Table 15 and

Figure 14 show costs for sequestering CO_2 in EHBM (to the theoretical limit of 71%) as a function of CH_4 displacement efficiency.

This section provides evidence for predicting that the displacement of hydrated methane by CO_2 will drop off exponentially after a rapid start, and have very slow continuing long-term exchange as CO_2 diffuses through the hydrate layer. The overall exchange rate is likely to be 5-10% at best, with the most economic scenario likely to be near US$1,360/tonne CO_2 sequestered. The amount of hydrate is so large that it is tempting to consider this option; if only 1% of the permafrost methane hydrate could be displaced, 126Gt CO_2 could be sequestered. However, EHBM is both theoretically limited and economically unsuitable, so this option is not likely to be used.

Table 12. Estimated CO2-EHBM Break Even Economics for 10% Displacement Efficiency

total Wells	1
Break Even, Initial Gas Price ($/Kscm; 1999)	$ 1,334
Incremental Production (%)	75%
Gas Proce Inflator (% per year)	
Royalty	0%
Severence Tax	0%
Discount Rate (per year)	10.0%
Section 29 Tax Credit (per Mcf; est. 1995)	

Operating Costs (Base; $ thousands per well-month)	$ 1.50
Operating Cost Inflator	
CO2 Costs ($ /Kscm)*	$ 60.03
Gas Gathering/Treat./Compr. Costs (per Kscm)	$ 8.83
Gas Shrinkage (Fuel, CO2)	8%
Injection Well Cost ($ thousands per Well)	$ 350
Stimulation Cost ($ per Well)	$ -
Drilling Cost ($ thousands per Well)	$ 200
Lease Equipment/ Gathering Cost ($ thousands per Well)	$ 150

*also includes CO^2 supply, compression, and separation

Item	Year	1999	2000	2001	2002	2003	2004	2005	2006	2007	2008	2009	2010	2011	2012	2013	2014	2015	2016	2017	2018	Total
Total Base Production (Kscm)		1953	2791	4186	5581	4911	4322	3803	3347	2945	2592	2281	2007	1766	1554	1368	1204	1059	932	820	722	50147
Gas Shrinkage (Kscm)		156	223	335	446	393	346	304	268	236	207	182	161	141	124	109	96	85	75	66	58	4012
Net Base Production (Kscm)		1797	2567	3851	5135	4519	3976	3499	3079	2710	2385	2098	1847	1625	1430	1258	1107	975	858	755	664	46135
Gas Price ($/Kscm)		$ 1,334	$ 1,334	$ 1,334	$ 1,334	$ 1,334	$ 1,334	$ 1,334	$ 1,334	$ 1,334	$ 1,334	$ 1,334	$ 1,334	$ 1,334	$ 1,334	$ 1,334	$ 1,334	$ 1,334	$ 1,334	$ 1,334	$ 1,334	
Gross Revenues ($ thousands)		$ 2,397	$ 3,425	$ 5,137	$ 6,850	$ 6,028	$ 5,304	$ 4,668	$ 4,108	$ 3,615	$ 3,181	$ 2,799	$ 2,463	$ 2,168	$ 1,908	$ 1,679	$ 1,477	$ 1,300	$ 1,144	$ 1,007	$ 886	$ 61,543
Royalty ($ thousands)		$ -	$ -	$ -	$ -	$ -	$ -	$ -	$ -	$ -	$ -	$ -	$ -	$ -	$ -	$ -	$ -	$ -	$ -	$ -	$ -	$ -
Gross Rev Less Royalty ($ thousands)		$ 2,397	$ 3,425	$ 5,137	$ 6,850	$ 6,028	$ 5,304	$ 4,668	$ 4,108	$ 3,615	$ 3,181	$ 2,799	$ 2,463	$ 2,168	$ 1,908	$ 1,679	$ 1,477	$ 1,300	$ 1,144	$ 1,007	$ 886	$ 61,543
Severence ($ thousands)		$ -	$ -	$ -	$ -	$ -	$ -	$ -	$ -	$ -	$ -	$ -	$ -	$ -	$ -	$ -	$ -	$ -	$ -	$ -	$ -	$ -
Net Revenues ($ thousands)		$ 2,397	$ 3,425	$ 5,137	$ 6,850	$ 6,028	$ 5,304	$ 4,668	$ 4,108	$ 3,615	$ 3,181	$ 2,799	$ 2,463	$ 2,168	$ 1,908	$ 1,679	$ 1,477	$ 1,300	$ 1,144	$ 1,007	$ 886	$ 61,543
Investment ($ thousands)		$ (350)																				$ (350)
Base Operating Costs ($ thousands)		$ 17	$ 17	$ 17	$ 17	$ 17	$ 17	$ 17	$ 17	$ 17	$ 17	$ 17	$ 17	$ 17	$ 17	$ 17	$ 17	$ 17	$ 17	$ 17	$ 17	$ 336
CO2 Costs ($ thousands)		$ 2,345	$ 3,350	$ 5,026	$ 6,701	$ 5,897	$ 5,189	$ 4,566	$ 4,018	$ 3,536	$ 3,112	$ 2,738	$ 2,410	$ 2,121	$ 1,866	$ 1,642	$ 1,445	$ 1,272	$ 1,119	$ 985	$ 867	$ 60,206
Gathering/Comprs Costs ($ thousands)		$ 17	$ 25	$ 37	$ 49	$ 43	$ 38	$ 34	$ 30	$ 26	$ 23	$ 20	$ 18	$ 16	$ 14	$ 12	$ 11	$ 9	$ 8	$ 7	$ 6	$ 443
Before Tax Net Cash Flow ($ thousands)		$ (332)	$ 33	$ 58	$ 83	$ 71	$ 60	$ 51	$ 43	$ 36	$ 29	$ 24	$ 19	$ 15	$ 11	$ 8	$ 5	$ 2	$ (0)	$ (2)	$ (4)	$ 208
Federal/State Taxes		$ -	$ -	$ -	$ -	$ -	$ -	$ -	$ -	$ -	$ -	$ -	$ -	$ -	$ -	$ -	$ -	$ -	$ -	$ -	$ -	$ -
Section 29 Tax Credit		$ -	$ -	$ -	$ -	$ -	$ -	$ -	$ -	$ -	$ -	$ -	$ -	$ -	$ -	$ -	$ -	$ -	$ -	$ -	$ -	$ -
After Tax Net Cash Flow ($ thousands)		$ (332)	$ 33	$ 58	$ 83	$ 71	$ 60	$ 51	$ 43	$ 36	$ 29	$ 24	$ 19	$ 15	$ 11	$ 8	$ 5	$ 2	$ (0)	$ (2)	$ (4)	$ 208
Discount Factor		1.000	0.909	0.826	0.751	0.683	0.621	0.564	0.513	0.467	0.424	0.386	0.350	0.319	0.290	0.263	0.239	0.218	0.198	0.180	0.164	
Net Disc. Cash Flow ($ thousands)		$ (332)	$ 30	$ 48	$ 62	$ 48	$ 37	$ 29	$ 22	$ 17	$ 12	$ 9	$ 7	$ 5	$ 3	$ 2	$ 1	$ 0	$ (0)	$ (0)	$ (1)	$ (0)

Financial Performance	
NPV @ 10.0%	$ (0)

Table 13. Estimated CO2-EHBM Break Even Economics for 25% Displacement Efficiency

total Wells	1
Break Even, Initial Gas Price ($/Kscm; 1999)	$ 1,138
Incremental Production (%)	75%
Gas Proce Inflator (% per year)	
Royalty	0%
Severence Tax	0%
Discount Rate (per year)	10.0%
Section 29 Tax Credit (per Mcf; est. 1995)	

Operating Costs (Base; $ thousands per well-month)	$ 1.50
Operating Cost Inflator	
CO2 Costs ($ /Kscm)*	$ 60.03
Gas Gathering/Treat./Compr. Costs (per Kscm)	$ 8.83
Gas Shrinkage (Fuel, CO2)	8%
Injection Well Cost ($ thousands per Well)	$ 350
Stimulation Cost ($ per Well)	$ -
Drilling Cost ($ thousands per Well)	$ 200
Lease Equipment/ Gathering Cost ($ thousands per Well)	$ 150

*also includes CO^2 supply, compression, and separation

Item	Year	1999	2000	2001	2002	2003	2004	2005	2006	2007	2008	2009	2010	2011	2012	2013	2014	2015	2016	2017	2018	Total
Total Base Production (Kscm)		1953	2791	4186	5581	4911	4322	3803	3347	2945	2592	2281	2007	1766	1554	1368	1204	1059	932	820	722	50147
Gas Shrinkage (Kscm)		156	223	335	446	393	346	304	268	236	207	182	161	141	124	109	96	85	75	66	58	4012
Net Base Production (Kscm)		1797	2567	3851	5135	4519	3976	3499	3079	2710	2385	2098	1847	1625	1430	1258	1107	975	858	755	664	46135
Gas Price ($/Kscm)		$ 1,138	$ 1,138	$ 1,138	$ 1,138	$ 1,138	$ 1,138	$ 1,138	$ 1,138	$ 1,138	$ 1,138	$ 1,138	$ 1,138	$ 1,138	$ 1,138	$ 1,138	$ 1,138	$ 1,138	$ 1,138	$ 1,138	$ 1,138	
Gross Revenues ($ thousands)		$ 2,046	$ 2,922	$ 4,383	$ 5,845	$ 5,143	$ 4,526	$ 3,983	$ 3,505	$ 3,084	$ 2,714	$ 2,389	$ 2,102	$ 1,850	$ 1,628	$ 1,432	$ 1,260	$ 1,109	$ 976	$ 859	$ 756	$ 52,512
Royalty ($ thousands)		$ -	$ -	$ -	$ -	$ -	$ -	$ -	$ -	$ -	$ -	$ -	$ -	$ -	$ -	$ -	$ -	$ -	$ -	$ -	$ -	$ -
Gross Rev Less Royalty ($ thousands)		$ 2,046	$ 2,922	$ 4,383	$ 5,845	$ 5,143	$ 4,526	$ 3,983	$ 3,505	$ 3,084	$ 2,714	$ 2,389	$ 2,102	$ 1,850	$ 1,628	$ 1,432	$ 1,260	$ 1,109	$ 976	$ 859	$ 756	$ 52,512
Severence ($ thousands)		$ -	$ -	$ -	$ -	$ -	$ -	$ -	$ -	$ -	$ -	$ -	$ -	$ -	$ -	$ -	$ -	$ -	$ -	$ -	$ -	$ -
Net Revenues ($ thousands)		$ 2,046	$ 2,922	$ 4,383	$ 5,845	$ 5,143	$ 4,526	$ 3,983	$ 3,505	$ 3,084	$ 2,714	$ 2,389	$ 2,102	$ 1,850	$ 1,628	$ 1,432	$ 1,260	$ 1,109	$ 976	$ 859	$ 756	$ 52,512
Investment ($ thousands)		$ (350)																				$ (350)
Base Operating Costs ($ thousands)		$ 17	$ 17	$ 17	$ 17	$ 17	$ 17	$ 17	$ 17	$ 17	$ 17	$ 17	$ 17	$ 17	$ 17	$ 17	$ 17	$ 17	$ 17	$ 17	$ 17	$ 336
CO2 Costs ($ thousands)		$ 1,994	$ 2,848	$ 4,272	$ 5,696	$ 5,012	$ 4,411	$ 3,881	$ 3,416	$ 3,006	$ 2,645	$ 2,328	$ 2,048	$ 1,803	$ 1,586	$ 1,396	$ 1,228	$ 1,081	$ 951	$ 837	$ 737	$ 51,175
Gathering/Comprs Costs ($ thousands)		$ 17	$ 25	$ 37	$ 49	$ 43	$ 38	$ 34	$ 30	$ 26	$ 23	$ 20	$ 18	$ 16	$ 14	$ 12	$ 11	$ 9	$ 8	$ 7	$ 6	$ 443
Before Tax Net Cash Flow ($ thousands)		$ (332)	$ 33	$ 58	$ 83	$ 71	$ 60	$ 51	$ 43	$ 36	$ 29	$ 24	$ 19	$ 15	$ 11	$ 8	$ 5	$ 2	$ (0)	$ (2)	$ (4)	$ 208
Federal/State Taxes		$ -	$ -	$ -	$ -	$ -	$ -	$ -	$ -	$ -	$ -	$ -	$ -	$ -	$ -	$ -	$ -	$ -	$ -	$ -	$ -	$ -
Section 29 Tax Credit		$ -	$ -	$ -	$ -	$ -	$ -	$ -	$ -	$ -	$ -	$ -	$ -	$ -	$ -	$ -	$ -	$ -	$ -	$ -	$ -	$ -
After Tax Net Cash Flow ($ thousands)		$ (332)	$ 33	$ 58	$ 83	$ 71	$ 60	$ 51	$ 43	$ 36	$ 29	$ 24	$ 19	$ 15	$ 11	$ 8	$ 5	$ 2	$ (0)	$ (2)	$ (4)	$ 208
Discount Factor		1.000	0.909	0.826	0.751	0.683	0.621	0.564	0.513	0.467	0.424	0.386	0.350	0.319	0.290	0.263	0.239	0.218	0.198	0.180	0.164	
Net Disc. Cash Flow ($ thousands)		$ (332)	$ 30	$ 48	$ 62	$ 48	$ 37	$ 29	$ 22	$ 17	$ 12	$ 9	$ 7	$ 5	$ 3	$ 2	$ 1	$ 0	$ (0)	$ (0)	$ (1)	$ 0

Financial Performance	
NPV @ 10.0%	$ 0

Table 14. Estimated CO2-EHBM Break Even Economics for 50% Displacement Efficiency

total Wells	1
Break Even, Initial Gas Price ($/Kscm; 1999)	$ 812
Incremental Production (%)	75%
Gas Proce Inflator (% per year)	
Royalty	0%
Severence Tax	0%
Discount Rate (per year)	10.0%
Section 29 Tax Credit (per Mcf; est. 1995)	

Operating Costs (Base; $ thousands per well-month)	$ 1.50
Operating Cost Inflator	
CO2 Costs ($ /Kscm)*	$ 60.03
Gas Gathering/Treat./Compr. Costs (per Kscm)	$ 8.83
Gas Shrinkage (Fuel, CO2)	8%
Injection Well Cost ($ thousands per Well)	$ 350
Stimulation Cost ($ per Well)	$ -
Drilling Cost ($ thousands per Well)	$ 200
Lease Equipment/ Gathering Cost ($ thousands per Well)	$ 150

*also includes CO_2 supply, compression, and separation

Item	Year	1999	2000	2001	2002	2003	2004	2005	2006	2007	2008	2009	2010	2011	2012	2013	2014	2015	2016	2017	2018	Total
Total Base Production (Kscm)		1953	2791	4186	5581	4911	4322	3803	3347	2945	2592	2281	2007	1766	1554	1368	1204	1059	932	820	722	50147
Gas Shrinkage (Kscm)		156	223	335	446	393	346	304	268	236	207	182	161	141	124	109	96	85	75	66	58	4012
Net Base Production (Kscm)		1797	2567	3851	5135	4519	3976	3499	3079	2710	2385	2098	1847	1625	1430	1258	1107	975	858	755	664	46135
Gas Price ($/Kscm)		$ 812	$ 812	$ 812	$ 812	$ 812	$ 812	$ 812	$ 812	$ 812	$ 812	$ 812	$ 812	$ 812	$ 812	$ 812	$ 812	$ 812	$ 812	$ 812	$ 812	
Gross Revenues ($ thousands)		$ 1,459	$ 2,085	$ 3,127	$ 4,169	$ 3,669	$ 3,229	$ 2,841	$ 2,500	$ 2,200	$ 1,936	$ 1,704	$ 1,499	$ 1,320	$ 1,161	$ 1,022	$ 899	$ 791	$ 696	$ 613	$ 539	$ 37,461
Royalty ($ thousands)		$ -	$ -	$ -	$ -	$ -	$ -	$ -	$ -	$ -	$ -	$ -	$ -	$ -	$ -	$ -	$ -	$ -	$ -	$ -	$ -	$ -
Gross Rev Less Royalty ($ thousands)		$ 1,459	$ 2,085	$ 3,127	$ 4,169	$ 3,669	$ 3,229	$ 2,841	$ 2,500	$ 2,200	$ 1,936	$ 1,704	$ 1,499	$ 1,320	$ 1,161	$ 1,022	$ 899	$ 791	$ 696	$ 613	$ 539	$ 37,461
Severence ($ thousands)		$ -	$ -	$ -	$ -	$ -	$ -	$ -	$ -	$ -	$ -	$ -	$ -	$ -	$ -	$ -	$ -	$ -	$ -	$ -	$ -	$ -
Net Revenues ($ thousands)		$ 1,459	$ 2,085	$ 3,127	$ 4,169	$ 3,669	$ 3,229	$ 2,841	$ 2,500	$ 2,200	$ 1,936	$ 1,704	$ 1,499	$ 1,320	$ 1,161	$ 1,022	$ 899	$ 791	$ 696	$ 613	$ 539	$ 37,461
Investment ($ thousands)		$ (350)																				$ (350)
Base Operating Costs ($ thousands)		$ 17	$ 17	$ 17	$ 17	$ 17	$ 17	$ 17	$ 17	$ 17	$ 17	$ 17	$ 17	$ 17	$ 17	$ 17	$ 17	$ 17	$ 17	$ 17	$ 17	$ 336
CO2 Costs ($ thousands)		$ 1,407	$ 2,010	$ 3,015	$ 4,021	$ 3,538	$ 3,113	$ 2,740	$ 2,411	$ 2,122	$ 1,867	$ 1,643	$ 1,446	$ 1,272	$ 1,120	$ 985	$ 867	$ 763	$ 671	$ 591	$ 520	$ 36,124
Gathering/Comprs Costs ($ thousands)		$ 17	$ 25	$ 37	$ 49	$ 43	$ 38	$ 34	$ 30	$ 26	$ 23	$ 20	$ 18	$ 16	$ 14	$ 12	$ 11	$ 9	$ 8	$ 7	$ 6	$ 443
Before Tax Net Cash Flow ($ thousands)		$ (332)	$ 33	$ 58	$ 83	$ 71	$ 60	$ 51	$ 43	$ 36	$ 29	$ 24	$ 19	$ 15	$ 11	$ 8	$ 5	$ 2	$ (0)	$ (2)	$ (4)	$ 208
Federal/State Taxes		$ -	$ -	$ -	$ -	$ -	$ -	$ -	$ -	$ -	$ -	$ -	$ -	$ -	$ -	$ -	$ -	$ -	$ -	$ -	$ -	$ -
Section 29 Tax Credit		$ -	$ -	$ -	$ -	$ -	$ -	$ -	$ -	$ -	$ -	$ -	$ -	$ -	$ -	$ -	$ -	$ -	$ -	$ -	$ -	$ -
After Tax Net Cash Flow ($ thousands)		$ (332)	$ 33	$ 58	$ 83	$ 71	$ 60	$ 51	$ 43	$ 36	$ 29	$ 24	$ 19	$ 15	$ 11	$ 8	$ 5	$ 2	$ (0)	$ (2)	$ (4)	$ 208
Discount Factor		1.000	0.909	0.826	0.751	0.683	0.621	0.564	0.513	0.467	0.424	0.386	0.350	0.319	0.290	0.263	0.239	0.218	0.198	0.180	0.164	
Net Disc. Cash Flow ($ thousands)		$ (332)	$ 30	$ 48	$ 62	$ 48	$ 37	$ 29	$ 22	$ 17	$ 12	$ 9	$ 7	$ 5	$ 3	$ 2	$ 1	$ 0	$ (0)	$ (0)	$ (1)	$ (0)

Financial Performance		
NPV @	10.0%	$ (0)

Table 15. Cost per tonne of CO_2 Sequestered as a Function of Methane Displacement Efficiency

Displacement Efficiency	Cost (thousands)	Cost per tonne CO_2 Sequestered (thousands)
10%	$ (33,291)	$ (1.36)
25%	$ (28,169)	$ (1.15)
50%	$ (19,631)	$ (0.80)
71%	$ (11,094)	$ (0.51)

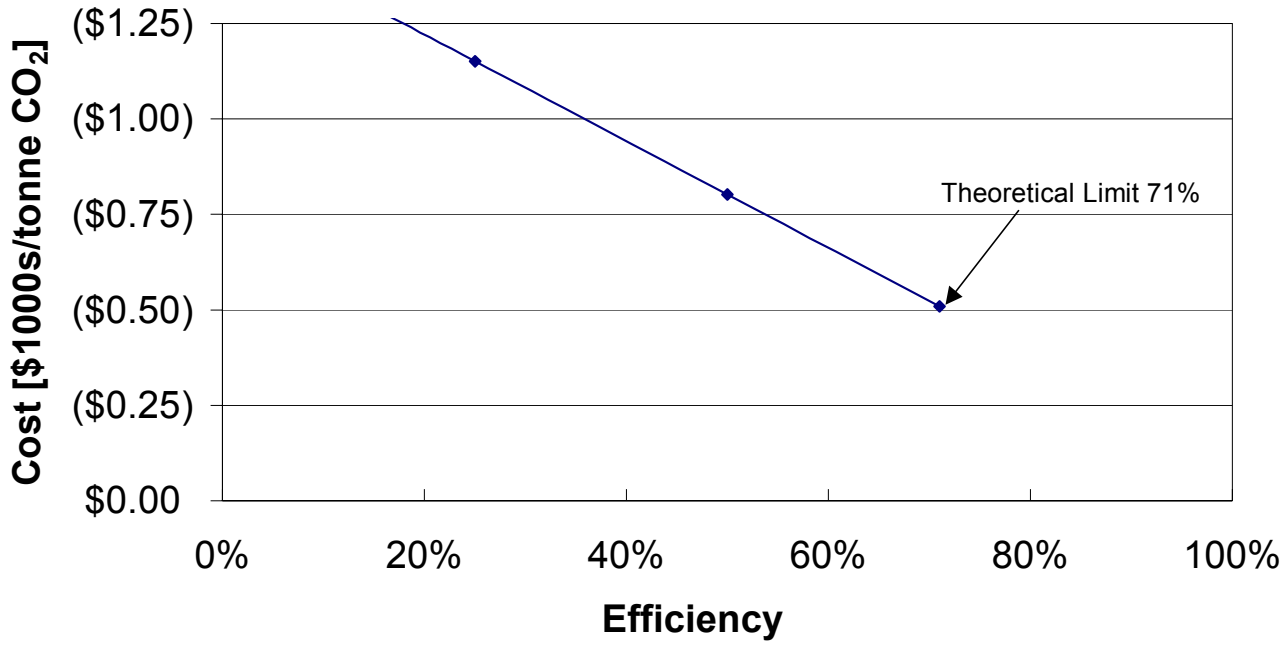

Figure 14. Cost per tonne of CO_2 vs. the Methane Displacement Efficiency

IV.D.2. Monitoring, Jurisdiction, Regulation, and Environmental Impact. With a limited number of permafrost injection and production wells, the input and discharge points of gases are well-defined. Figure 7 and accompanying discussion illustrates a typical "five-spot" injection/production scheme, which controls the gas escape in the system via the integrity of cap and basement reservoir rock and the well cement seals. The injected amount of CO_2 can be obtained through positive displacement (piston) compressors or via gas flow meters. The amount of produced gas can be obtained by flow metering, with chromatographic measurement of compositions of CH_4, CO_2, and other gases at the production wells.

However, the injection/production system will never be at steady state, so a mass balance (CO_2 in – CO_2 out) will not indicate CO_2 leakage. Using gas chromatography and pH meters, regular, periodic monitors should occur for CO_2 contents in the area above the reservoir and in groundwater aquifers. Reservoir CO_2 accumulations will only be known via discharge measurements or via assuming that CO_2 neither escapes nor enters the reservoir at points other than the wells.

The jurisdiction of EHBM in permafrost should be straightforward. Since permafrost depressurization will be the first hydrate production method, a free gas reservoir will contact the hydrates. When normal leases are obtained for the free gas, the associated hydrated gas may also be leased. Jurisdiction issues are much less certain in ocean environments but, as indicated earlier, it is unlikely that ocean methane hydrates will be either produced or displaced in the foreseeable future.

Regulation of CO_2 injection into existing permafrost hydrate reservoirs should be very similar to those for injecting CO_2 into depleted terrestrial hydrocarbon reservoirs. Since such reservoirs were once the natural containers of hydrocarbon gases, this storage technique has intuitive public appeal and is currently favored over other CO_2 storage. Additional governmental regulations such as Norway's CO_2 tax, or the possibility of carbon sequestration exchange credits could positively impact the EHBM economics.

However, the environmental impact of CO_2 injection into permafrost should be carefully considered from geological, chemical, or biological viewpoints. At the Colorado School of Mines, Harrison et al., (1993) have shown via thermodynamic calculations that CO_2 can either become carbonate rock, acidify the sea water, or become hydrates in deep oceans, as a function of the geological environment,. Two other, as yet unstudied considerations are: (a) melting the permafrost around the injection well due to heat of compression of CO_2, (b) acidification of aquifers may affect flora and fauna contacted by the water (see Caulfield et al., (1997) and Auerbach et al., (1997)). If EHBM is to be seriously considered, thermodynamic studies should be done to determine terrestrial outcomes similar to those predicted by Harrison et al. (1995) for ocean environments.

V. Conclusions and Recommendations

V.A. Conclusions

The conclusions are separated into the reported five segments:

1. Relative amounts of conventional natural gas and hydrated methane,
2. Most likely means of methane recovery from hydrates
3. Potential for fugitive emissions and geohazards from hydrates,
4. Estimate of the hydrate impact on carbon dioxide ocean sequestration, and
5. Potential for displacement of hydrated methane with carbon dioxide.

V.A.1. Relative Amounts of Conventional Natural Gas and Hydrated Methane,

- The worldwide estimates of methane in conventional reserves and in hydrate deposits are 164 TCM and 21,000 TCM respectively.

- The total amount of methane in sea floor hydrates is two orders of magnitude greater than the methane in permafrost hydrates; however deep ocean hydrates are much more dispersed over a wider area.

- The concentration of methane in the best-known permafrost hydrated deposit is maximized at 30% of the bulk volume in the hydrate stability region. In contrast the concentration of methane in the best-known ocean hydrated deposit is 3%. Such concentrations may typify local ocean and permafrost deposits.

- The gas in hydrates is almost pure methane, with few exceptions.

- Very high CO_2 content natural gases reserves are in four worldwide locations: (1) Pacific Rim, (2) Asia, (3) Eastern Europe, and (4) the former Soviet Union. These locations should be closely monitored for fugitive green house gas emission associated with normal gas production.

V.A.2. Potential for Methane Recovery from Hydrated Methane

- The first pilot demonstration of methane recovery from hydrate will likely be done by 2010 at a permafrost site such as the Mallik 2L-38 site in the Canadian Mackenzie Delta. Field methane recovery will be accomplished by depressurizing the free gas associated at subsurface depths between 130-2,000m, using the heat of the earth to provide the dissociation energy.

- The Messoyakha Field in the Siberian permafrost field is one case in which methane may have been recovered via depressurization of hydrates over a decade. Questions exist regarding the extent of hydrated methane contribution to gas production.

- Economics for permafrost hydrate production by depressurization are comparable to free gas production economics. Production by thermal stimulation and inhibitor injection are much more expensive. However, in many permafrost regions such as the Alaskan North Slope, high transportation costs control the economics of gas production from conventional and from hydrated reserves.

- Methane recovery from ocean hydrates will probably not be done until after 2050, due to two factors: (1) the dispersed nature of the ocean hydrate deposits and (2) the minimum ocean hydrate stability depth is greater than 500m of water, 100-1,100m below the seafloor, which prevents easy access.

V.A.3. Potential for fugitive emissions and geohazards from hydrates,

- The risk of methane evolution upon hydrate production in the permafrost is no greater than conventional gas production.

- As shown in Appendix C, in the ocean 70% of the hydrates are well away from the unstable condition. As a result, uncertainty in future global warming due to methane clathrate destabilization is less than the uncertainty due to future fossil fuel use.

- The hydrates most susceptible to climate dissociation are those in near shore Arctic oceans close to permafrost regions and, to a lesser extent, those in warmer, deeper oceans subject to eddy heating. The preliminary models indicate a small rate of methane evolution from permafrost shoreline hydrates with warming, but further studies are needed.

- In the Late Paleocene, 55.5 million years ago, methane from dissociated hydrates is hypothesized to account for a 8^{o}C warming in worldwide climates (see Appendix C). Such an event could not reoccur in the present era, due to deeper oceans.

- Hydrates in the deep ocean do present geohazards, but to an unknown extent. It is the concern for geohazards which will first unite the communities concerned with hydrates inside and outside the hydrocarbon pipeline.

V.A.4. Estimate of the hydrate impact on carbon dioxide ocean sequestration

- Ocean injection studies are moving away from concepts, models, and laboratory studies to field studies and pilot injections into the deep oceans. Such data are the most reliable for deep sea CO_2 stability predictions.

- If injected at depths less than 2600m liquid CO_2 will be buoyant and droplets nominally 1cm in diameter will rise at an approximate rate of 6m/min. A flexible hydrate film will cover the droplet-water interface, controlling the rate of CO_2 dissolution into sea water, slowing it by a factor of about 1.6-3.2. When the liquid CO_2 droplets rise to a depth of 200-300m they will vaporize and rapidly dissolve.

- CO_2 injected into ocean trenches at depths greater than 3700 m has the best chance of long-range stability, because the CO_2 density is greater than sea water and will form solid hydrates. The time for CO_2 hydrate dissolution from such a deep lake into stagnant sea water can be very long.

- Effects on the deep sea environment have been modeled, but no long term data are available to estimate the ecological effects of primary variables such as pH and the CO_2 partial pressure. The accumulation of long term stability and environmental data should be an area of active research.

V.A.5. Potential for Displacement of Hydrated Methane with Carbon Dioxide

- Enhanced Hydrate Bed Methane (EHBM) displacement by CO_2 is still in the conceptual stage. Each of four technical challenges should be fulfilled before the process can be realized: (1) large laboratory or pilot-scale experiments should indicate the viability of the method, (2) permafrost development of hydrate bed methane should provide a commercial foundation for EHBM, (3) an inexpensive CO_2 source must be located for the EHBM site, (4) a gathering, separation, and marketing system should be available for the product gases.

- There are a number of Japanese laboratory measurements showing marginal thermodynamic and kinetic feasibility at the preliminary level. A pilot plant will be built and operated in the period 2000-2002 in Japan. Until such large scale studies are available for the displacement process, reliable economics cannot be done.

- The EHBM process economics have an upper limit in the analogous process for the displacement of methane from coal beds by CO_2, (ECBM). The cost of EHBM may range between \$100 - \$1,360/tonne CO_2 sequestered.

- The overall exchange rate of CO_2 for hydrated CH_4 is likely to be 5-10% at best in the field, with the most economic scenario likely to be near US\$1,360/tonne CO_2 sequestered. EHBM is both theoretically limited and economically unsuitable, so this option is not likely to be used.

V.B.Recommendations

- Accurate worldwide compositional data should be obtained for four locations of high CO_2 gas content indicated in a preliminary way in this report: (1) the Pacific Rim (2) Asia (3) Eastern Europe and (4) the former Soviet Union.

- The natural hydrate resource must be characterized more accurately in terms of availability and producibility, to provide for applications in production, global climate change, or geohazards.

- There is an imminent need for a methane production demonstration via depressurization of permafrost hydrates associated with a free gas reservoir. Learning about methane recovery from permafrost hydrates will provide a foundation for the future ocean recovery.

- The technology is not yet available for methane recovery from ocean hydrates, and technical breakthroughs are needed.

- More accurate evaluations are needed to assess methane hydrate evolution and climate effects at continental permafrost margins.

- More accurate assessments are needed for geohazards associated with hydrates.

- The impact of MBARI CO_2 ocean injection experiments should be evaluated for pilot studies for CO_2 injection in the ocean, such as the planned 2001 international experiment for CO_2 sequestration off the Hawaiian Coast.

- Long-term studies are required for evaluation of the thermodynamic, kinetic, and environmental effects of CO_2 sequestration in the ocean.

- Large scale laboratory and pilot scale experiments in Japan should be monitored for CO_2 displacement of CH_4 in hydrates.

Appendix A. Gas Hydrate Structures, Properties, and Kinetics

The following discussion is excerpted from the monograph by Sloan (1998, Chapters 2 and 3), to which the reader may wish to turn for a more complete explanation. Two hydrate conference summaries (Sloan et al., 1994; Monfort 1996) also provide research and applied perspectives of the hydrate community.

Gas clathrates are crystalline compounds which occur when water forms a cage-like structure around smaller guest molecules. While they are more commonly called hydrates, a careful distinction should be made between these non-stoichiometric clathrate hydrates of gas and other stoichiometric hydrate compounds which occur for example, when water combines with various salts.

Gas hydrates of current interest are composed of water and the following eight molecules: methane, ethane, propane, isobutane, normal butane, nitrogen, carbon dioxide, and hydrogen sulfide. Yet other apolar components between the sizes of argon (3.5 Å) and ethylcyclohexane (9Å) can form hydrates. Hydrate formation is a possibility where water exists in the vicinity of such molecules at temperatures above and below 32^{o}F. Hydrate discovery is credited in 1810 to Sir Humphrey Davy. Due to their crystalline, non-flowing nature, hydrates first became of interest to the hydrocarbon industry in 1934, the time they first were observed blocking pipelines. Hydrates concentrate hydrocarbons: 1 ft^3 of hydrates may contain 180 SCF of gas.

Hydrates normally form in one of three repeating crystal structures shown in Figure A.1. Structure I (sI), a body-centered cubic structure forms with small natural gas molecules found *in situ* in deep oceans. Structure II (sII), a diamond lattice within a cubic framework, forms when natural gases or oils contain molecules larger than ethane but smaller than pentane. sII represents hydrates which commonly occur in hydrocarbon production and processing conditions, as well as in many cases of gas seeps from faults in ocean environments.

The newest hydrate structure H (sH) named for its hexagonal framework, has cavities large enough to contain molecules the size of common components of naphtha and gasoline. Some initial physical properties, phase equilibrium data, and models have been determined for sH and one instance of *in situ* sH in the Gulf of Mexico has been found. Since information on structure H is in the fledgling stages, and since it may not occur commonly in natural systems, most of this appendix concerns sI and sII.

A.1. Hydrate Crystal Structures.

Table A.1 provides a hydrate structure summary for the three hydrate unit crystals (sI, sII, and sH) shown in Figure A.1. The crystals structures are given with reference to the water skeleton, composed of a basic "building block" cavity which has twelve faces with five sides per face, given the abbreviation 5^{12}. By linking the vertices of 5^{12} cavities one obtains sI; linking the faces of 5^{12} cavities results in sII; in sH a layer of linked 5^{12} cavities provide connections.

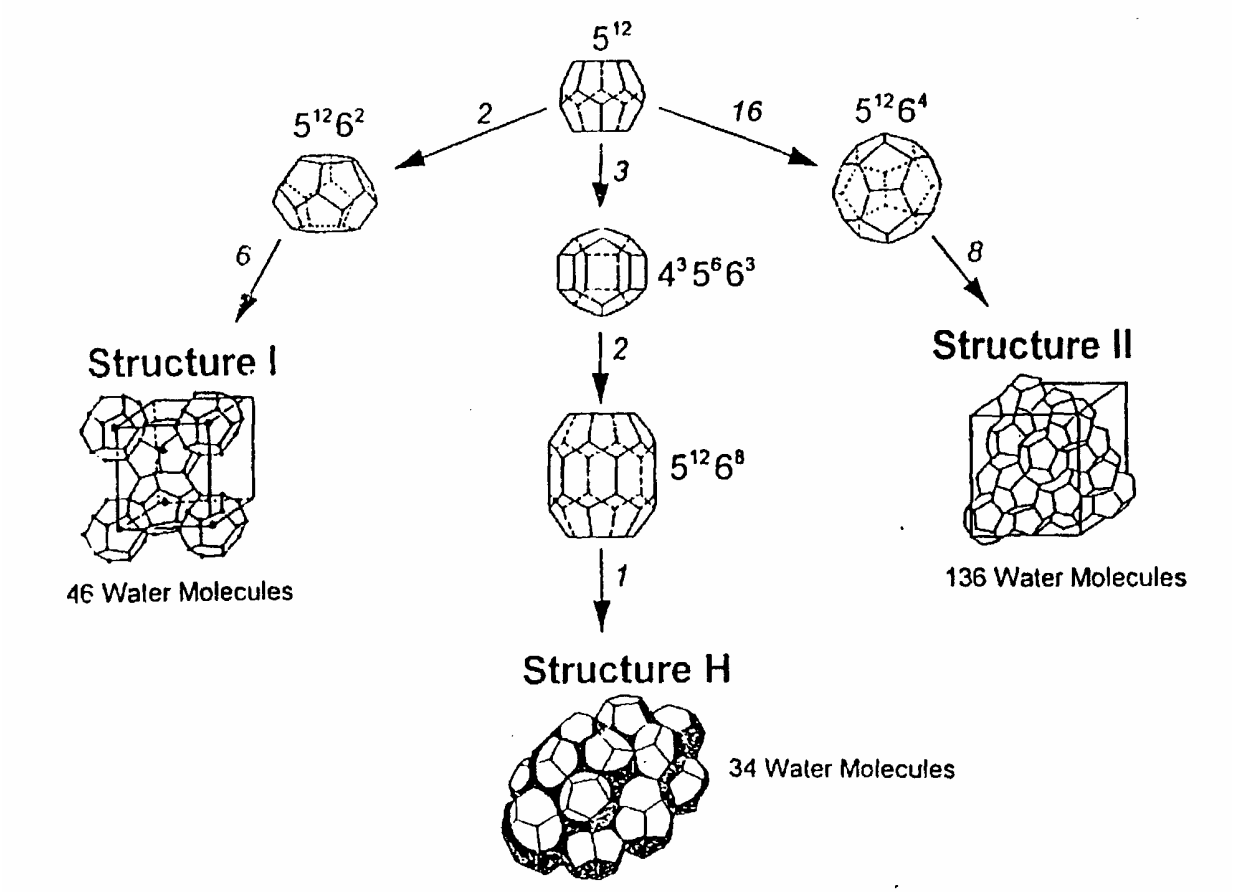

Figure A-1: Three Hydrate Unit Crystals and Constituent Cavities (from Sloan, 1998)

Spaces between the 5^{12} cavities are larger cavities, which contain twelve pentagonal faces and either two, four, or eight hexagonal faces: (denoted as $5^{12}6^2$ in sI, $5^{12}6^4$ in sII, or $5^{12}6^8$ in sH). In addition sH has a cavity with square, pentagonal, and hexagonal faces ($4^3 5^6 6^3$). Figure A.1 depicts the five cavities of sI, sII, and sH. In Figure

A.1 an oxygen atom is located at the vertex of each angle in the cavities; the lines represent hydrogen bonds with which one chemically-bonded hydrogen connects to an oxygen on a neighbor water molecule.

Table A.1 Geometry of Cages in Three Hydrate Crystal Structures in Figure A.1

Hydrate Crystal Structure	I		II		H		
Cavity	Small	Large	Small	Large	Small	Medium	Large
Description	5^{12}	$5^{12}6^2$	5^{12}	$5^{12}6^4$	5^{12}	$4^35^66^3$	$5^{12}6^8$
Number of Cavities/Unit Cell	2	6	16	8	3	2	1
Average Cavity Radius, Å	3.95	4.33	3.91	4.73	3.91[3]	4.06[3]	5.71[3]
Variation in Radius[1], %	3.4	14.4	5.5	1.73	Not Available		
Coordination Number[2]	20	24	20	28	20	20	36
Number of Waters/Unit Cell	46		136		34		

1. Variation in distance of oxygen atoms from center of cage.
2. Number of oxygens at the periphery of each cavity.
3. Estimates of structure H cavities from geometric models

Inside each cavity resides a maximum of one of the small guest molecules, typified by the eight guests associated with 46 water molecules in sI ($2[5^{12}]\bullet6[5^{12}6^2]\bullet46H_2O$), indicating two guests in the 5^{12} and 6 guests in the $5^{12}6^2$ cavities of sI. Similar formulas for sII and sH are ($16[5^{12}]\bullet8[5^{12}6^4]\bullet136H_2O$) and ($3[512]\bullet2[4^35^66^3]\bullet1[5^{12}6^8]\bullet34H_2O$) respectively.

Structure I, a body-centered cubic structure, forms with natural gases containing molecules smaller than propane; consequently sI hydrates are found *in situ* in deep oceans with biogenic gases containing mostly methane, carbon dioxide, and hydrogen sulfide. Structure II, a diamond lattice within a cubic framework, forms when natural gases or oils contain molecules larger than ethane; sII represents hydrates from most natural gas systems gases. Finally structure H hydrates must have a small occupant (like methane, nitrogen, or carbon dioxide) for the 5^{12} and $4^35^66^3$ cages but the molecules in the $5^{12}6^8$ cage can be as large as 0.9 Å (e.g. ethylcyclohexane). Structure H has not been commonly determined in natural gas systems to date.

A.2. Properties Derive from Crystal Structures.

A.2.a. Mechanical Properties of Hydrates. As may be calculated via Table A.1, if all the cages of each structure are filled, all three known hydrates have the amazing property of being approximately 85% (mol) water and 15% gas. The fact that the water content is so high suggests that the mechanical properties of the three hydrate structures should be similar to those of ice. This conclusion is true to a first approximation as shown in Table A.2, with the exception of thermal conductivity and thermal expansivity. Many sH mechanical properties of have not been measured.

Table A.2 Comparison of Properties of Ice and sI and sII Hydrates

Property	Ice	Structure I	Structure II
Spectroscopic			
Crystallographic Unit Cell			
Space Group	$P6_3/mmc$	Pm3n	Fd3m
No. H_2O molecules	4	46	136
Lattice Parameters at 273K	a =4.52 c =7.36	12.0	17.3
Dielectric Constant at 273 K	94	~58	58
Far infrared spectrum	Peak at 229 cm^{-1}.	Peak at 229 cm^{-1} with others	
H_2O Diffusion Correl Time, (μsec)	220	240	25
H_2O Diffusion Activ. Energy(kJ/m)	58.1	50	50
Mechanical Property			
Isothermal Young's modulus at 268 K (10^9 Pa)	9.5	8.4^{est}	8.2^{est}
Poisson's Ratio	0.33	~0.33	~0.33
Bulk Modulus (272 K)	8.8	5.6	NA
Shear Modulus (272 K)	3.9	2.4	NA
VelocityRatio(Comp/Shear):272K	1.88	1.95	NA
Thermodynamic Property			
Linear. Therm. Expn: 200K (K^{-1})	$56x10^{-6}$	$77x10^{-6}$	$52x10^{-6}$
AdiabBulkCompress:273K(10^{-11}Pa)	12	14^{est}	14^{est}
Speed Long Sound:273K(km/sec)	3.8	3.3	3.6
Transport			
Thermal Condctivity:263K(W/m-K)	2.23	0.49±.02	0.51±.02

A.2.b. Guest: Cavity Size Ratio: a Basis for Property Understanding. The hydrate cavity occupied is a function of the size ratio of the guest molecule within the cavity. To a first approximation, the concept of "a ball fitting within a ball" is a key to understanding many hydrate properties. Figure A.2 may be used to illustrate five points regarding the guest:cavity size ratio for hydrates formed of a single guest component in sI or sII.

1. The sizes of stabilizing guest molecules range between 3.5 and 7.5 Å. Below 3.5Å molecules will not stabilize sI and above 7.5 Å molecules will not stabilize sII.
2. Some molecules are too large to fit the smaller cavities of each structure (e.g. C_2H_6 fits in the $5^{12}6^2$ of sI; or i-C_4H_{10} fits the $5^{12}6^4$ of sII).
3. Other molecules such as CH_4 and N_2 are small enough to enter both cavities (5^{12}+$5^{12}6^2$ in sI or 5^{12}+$5^{12}6^4$ in sII) when hydrate is formed of single components.
4. The largest molecules of a gas mixture usually determines the structure formed. For example, because propane and i-butane are present in many natural gases, they will cause sII to form. In such cases, methane will distribute in both cavities of sII and ethane will enter only the $5^{12}6^4$ cavity of sII.
5. Molecule sizes which are close to the hatched lines separating cavity sizes exhibit the most non-stoichiometry, due to their inability to fit securely within the cavity.

Table A.3 shows the size ratio of several common gas molecules within each of the four cavities of sI and sII. Note that a size ratio (guest molecule: cavity) of approximately 0.9 is necessary for stability of a simple hydrate, given by the superscript "^{g}". When the size ratio exceeds unity, the molecule will not fit within the cavity and the structure will not form. When the ratio is significantly less than 0.9 the molecule cannot lend significant stability to the cavity.

Table A.3 Ratios of Guest: Cavity Diameters for Natural Gas Hydrate Formers

		(Molecular Diameter) / (Cavity Diameter)			
		Structure I		Structure II	
	Cavity Type=>	5^{12}	$5^{12}6^2$	5^{12}	$5^{12}6^4$
Molecule	Guest Dmtr (Å)				
N_2	4.1	0.804	0.700	0.817^g	0.616^g
CH_4	4.36	0.855^g	0.744^g	0.868	0.655
H_2S	4.58	0.898^g	0.782^g	0.912	0.687
CO_2	5.12	1.00	0.834^g	1.02	0.769
C_2H_6	5.5	1.08	0.939^g	1.10	0.826
C_3H_8	6.28	1.23	1.07	1.25	0.943^g
i-C_4H_{10}	6.5	1.27	1.11	1.29	0.976^g
n-C_4H_{10}	7.1	1.39	1.21	1.41	1.07

"^{g}" indicates the cavity occupied by the simple hydrate former

As seen in Table A.3, ethane as a single gas forms in the $5^{12}6^2$ cavity in sI, because ethane is too large for the small 5^{12} cavities in either structure and too small to give much stability to the large $5^{12}6^4$ cavity in sII. Similarly propane is too large to

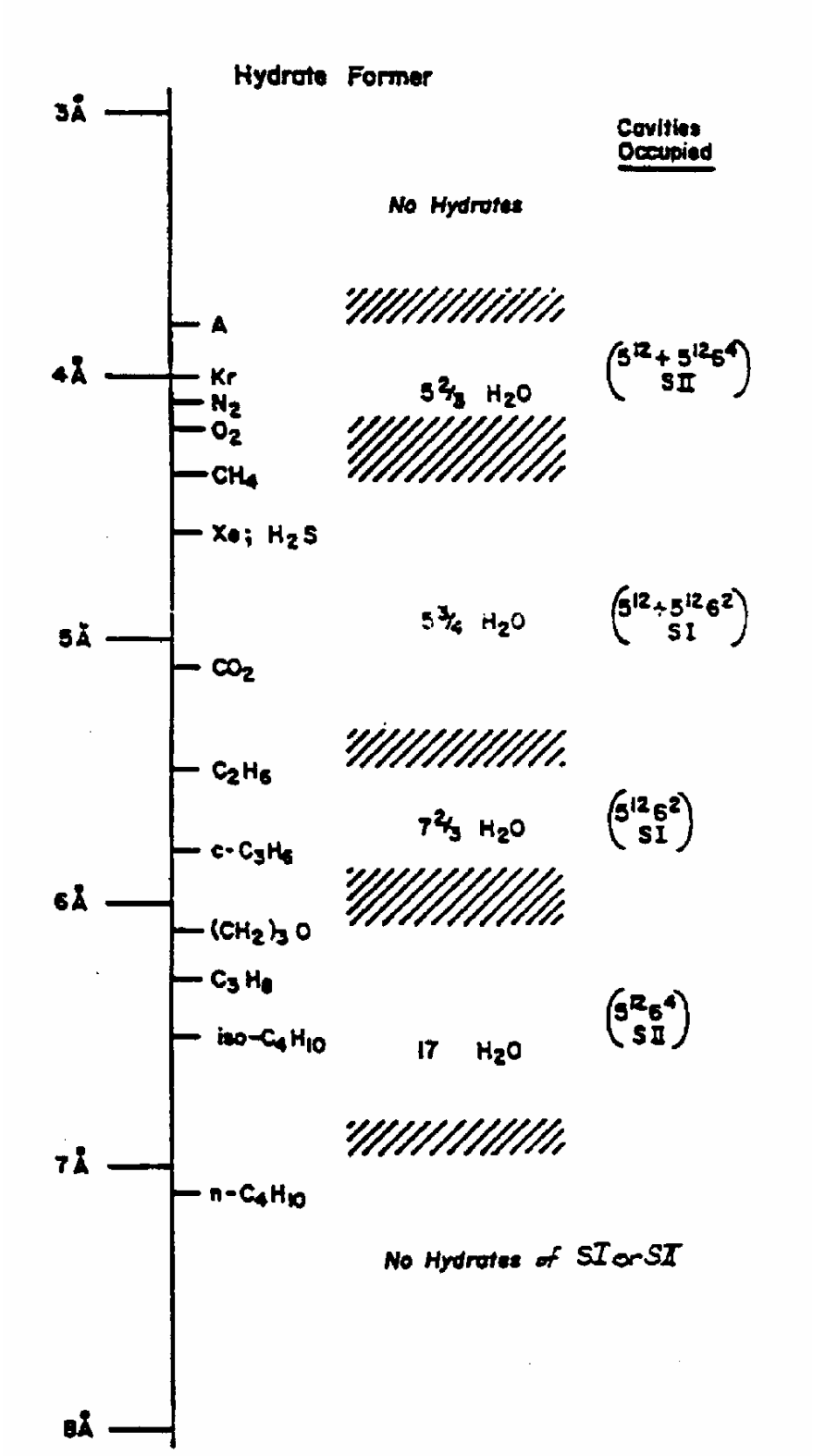

Figure A-2: Relative Sizes of Hydrate Guest and Host Cavities (from Sloan, 1998)

fit any cavity except the $5^{12}6^4$ cavity in sII, so that gases of pure propane form sII hydrates from free water. On the other hand, methane's size is sufficient to lend stability to the 5^{12} cavity in either sI or sII, with a preference for sI, because CH_4 lends slightly higher stability to the $5^{12}6^2$ cavity in sI than the $5^{12}6^4$ cavity in sII.

A.2.c. Phase Equilibrium Properties. In Figure A.3 pressure is plotted against temperature with gas composition as a parameter, for methane+propane mixtures. Consider a gas of any given composition (marked 0 through 100% propane) on a line in Figure A.3. At conditions to the right of the line, a gas of that composition will exist in equilibrium with liquid water. As the temperature is reduced (or as the pressure is increased) hydrates form from gas and liquid water at the line, so three phases (liquid water + hydrates + gas) will be in equilibrium. With further reduction of temperature (or increase in pressure) the fluid phase which is not in excess (water in pipeline environments) will be exhausted, so that to the left of the line the hydrate will exist with the excess phase (gas).

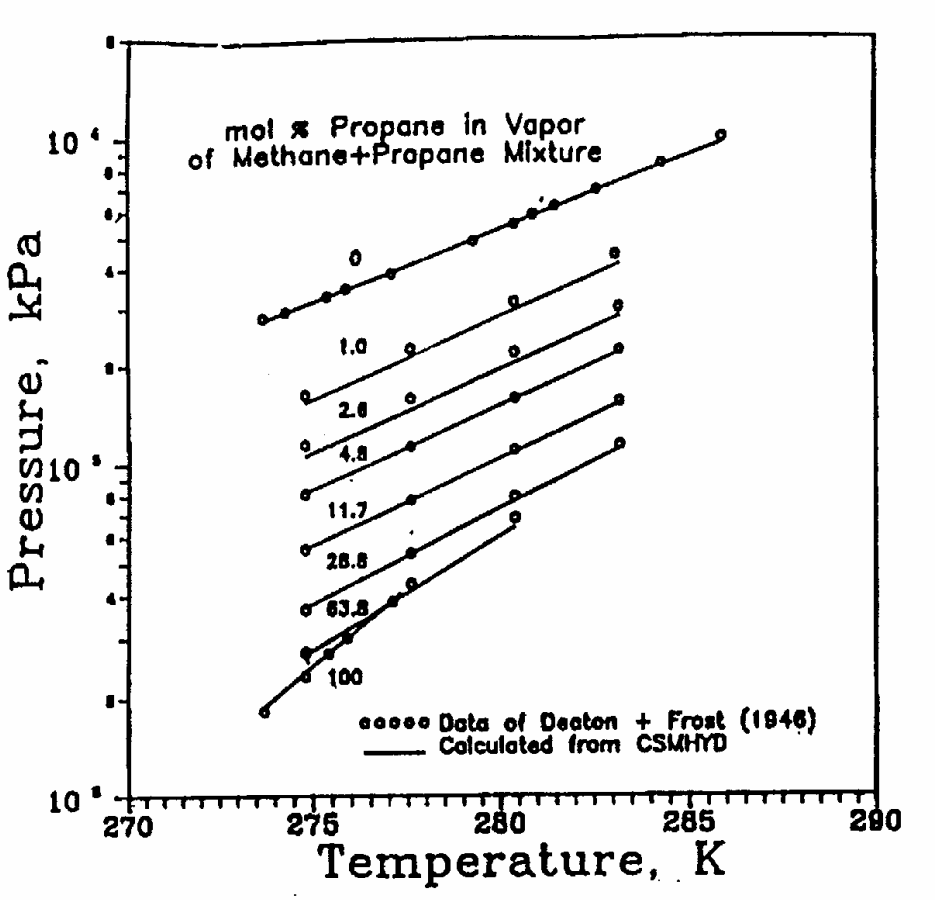

Figure A-3: Three-Phase (Lw-H-V) Equilibria of Methane+Propane Mixtures

All of the conditions given in Figure A.3 are for temperatures above 273K and pressures along the lines vary exponentially with temperature. Put explicitly, hydrate stability at the three-phase (L_W-H-V) condition is always much more sensitive to

temperature than to pressure. Figure A.3 also illustrates the dramatic effect of gas composition on hydrate stability; as any amount of propane is added to methane the structure changes (sI → sII) to a hydrate with much wider stability conditions. Note that a 50% decrease in pressure is needed to form sII hydrates, when as little as 1% propane is in the gas phase.

Any discussion of hydrate dissociation would be incomplete without indicating that hydrates provide the most industrially useful instance of statistical thermodynamics prediction of phase equilibria, which was formulated after the determination of sI and sII structures shown in Figure A.1. With the model, one may predict the three-phase pressure or temperature of hydrate formation, by knowing the gas composition. For further detailed discussion the reader is referred to Sloan (1998, Chapter 5).

A.2.d. Heat of Dissociation. The heat of dissociation (ΔH_d) may be considered to be the heat (rigorously, enthalpy change) required to dissociate hydrates to a vapor and aqueous liquid, with values given below at temperatures just above the ice point. For sI and sII, to a fair engineering approximation (±10%) ΔH_d depends mostly on crystal hydrogen bonds, but also the cavity occupied within a wide range of component sizes.

Enthalpies of dissociation may be determined via the univariant slopes of phase equilibrium lines (ln P vs. 1/T) in previous paragraphs, using the Clausius-Clapeyron relation [$\Delta H_d = -zR\ d(\ln P)/d(1/T)$]. As one illustration, simple hydrates of C_3H_8 or i-C_4H_{10} have similar ΔH_d of 129,000 and 133,000 KJ/(kgmol gas) because they both occupy $5^{12}6^4$ cavities, although their guest:cavity size ratios differ (0.943 and 0.976).

As a second illustration, similar slopes of lines in Figure A.3 show that mixtures of CH_4 + C_3H_8 have a value of ΔH_d = 79,000 KJ/(kgmol gas) over wide ranges of composition, wherein C_3H_8 occupies most of the $5^{12}6^4$ cavities, while CH_4 occupies a small number of $5^{12}6^4$ and many 5^{12}. Figure A.4 shows similar line slopes (and thus ΔH_d values) for binary mixtures of methane when the large guest is changed from C_3H_8, to i-C_4H_{10}, to n-C_4H_{10}. Since natural gases almost always contain such components, ΔH_d = 79,000 KJ/(kgmol gas) is valid for most natural gas hydrates.

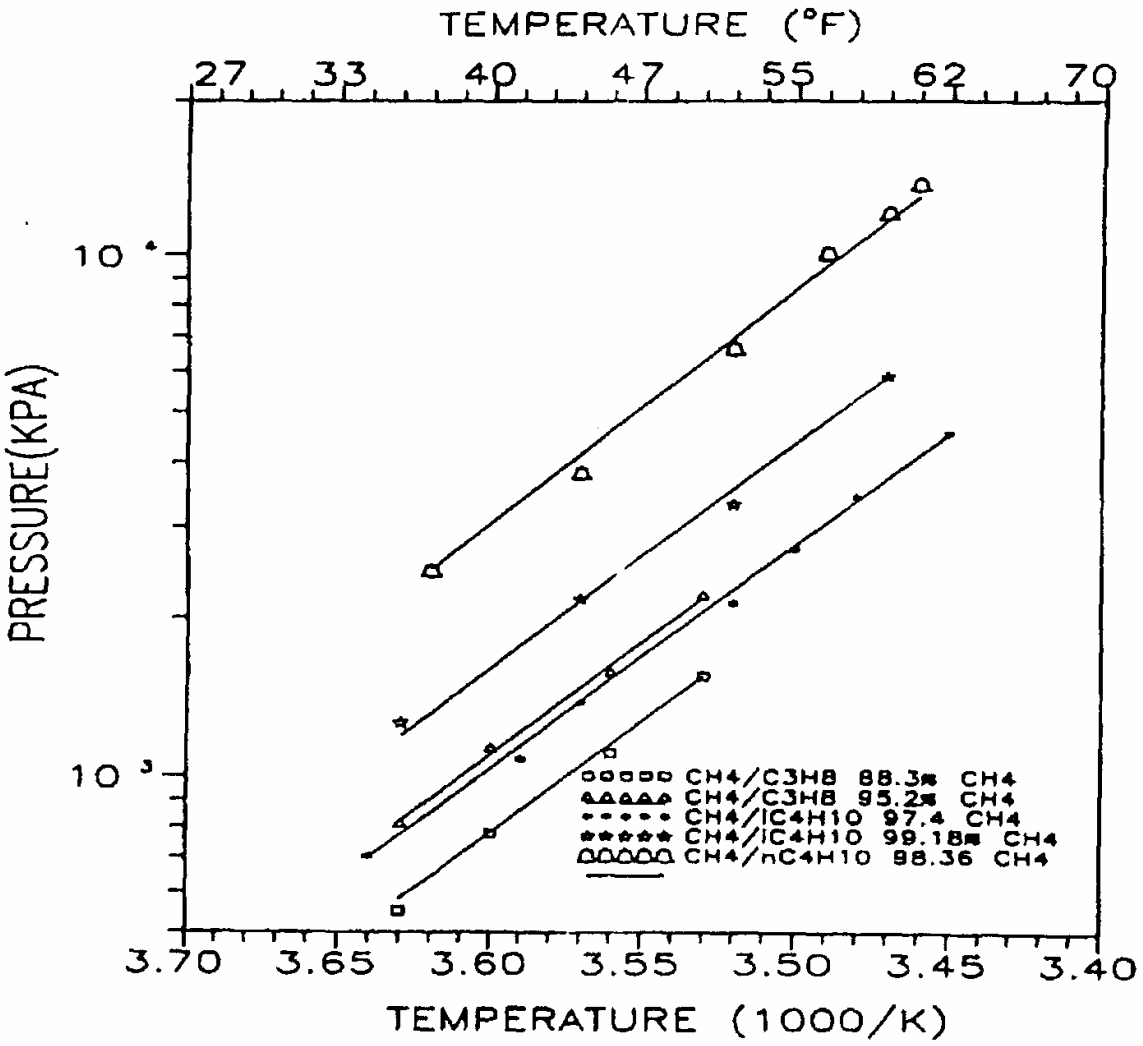

Figure A-4: Three-Phase Diagram (Lw-H-V) Equilibria of Methane + (Propane and Two Butanes) (from Sloan, 1998)

A.3. Formation Kinetics Relate to Hydrate Crystal Structures.

The answer to the questions, "What are hydrates?" and “Under what condition do hydrates form?” in the previous sections is much more certain than answers to "How do hydrates form?". We don’t know how hydrates form, but we can make some educated guesses about kinetics. The mechanism and rate (i.e. the kinetics) of hydrate formation are controversial topics at the forefront of current research.

The kinetics of hydrate formation are clearly divided into three parts: (a) nucleation of a critical crystal radius, (b) growth of the solid crystal, and (c) the transport of components to the growing solid-liquid interface. All three kinetic components are under study, but an acceptable model for any has yet to be found.

A.3.a. Conceptual Picture of Hydrate Growth. In a conceptual picture, this laboratory proposed that clusters at the water-gas interface may grow to achieve a critical radius as shown schematically in Figure A.5, by the following steps:

1. When natural gases dissolve in water there is conclusive evidence that water molecules organize themselves to maximize hydrogen bonding around each apolar molecule. The resulting liquid clusters resemble the solid hydrate cavities of Figure A.1. These fluid clusters are envisioned to join other clusters as the beginning of the hydrate crystallization process.
2. Figure A.5 indicates an autocatalytic reaction mechanism hypothesized for hydrate formation based upon limited experimental evidence. The figure depicts the progress of molecular species from water [A], through metastable species [B] and [C], to stable nuclei [D] which can grow to large species.
3. At the beginning of the process (point A), hydrogen-bonded liquid water and gas are present in the system. Water clusters around gas molecules to form both large and small clusters [B] similar to the hydrate cages of sI and sII. At point [B], the cages are termed "labile" - they are relatively long-lived but unstable.
4. The cages may either dissipate or grow to hydrate unit cells or agglomerations of unit cells [C], thus forming metastable nuclei. Since these metastable unit cells at [C] are of subcritical size, they may either grow or shrink in a stochastic process. The metastable nuclei are in quasi-equilibrium with the liquid-like cages until the nuclei reach a critical radius. After attaining the critical radius [D], the crystals grow rapidly in a period sometimes called catastrophic growth.
5. In our conceptual picture, when the system is heated, it is driven to the left in Figure A.5, and stable hydrate crystals are dissociated. Once the hydrate dissociation point is reached and passed, there are still labile microscopic species in the water that range in size from multiple hydrate unit cells [C] to metastable nuclei [B]. These residual structures are present up to a certain level of thermal energy above dissociation. At temperatures below that upper boundary, these species causes a decrease in induction or metastability time of a successive run, because the "building blocks" of crystals remain in the liquid. However, once about 40ºC is passed, no residual structure remains to promote hydrate formation.

The above cluster model conceptual picture is most likely to occur at the interface, either in the liquid or the vapor side. The reader should note that the above is a largely unproven hypothesis, whose only justification is to serve as a mental picture for qualitative predictions and future corrections.

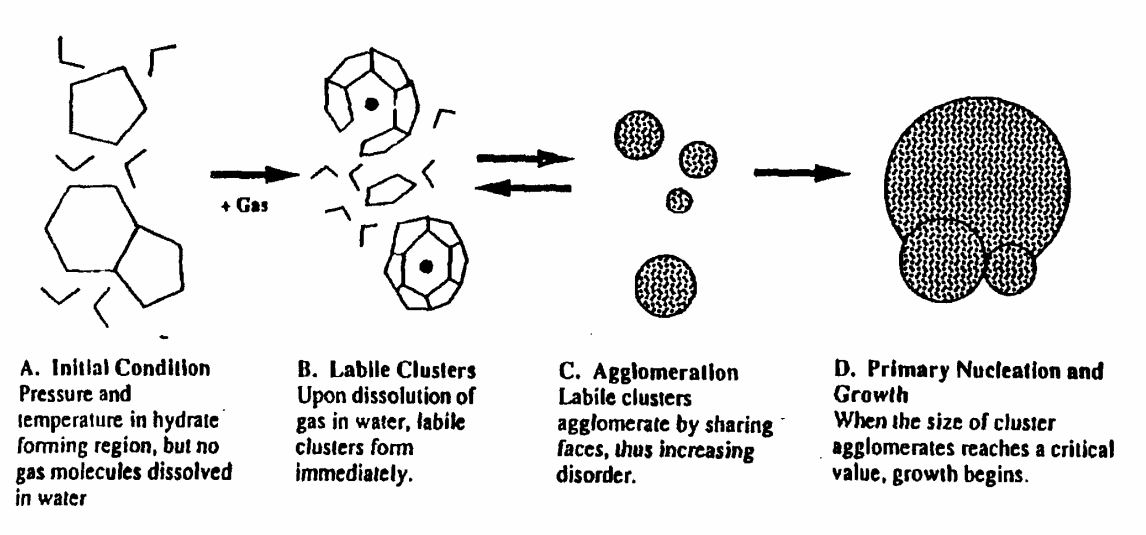

Figure A-5: Schematic Model of Hydrate Cluster Growth (from Sloan, 1998)

In contrast to well-determined thermodynamic properties, kinetic characterization of hydrates is very ill-determined. The following unsettling facts act as a state-of-the-art summary:

- Hydrate nucleation is both heterogeneous and stochastic, and therefore is only approachable by very approximate models. Most hydrate nucleation models assume homogeneous nucleation and typically cannot fit more than 80% of the data generated in the laboratory of the modeller.
- Hydrate growth kinetics are apparatus-dependent; the results from one laboratory are not transferable to another laboratory or field situation.
- In both kinetics and thermodynamics the hydrate phase is almost never measured.
- The hydrate dissociation models derived from solid moving-boundary differential equations do not account for the porous, surface formation, and occlusion nature of hydrates on a macroscopic scale.
- No satisfactory kinetic model currently exists for formation or dissociation. Due to the unsatisfactory state of hydrate kinetics knowledge, this area is the subject of intensive research at the present.

Appendix B. Two Hydrate Recovery Sites and the Messoyaka Depressurization Case

B.1: Permafrost Hydrates: the Mallik 2L-38 Well.

This material was excerpted from the detailed monograph, Scientific Results from JAPEX/JNOC/GSC Mallik 2L-38 gas Hydrate Research Well, MacKenzie Delta, Northwest Territories, Canada, Dallimore, S.R., Uchida, T., and T.S. Collett, Eds., Geological Survey of Canada Bulletin 544, (1999). This work contains 19 papers reviewing Mallik cores, 15 papers on core properties, 5 papers on downhole geophysics, and three papers providing the implications of the Mallik hydrate occurrence.

Mallik 2L-38 on Richards Island in the Mackenzie Delta of Canada was drilled to a depth of 1150m specifically for hydrates by the Japan National Oil Corporation (JNOC) and the Canadian Geological Survey (GSC). The well, completed on March 30, 1998, had the first confirmed hydrate samples collected beneath the permafrost in the world.

Gas hydrate occurred primarily in sand sediments with a porosity of 32-45% and in gravel with a lower porosity of 23-29%. An impermeable ($2x10^{-19}$ to $2x10^{-21}$ m^2) silt occurred at the top of the hydrate region (897 to 926m) suggesting that it acts as an impermeable seal. The log data confirm that hydrate occurred in four major and six minor intervals in the region (897-1110m) which were below the permafrost (640m). There was a thin 1.5m free gas zone from 1108.4 to 1109.8m at the base of the hydrate, which might impact the chance to produce via depressurization.

The well methane was highest in the hydrate zone. A high proportion of thermogenic gases was suggested by three markers: (1) methane carbon isotopes of $\delta^{13}C_1 = -43‰$, (2) ratios of $iC_4/nC_4 <1$, (3) ratios of $iC_5/nC_5 >10$. Gas hydrate was visually observed as mainly fine grained (<2mm), filing the intergranular pores and/or coating mineral grains. Rare thin veins (1-2mm) and nodules of hydrate (<0.5mm) were observed in sands and the largest piece of gas hydrate (~2cm) formed the matrix of a granular sand. The bulk of the gas hydrate samples were structure I methane (>98%), with small quantities (<1.2%) of carbon dioxide and propane, but no conclusive evidence of structure II hydrate was determined via diffraction, spectroscopy, or calorimetry. Gas hydrate bearing sands had shear strengths three to nine times greater than those without gas hydrates.

A summation of the hydrate interval is as follows:

1. In the hydrate depths of 897 – 1110m the temperature ranges from 7°C to 14°C.
2. The gas was mostly methane forming structure I hydrate.
3. The average sediment porosity was 34%.
4. The average gas hydrate concentration is 64%.
5. A thin (1.5m) free gas zone underlay 10 distributed hydrate deposits.
6. The Mallik methane accumulation in hydrate is estimated at $110\times10^9 m^3$ total, or about $4.15\times10^9 m^3$ in a 1 km^2 area surrounding the Mallik 2L-38 drill site.

7. Four significant gas hydrate accumulations are characterized in and around the Mallik well area, with a total amount of trapped gas hydrate estimated at 187.2×10^9 m^3 of methane.
8. Modeling of Mallik has shown it unlikely that methane will naturally evolve from hydrates in amounts to affect climate change. Over 13,300 years the hydrate stability field will only rise 70m, considered to be a relatively insignificant amount with a small rate of methane release.

B.2. Oceanic Hydrates: Leg 164 Three Wells in the Blake-Bahama Ridge

This discussion is exerpted from Leg 164 Scientific Party Report Edited by Paull, Matsumoto, and Wallace (1996). The Ocean Drilling Program (ODP) Leg 164, represented a drilling effort in late 1995 to understand the amounts of gas associated with the famous Blake-Bahama Ridge bottom simulating reflector (BSR) which was known since the late 1960's. Samples indicating the presence of hydrates were obtained earlier in this BSR vicinity at Deep Sea Drilling Project (DSDP) Leg 11, Site 102, 103 and Leg 76, Site 553. Figure 5a (in the main report body) gives the location of earlier sites, as well as those of Leg 164 (Sites 991 through 997).

On ODP Leg 164, three sites were drilled below the base of hydrate stability over a short distance (9.6 km) in the same stratigraphic interval. Figure 5b shows the three Leg 164 holes: Site 994 without a BSR, Site 995 with a weak BSR, and Site 997 with a strong BSR on the ridge crest. Site 996 was drilled some distance away from the BSR, to investigate migration in a fault zone where methane was leaking from the rise.

Common Hydrate Indicators. At all three sites, six indirect indicators were found: (1) large gas exsolution from cores, (2) high methane sediment concentration, (3) acoustic data, (4) low interstitial-water chlorinity, (5) low core temperatures recovered on the catwalk of the ship, and (6) P-wave velocity logs and resistivity logs.

The similarity of the hydrate indicators in the three sites is exemplified by the chlorinity anomalies in the hydrate regions of Figure B.1. There is a minimum of ~1.4vol%, 1.7% and 2.1% gas hydrate at Sites 994, 995, and 997, respectively assuming a low chlorinity baseline, and a sediment porosity of 50%. The amount of gas hydrate appears to increase from the ridge flank (Site 994) to the ridge crest (Site 997) with various indicators shown in Table B.1.

Table B.1. Fraction of Bulk Sediment as Hydrates at Leg 164 Sites

Detection Means	Bulk Hydrate Vol
Chlorinity	1-2% (minimum) as high as 12%
Log Suite	8%
Acoustic VSP	6-7%

At all three Sites there was significant direct and indirect evidence to indicate the base of the hydrate to be at 450 ± 10 mbsf. However there was a discrepancy between hydrates signals and the phase boundary. The temperature gradient indicated that the boundary should have been significantly lower (at 490-570 m) than observed.

Paull et al. (1997) cited four possible reasons for the above discrepancy:

1. The inferred base is a fossil depth reflecting conditions during a previous sea level stand or bottom water temperature regime.
2. Experimental (P-T) data do not adequately characterize hydrates, particularly in fine-grained sediments. Clennell et al. (1996) used surface effects to explain this discrepancy.
3. Gas hydrate existed below 450±10 mbsf, but was undetected.
4. The hydrate depth is limited by the gas supply.

In all samples there was a large (10% vol) amount of gas below the hydrates and as much as 50% water, so three phases were present in all cases. However, most of the hydrates were recovered in disseminated form - that is they had decomposed by the time the core barrel reached the deck. In two instances (Sites 994 and 997) samples of hydrates were recovered.

B.3. Messoyakha: A Case Study in Depressurization and Inhibitor Injection. The Messoyakha gas hydrate field is the only available exemplar for gas production from hydrate, although the extent of the hydrate contribution has recently been questioned by Collett and Ginsburg (1998) . Hydrates were produced from this field semi-continuously for over 17 years. The field is located in the north-east of western Siberia, close to the junction of the Messoyakha River and the Yenisei River, 250 km west of the town of Norilsk, as shown in Figure B-1.

Figure B-2 provides a cross-section of the field, showing the hydrate deposit overlying the free gas zone. The depth-temperature plot of Figure B-3 from Sheshukov (1972) shows the hydrate layer to extend to the intersection of the 281 K geotherm. The gas in the hydrate zone is both in the free and in the hydrated state. Makogon (1988b) provided summary information regarding the properties of the field, as abbreviated in Table B-1.

The Messoyakha field has been produced through both inhibitor injection and depressurization, as well as combinations of the two. The inhibitor injection tests, presented in Table B-2 from the combined results by Sumetz (1974) and Makogon (1981, p.174), frequently gave dramatic short-term increases in production rates, due to hydrate dissociation in the vicinity of each injected well bore. The figures in the table are the results of methanol and mixtures of methanol and calcium chloride were injected under pressure, using a "cement aggregate." For long-term dissociation of hydrates, depressurization was used.

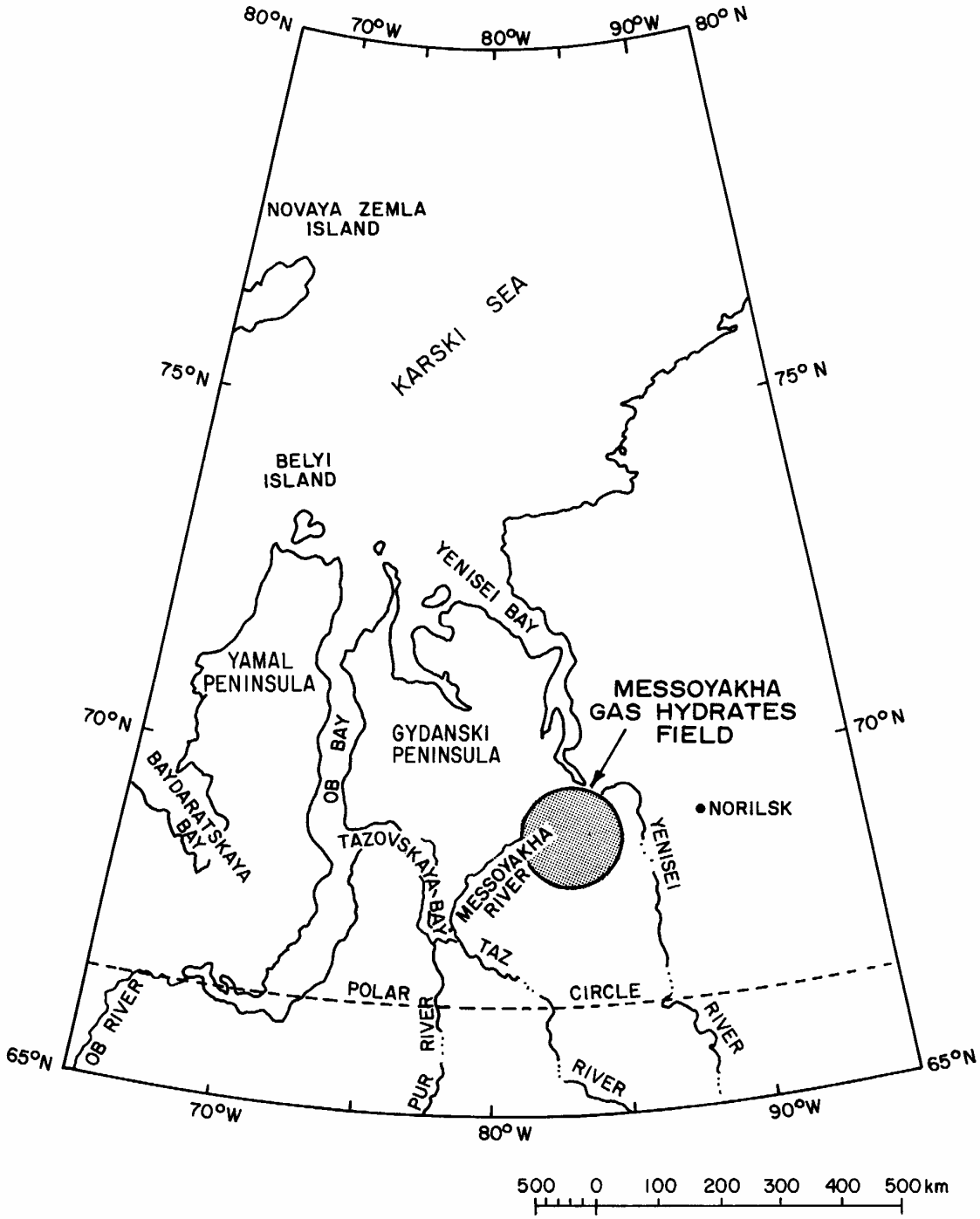

Figure B-1. Messoyakha Field Location (from Krason and Ciesnik, 1985)

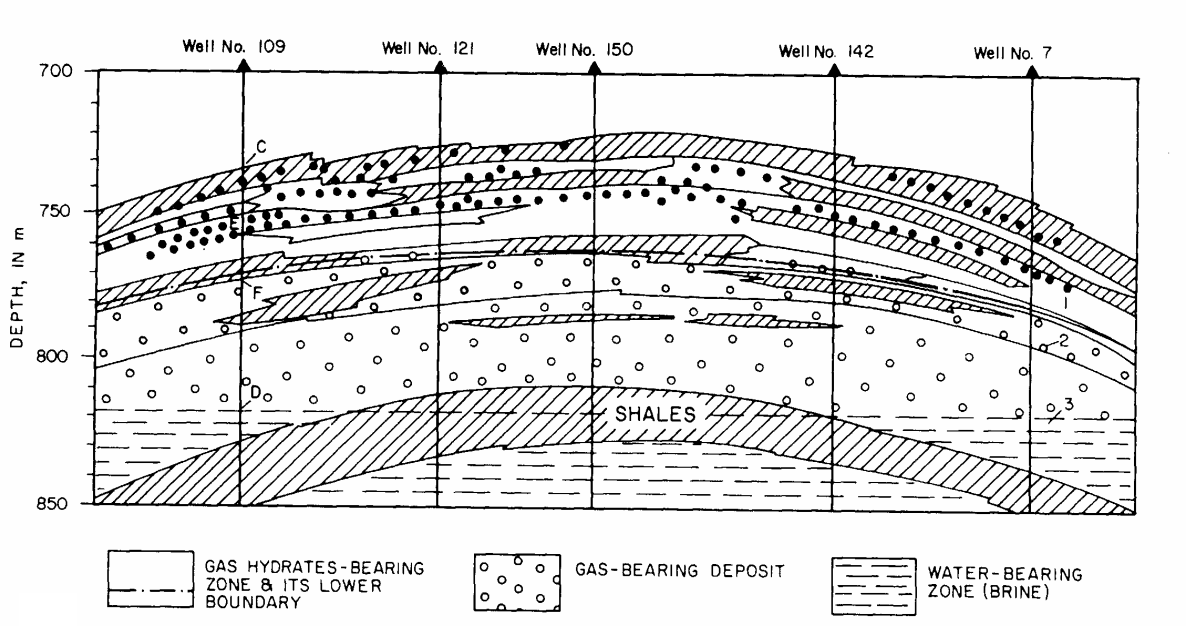

Figure B-2. Cross Section of Messoyakha Gas Hydrate Field Showing Placement of Hydrates (from Makogon, 1988)

Table B-1 Properties of Messoyakha Gas Hydrate Field (after Makogon, 1988b)

Area of the pay zone,	12.5 km^2
Thickness of the pay zone	84 m
Open porosity	16-38% (average 25%)
Residual water saturation	29-50% (average 40%)
Initial reservoir pressure	7.8 MPa
Reservoir temperature range	281 - 285 K
Reservoir water salinity	< 1.5 wt%
Water-free gas composition	98.6% CH_4
	0. 1% C_2H_6
	0. 1% $C_3H_8^+$
	0.5% CO_2
	0.7% N_2

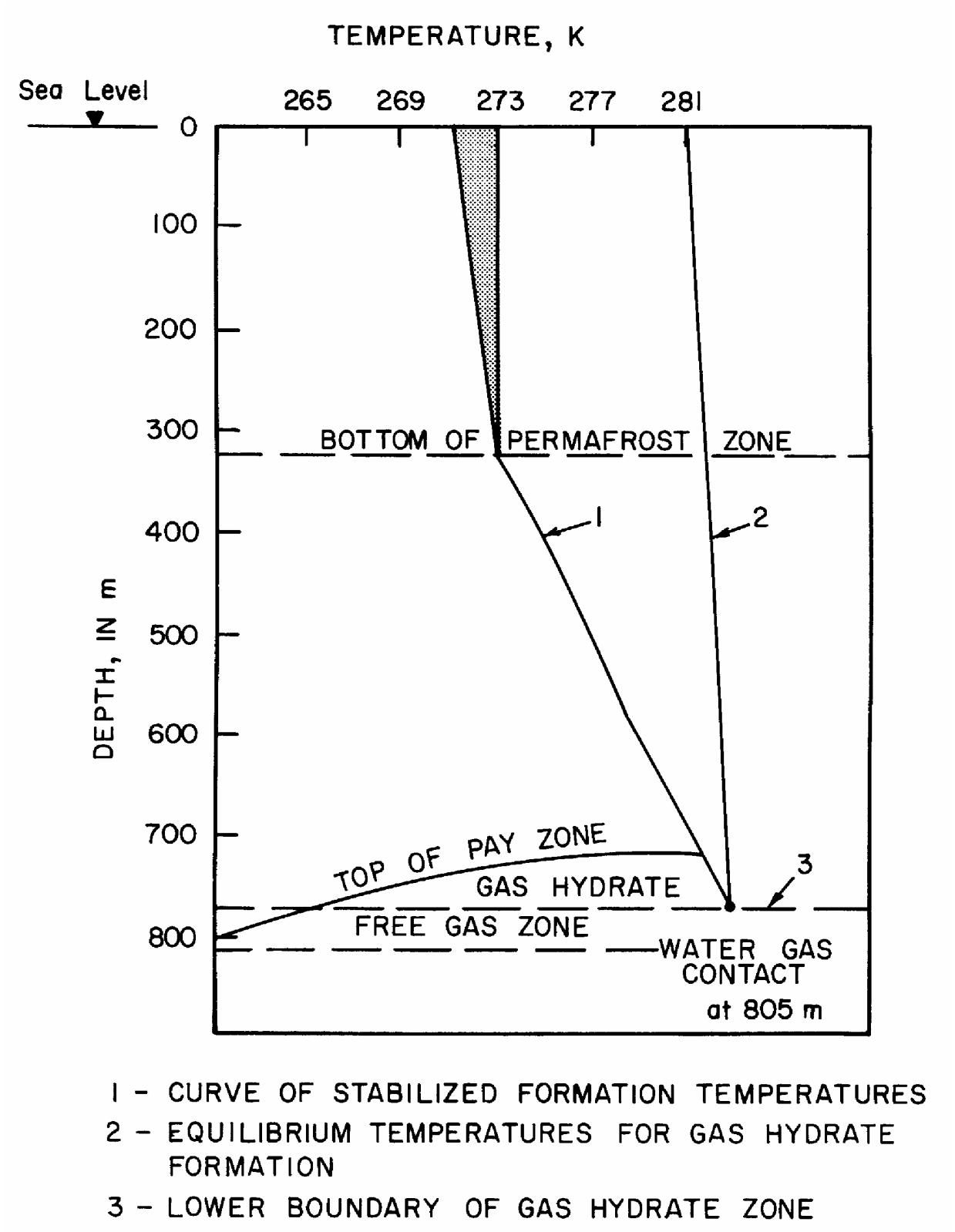

Figure B-3. Messoyakha Hydrate Stability Zone with Phase Boundary and Geothermal Gradient (from Sheshukov, 1972)

Table B-2. Test Results from Inhibitor Injection in the Messoyakha Field (from Sumetz, 1974 and Makogon, 1981, p. 174)

Well No.	Type of Inhibitor	Volume of Inhibitor	Gas Flow Before Treatment	Gas Flow After Treatment
		m^3	1000 m^3 /day	1000 m^3 /day
2	96 wt% methanol	3.5	Expected results Not Achieved	
129	96 wt% methanol	3.5	30	150
131	96 wt% methanol	3.0	175	275
133	methanol	unknown	25	50
			50	50
			100	150
			150	200
138	Mixture 10% MeOH 90 vol% of 30 wt% $CaCl_2$	4.8	200	300
139	Mix of Well 138	2.8		
141	Mix of Well 138	4.8	150	200
142	methanol	unknown	5	50
			10	100
			25	150
			50	200

Makogon (1988b) indicates that of all the complex studies obtained during the 19 years of the production life of the Messoyakha field, the most informative results came from an analysis of the reservoir pressure change as a function of the gas withdrawal rate. A diagram showing pressure and gas production as a function of time is shown in Figure B-4, with the accompanying pressure-temperature relationship in Figures B-5a,b. While Figure B-5a may represent the measured pressure-temperature values (Makogon, 1988b) far away from the hydrate, Poettmann (1988) suggested that the values in the neighborhood of the hydrate interface are better represented by Figure B-5b, for reasons given below. The combination of these three figures represents the only example in slow depressurization, done via the production of the free gas reservoir over a period of years.

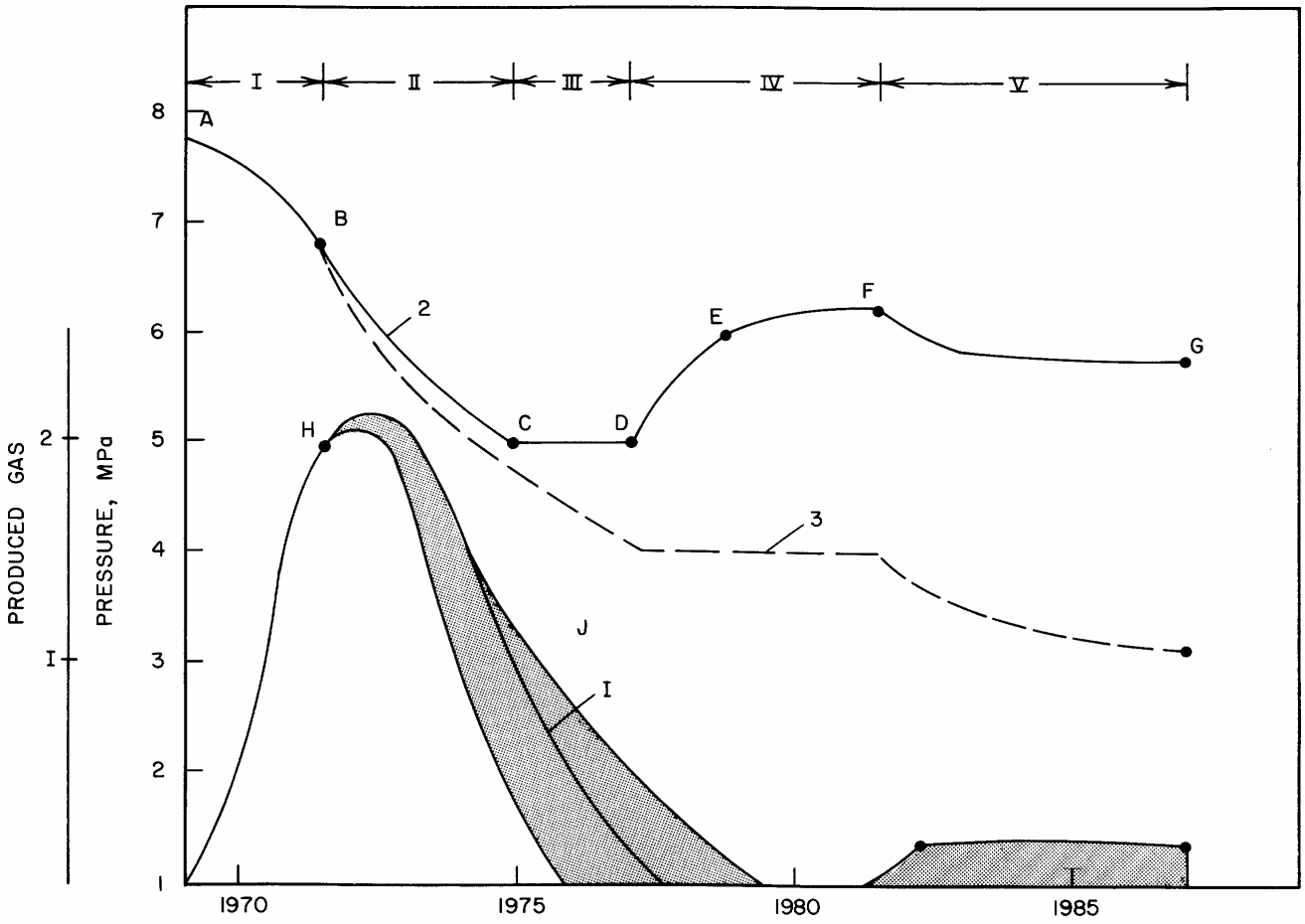

Figure B-4. Gas Produced from Hydrates at Messoyakha (Gray regions) During 1970 - 1985. (Makogon 1988b)

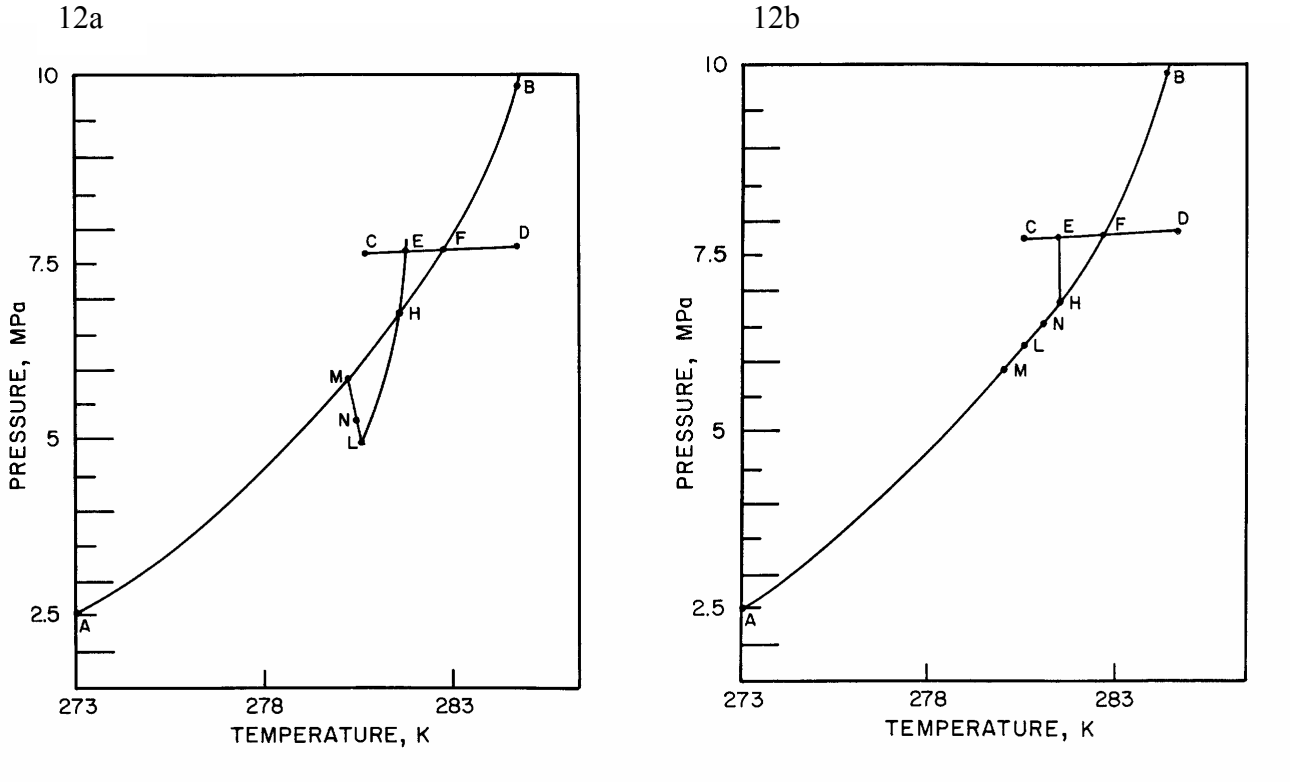

Figure B-5. Pressure-Temperature Curves During the Hydrate Dissociation Shown in Figure B-4. (a) away from the hydrate face, and (b) at the hydrate face.

In Figures B-5a,b, the following initial points are used: AB = hydrate equilibrium line; C = temperature at the top of the pay zone; D = temperature at a level of gas and water contact; E average gas-hydrate temperature; F = temperature at boundary surface between gas and gas-hydrate reserves; H = beginning dissociation pressure for gas hydrates.

As the production of the field was begun from 1969 to mid-1971, the pressure decreased from E to just above the hydrate dissociation point at H in Figures B-4, and B-5a,b. During this period only free gas was produced because the pressure was above the hydrate equilibrium value.

When the pressure reached the hydrate equilibrium value at point H, the hydrates began to dissociate, adding the shaded portion to the gas production curve at the lower half of Figure B-4. The top half of Figure B-4 shows the reservoir pressure was maintained at a higher value (solid line 2) than the expected pressure (dashed line 3) due to the addition of gas to the reservoir by the hydrates. After Point H in Figure B-5a, Makogon (1988a) indicated that the pressure away from the hydrate decreased below the equilibrium value, with a slight decrease in temperature. The pressure at the hydrate interface in Figure B-5b however, should not deviate from the equilibrium line, unless all hydrates were dissociated. Consequently, the pressure and temperature at the hydrate

interface decreased along the equilibrium curve as the reservoir was depressurized. Between the third and sixth year of the field development, there was probably a pressure drop between the hydrate interface, from H to L in Figure B-5b, and the measured pressure from H to L in Figure B-5a, due to the flow of gas in porous media.

As the Messoyakha reservoir attained the pressure at point L, the average pressure stabilized for two years to point M, indicating that the volume of gas recovered was replenished by the gas liberated from the hydrate. The difference between curves I and J in Figure B-4 indicates that the total free gas produced (curve I) was slightly less than the gas liberated (curve J) including the hydrates. During this period, from the seventh to the eight year of the life of the reservoir, the pressure away from the hydrate face in Figure B-5a rose slightly (L→M), compensated by a corresponding pressure decrease at the hydrate face in Figure B-5b.

At point M. the reservoir was shut in, while other higher pressure reservoirs were produced (Makogon, 1988a). During that period, the average pressure of the reservoir began to rise from point M to point N in Figure B-5b. The difference between curves I and J in Figure B-4 indicates that gas continued to be liberated by the hydrate until the reservoir pressure was uniform at in mid-1981. As the average gas pressure approached the equilibrium value the amount of gas produced decreased exponentially. Makogon indicated that the temperature of the reservoir tended to be restored to its original value, after a period of time. The equilibrium pressure itself rose slightly as the high reservoir heat capacity increased the temperature of the hydrate mass.

Since 1982 there has only been a modest production of the Messoyakha reservoir. The total amount of gas liberated from hydrates thus far has amounted to 36% of the total gas withdrawn from the field. It is noted further that the position of the gas-water interface did not change over the seventeen year period of the production of the field.

It is generally accepted that gas hydrates did play some role in the production of the Messoyakha field. However, the question of whether hydrates contributed significantly to the total gas production was raised through a recent compilation of direct and indirect observations by Collett and Ginsburg (1998).

Appendix C. The Potential for Hydrate Effects on Modern and Ancient Climate Change

Hydrates have a potential to affect both modern and ancient climates. This appendix is bifurcated to discuss both potentials.

C.1. The Potential for Climate Change in the Modern Era. In a database summarizing the *in situ* recovered hydrate sample database, Booth et al. (1996) gave three important facts:

1. About 70% of the recovered hydrate samples were located at higher pressures or lower temperatures than the three-phase (L_W-H-V) boundary prediction. Evidence for this generalization is shown in a phase diagram on Figure C.1, which shows hydrate recovery locations and conditions in the shaded region of the more general Figure 3b. The result in Figure C.1 suggests that most *in situ* hydrate systems are in two-phase (L_W-H) equilibrium, wherein the gas phase is exhausted and the liquid phase (with dissolved methane) exists in equilibrium solely with hydrates.
2. The extreme of any hydrate equilibria condition is coincident with the three phase condition predicted using salt water.
3. Most recovered samples have been small, dispersed (even dissociated) particles with isolated examples of massive hydrates

The importance of the above facts can be assessed by a phase equilibrium calculation . Consider the case for the dissociation of a hydrate sample such as MAT Guatemala 2 (the uppermost point on Figure C.1) which is over 15^{o}C cooler than the three-phase boundary. Before the hydrate melts, it must be heated to the three phase boundary at constant pressure. At that point, any gas evolved from melted hydrates will likely exceed the low solubility, and form a free gas phase.

The hydrate and the surrounding media must have a considerable sensible heat input term ($\Delta H = m \times Cp \times \Delta T$, where H is enthalpy, m is mass, Cp is heat capacity, and ΔT is the temperature difference required to move the system to the three-phase boundary). The required heat input is more than the few degrees usually cited as a consequence of global warming or warming by an eddy from the Gulf (of Mexico) Stream. At the three phase boundary, hydrates melt at constant temperature and pressure as the heat of dissociation ($\Delta H = m \times \Delta H_d$) is input.

The above example stands in contrast to those anecdotal cases by MacDonald et al. (1994) who reported incidences of Gulf of Mexico hydrate dissociation over a short period. In those cases, hydrates formed from seeping gas at a fault; these hydrates were already at the three-phase boundary, so they could be dissociated by small heat input from the surrounding water.

On the other hand the hydrate samples found by MacDonald et al. at faults indicates that methane did not escape as rapidly as it would have if hydrates had not formed. In such cases it is clear that hydrates act as a trap/storage for venting methane, as well as a release of methane.

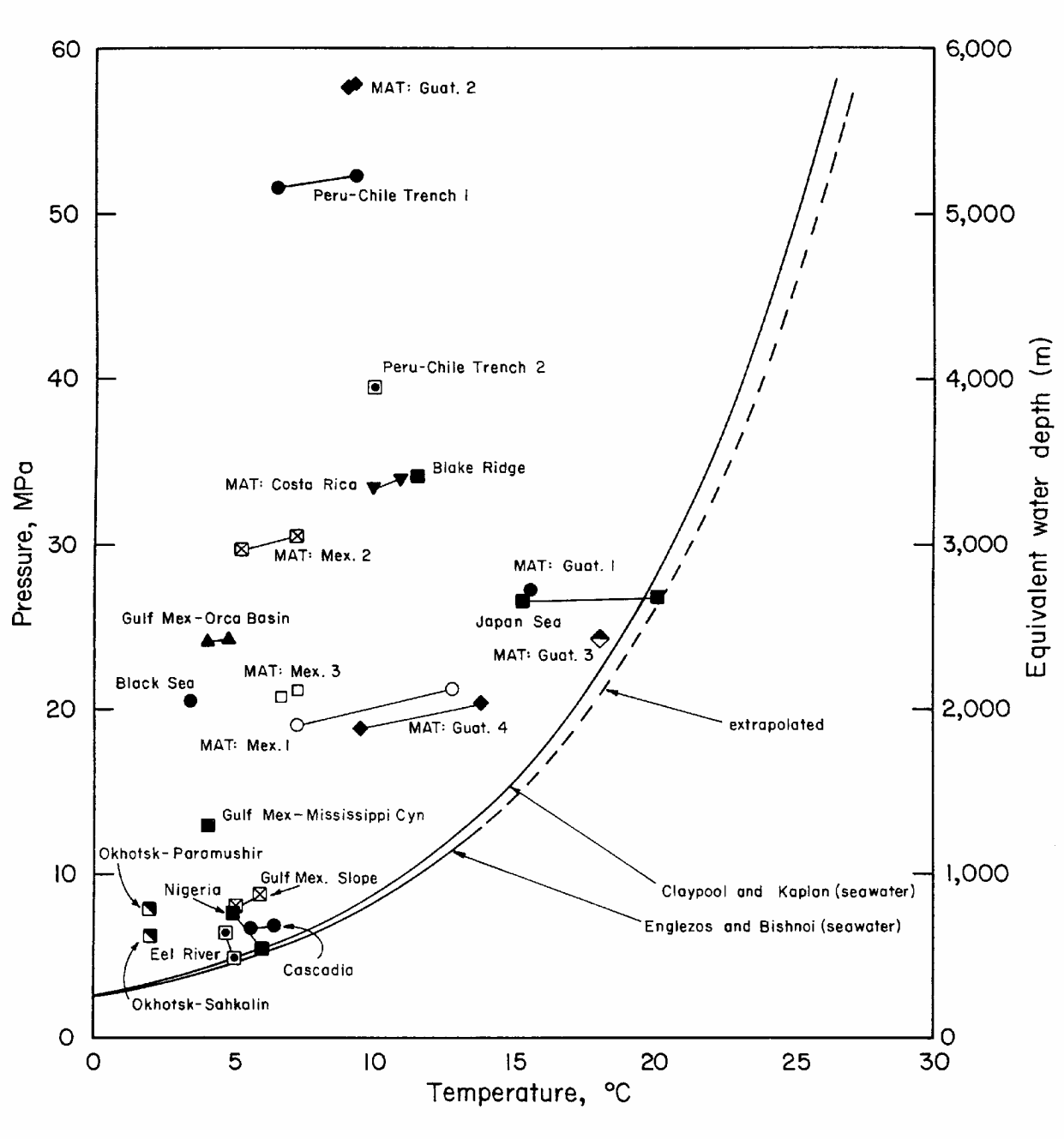

Figure C.1. Compilation of Hydrate Recovered Core Data Relative to Three-Phase Boundary (from Booth et al., 1996)

The original concern for hydrates as an input to the climate arose as a result of the review by Kvenvolden and McMenamin (1980), Shortly thereafter Bell (1982), Kvenvolden (1988b), MacDonald (1990a), and Nisbet (1989) expressed concern about methane release by *in situ* hydrates. In an alarmist perspective, Leggett (1990) noted

that, "the uncertainties are enormous and the stakes are probably higher than with any other potential feedback (mechanism)."

The original concerns for current release of methane from hydrates were highly speculative and have since been mitigated by many researchers. Makogon (1997) noted that if the sea temperature were $1^{o}C$ higher and if the geothermal gradient were increased by $1^{o}C/100m$, then up to 3×10^{9} m^3 of free methane can be released per km^2 of hydrate deposits. However, currently a consensus view that only small amounts of methane are being discharged from melting hydrates is held by researchers such as Fei (1991); Cranston (1994); Yakushev (1994); Kvenvolden et al., (1993a,b). Yet Brewer (1999) points out that hydrates are decomposing at the three-phase boundary which can be affected by small warming trends, such as at the shoreline in permafrost regions.

Kvenvolden (1988) pointed out that the amount of methane currently released and that to be released in the 21^{st} century is probably small; however, with the present knowledge base, it is not possible to predict the amount of methane being released as a result of permafrost degradation in the nearshore environment (to water depths of 100m). The primary concern is for degradation in the nearshore environment of the Arctic shelves, particular the huge Siberian shelf. Two dimensional modeling by Romanovskii and Tipenko, (1998) show that Russian hydrate zones are typically thin layers and probably need not be included in the model.

The most detailed mathematical models (with the fewest assumptions) have been done by Englezos (1992), Hatzikiriakos and Englezos (1993), and Harvey and Huang (1995). Both sets of modellers assume "worst case" conditions for methane release. The conclusions of Englezos and co-workers agree with the final conclusion from Harvey and Huang (1995):

> "Uncertainty in future global warming due to potential methane clathrate destabilization is thus smaller than the uncertainty due to future fossil fuel use or climate sensitivity."

Finally one must state that only models are available to assess the magnitude of modern hydrate methane emissions to the environment. There is general agreement that some hydrate dissociation is occurring at the three phase boundary, but the magnitude is unknown and assessed as small. Data are needed to determine the dimension of fugitive methane from hydrates.

C.2. The Potential for Ancient Climate Change. Dickens et al., (1995, 1997) and Kaiho et al., (1996) indicate that an ancient, massive ocean methane hydrate dissociation explains a $4\text{-}8^{o}C$ temperature rise over a brief geologic time interval (10^3 years) called the Late Palaeocene Thermal Maximum (LPTM) which occurred 55.5 million years ago. This is documented in deep ocean drilling samples as a prominent negative carbon isotope ($\delta^{13}C$ of $-2.5‰$) in all ocean sediments, in fossil tooth enamel, and in carbonates and organic sediments in terrestrial sequences. This $\delta^{13}C$ reduction in the ocean and the

recovery over the ensuing 200x 10^3 years (see Figure C.2a) is consistent with pronounced dissolution of calcium carbonate in the deep sea sediment deposited during the LPTM, shown in Figure C.2b.

The evolution of a large amount ($1.12x10^{18}$ g of CH_4) of methane from hydrates is the only plausible hypothesis which has been offered to explain this environmental perturbation. The abnormal $\delta^{13}C$ isotope indicates that source was external to the normal ocean-atmospheric-biomass carbon pool. Figure C.2c shows a rapid evolution of methane from hydrates, which is hypothesized to be oxidized to CO_2 greatly enriched in $\delta^{12}C$ (Dickens et al., 1995; Thomas and Shackleton, 1996)

Figure C.2d shows the hydrate equilibrium curve as a function of depth and temperature, in the ocean. Hydrates are only stable between equilibrium line and the original geotherm to the left of the curved line, at depths below the sediment surface, shown by the small vertical rectangle at A. If the ocean were warmed by 4^oC, the hydrates between the original geotherm and the equilibrium curve would melt, as the new geotherm was established. The warming from the original to the new geotherm would result in methane expulsion to the environment, where it would be oxidized to CO_2, resulting in significant further warming. It was hypothesized that the resulting CO_2 was re-absorbed by the ocean over the ensuing $200x10^3$ years.

Dickens (1999) cautions that a modern similar re-occurrence is prevented by much deeper oceans. However, the importance of the LPTM perturbation is that it is the only analog available in the geological record for understanding how the global carbon cycle and other systems related to a rapid, massive input of fossil fuel such as may be occurring in modern industrial times.

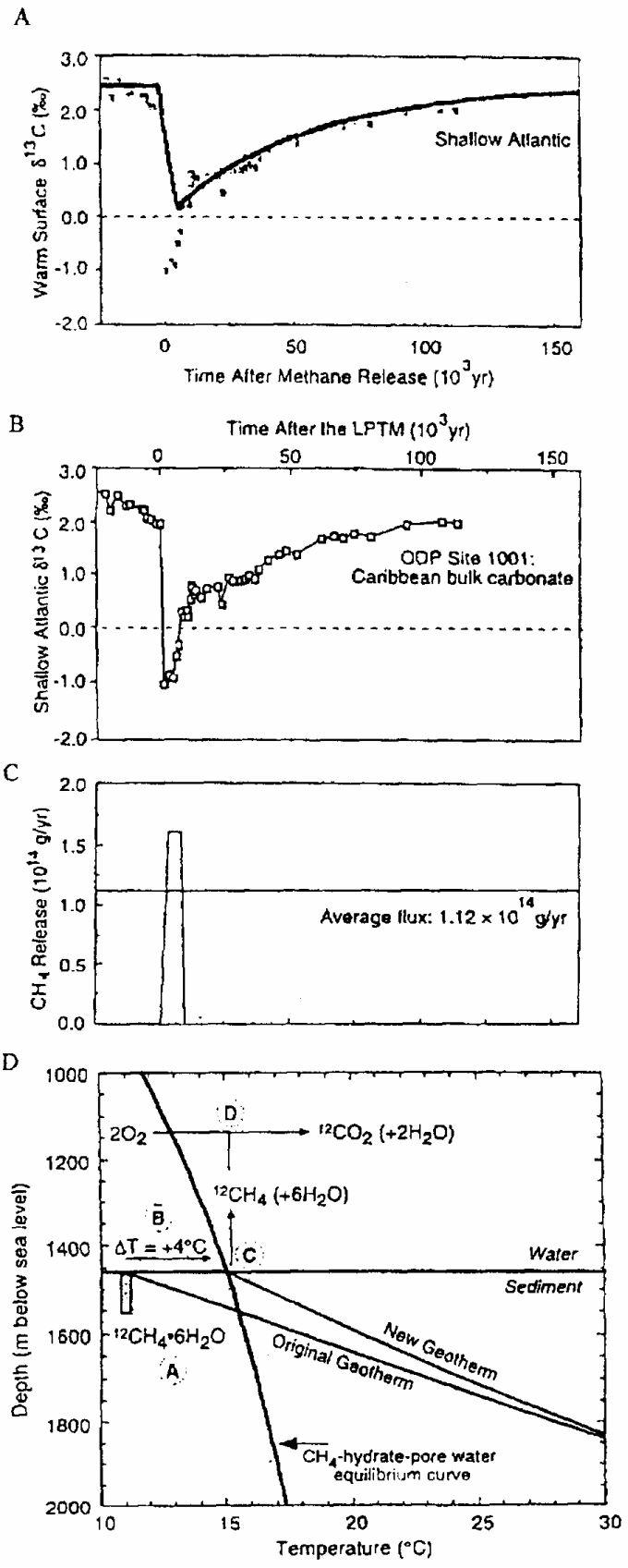
A
Warm Surface δ13C (‰)
Shallow Atlantic
Time After Methane Release (10^3 yr)
B
Time After the LPTM (10^3 yr)
Shallow Atlantic δ13 C (‰)
ODP Site 1001:
Caribbean bulk carbonate
C
CH4 Release (10^14 g/yr)
Average flux: 1.12 × 10^14 g/yr
D
2O2
12CO2 (+2H2O)
12CH4 (+6H2O)
ΔT = +4°C
Water
Sediment
12CH4•6H2O
New Geotherm
Original Geotherm
CH4-hydrate-pore water
equilibrium curve
Depth (m below sea level)
Temperature (°C)

Appendix D. Hydrates and the Ocean Sequestration of CO_2

This Appendix is organized by providing a general background for CO_2 sequestration in Section D.1, before giving a summary of CO_2 sequestration models in Section D.2. The physical phenomena which control CO_2 sequestration in hydrates are presented in Section D.3, to complement Section III which summarizes the *in situ* CO_2 ocean injection data. With data as a basis, Section D.4 provides a prediction for CO_2 injection in the ocean, completed by Section D.5, an economical analysis.

D.1. Background

Only a brief general background is given for CO_2 sequestration, in order to provide a setting. Readers interested in a more comprehensive summary may wish to consider the recent state-of-the-science summary by the U.S. Department of Energy (1999b), or the excellent summaries from the MIT Energy Laboratory (Herzog et al., 1997, Herzog 1999a,b).

Between August 1995 and October 1996 the IEA Greenhouse Gas R&D Programme sponsored a series of four workshops to address four aspects of ocean storage of CO_2: (1) Ocean Circulation and Sequestration Efficiency (Ormerod, 1996a), (2)Environmental Impact (Ormerod and Angel, 1996), (3) International Links and Concerns (Ormerod, 1996b), and (4) Practical and Experimental Approaches (Ormerod, 1997). The international experts made the ocean storage recommendations summarized for each workshop in Box D-1. Two other IEA Greenhouse Gas R&D Programme reports deal with ocean carbonate and CO_2 hydrate chemistry (Wong and Hirai, 1997) and ocean fertilization (Ormerod and Angel, 1998).

The IEA Greenhouse Gas R&D Programme provided ranges for worldwide storage locations (Ormerod, 1994), as shown in Table D-1. When the values in the table are contrasted with the annual world production of 22 billion tonnes of CO_2 from energy (Herzog et al, 1997) the storage capacities seem more than adequate.

Table D-1. Worldwide Storage Potential for CO_2

Storage Site	Capacity Range (billions of tonnes)
Deep Ocean	5,100 - > 100,000
Deep Aquifers	320 – 10,000
Depleted Gas Reservoirs	500 – 1,100
Depleted Oil Reservoirs	150-700

Currently, the public and political climates are more favorable for CO_2 injection into spent hydrocarbon reservoirs or in aquifers. However, the capacity of such aquifers and reservoirs is limited, and it is clear that the ocean represents the largest reservoir in which to store CO_2. The ocean is currently absorbing about 9 billion tonnes of CO_2 per year from the atmosphere so that the pH of typical surface ocean water will change from about 8.2 in the year 1800 to a pH of 7.78 in the year 2100 (Brewer, 1999).

The projected future atmospheric equilibrium CO_2 concentration will increase from its current level of about 350 ppm to about 1150 ppm after 3000 years (Hoffert et al., 1979). CO_2 ocean sequestration efforts can prevent peak atmospheric concentrations of 2800 ppm, before the decrease occurs toward equilibrium. Direct ocean injection of CO_2 will cause an additional pH decrease of only 0.1, principally because carbonate dissolved in benthic sediments and in sea water act as a buffer.

Two fundamental questions arise concerning the injection of CO_2 into the ocean: (1) How will the injection affect aquatic life? and (2) How long will the CO_2 remain sequestered? It is clear that the formation of CO_2 hydrates will have a positive affect on both questions, because hydrates are less transportable than vapor or liquid CO_2.

There are five principal scenarios for CO_2 sequestration in the ocean shown schematically in Figure D-1:

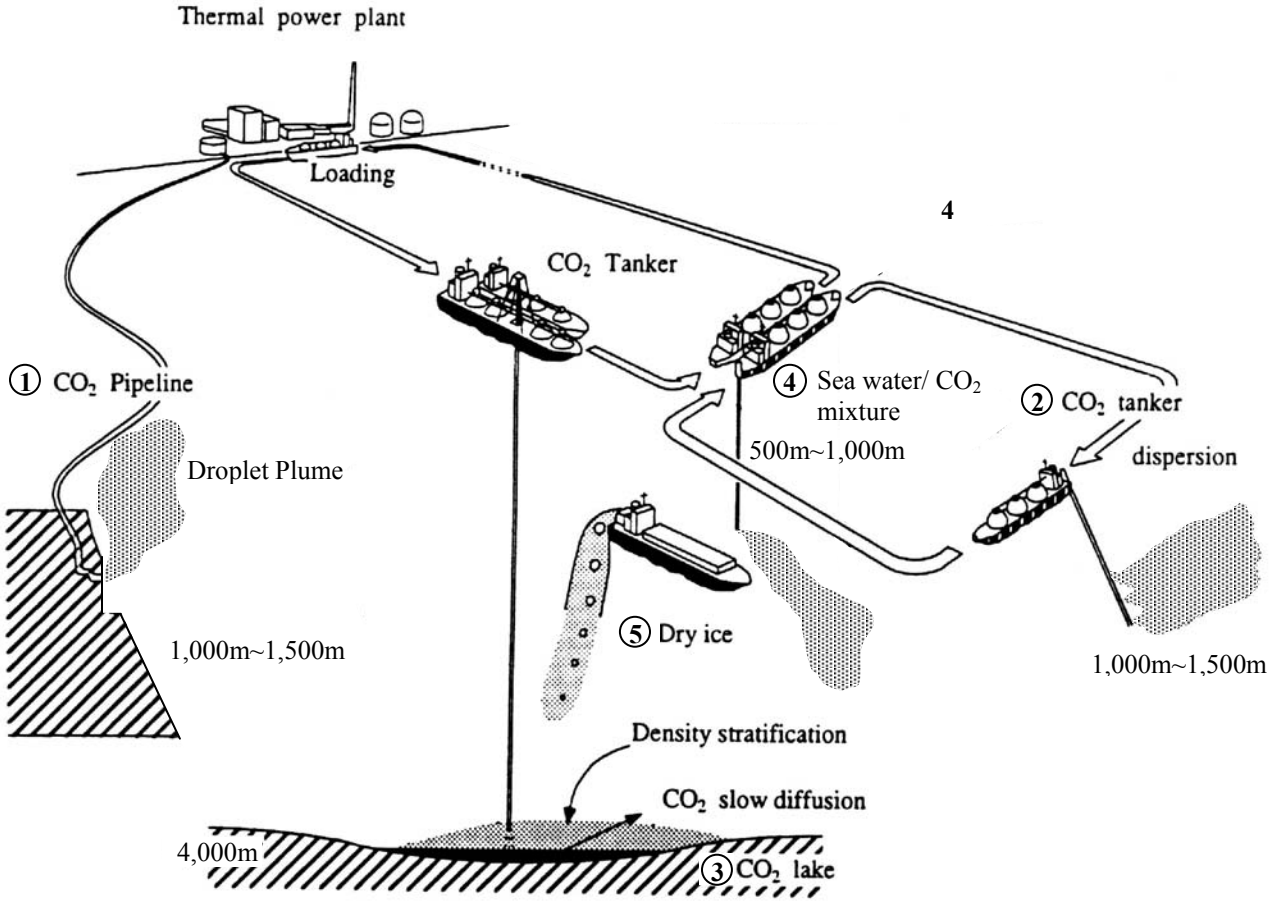

Figure D-1. Five Schemes for CO_2 Ocean Sequestration, (modified from Fujioka et al., 1997)

1. Transport the liquid CO_2 from shore in a pipeline and discharge it from a manifold lying on the ocean below the thermocline at depths of 1000-1500m forming a droplet plume about 100m high (Liro et al., 1992)
2. Transport the liquid CO_2 from shore in a tanker and discharge it as a droplet plume at depths of 1000-1500m from a pipe towed by a moving ship (Ozaki et al., 1995).
3. Inject liquid CO_2 into a sea floor depression, forming a stable lake at a depth of 4000m (Ohsumi, 1993)
4. Create a dense CO_2-sea water solution at a depth of 500-1000m which will sink to the bottom due to gravity (Drange and Haugen, 1992)
5. Form solid CO_2 (dry ice); release it to the ocean from a ship (Nakashiki et al., 1995).

Of the latter two disposal options, the dry ice concept is too expensive due to the cost of production, while the dense sea water mixture has over-riding environmental questions concerning the concentration and resulting effect on aquatic life. However, in the first three concepts, hydrates will play an important (perhaps governing) role as shown in the following discussion.

D.2. Summary of Sequestration Models which Have Considered Hydrates

Many modeling studies have been done to determine the fate of CO_2 injections in the deep ocean. Because, in the low temperature interactions of CO_2 with water, hydrates are a physical reality which cannot be ignored (for example, hydrates may control the rate of CO_2 dissolution in the ocean) those models which have not explicitly included hydrates have been omitted. Without an attempt to be comprehensive, sequestration models which have included hydrates are listed in Table D.2.

Table D.2. Ocean CO_2 Sequestration Mathematical Models which Consider Hydrates

Authors(Date)	Comments
Golomb et al.,(1992)	CO_2 released from diffuser at 500m depth
Adams et al.,(1995)	Droplet plume release to confinement vessel at depths >500m
Holder et al., (1995)	Injection depth & droplet size for a sinking CO_2 droplet at 500m
Shindo et al., (1995)	CO_2 droplet injected at > 3700m depth; lab experiments
Hirai et al., (1997)	CO_2 droplet released at 1000m depth from (a)pipe or (b)ship
Wong &Hirai (1997)	CO_2 drop released from ship at 1500m or in pool at 5182m
Teng et al., (1997a)	Effect of ocean currents on CO_2 injection dispersion at 3000m
Aya et al., (1999)	Large (>200cm) CO_2 droplet injection at 500-700m depth
Hirai et al., (1999b)	CO_2 droplets released from ship via towed pipe at 1500m
Sasaki &Akibayashi (1999)	CO_2 injection in aquifer 200m below sea bottom, 500m below sea surface (700m total depth of aquifer)

Box D-1. Recommendations from Four IEA Ocean Storage Workshops

Workshop 1: Ocean Circulation – To improve predictions of Ocean Global Circulation Models (OGCMs) which predict CO_2 sequestration efficiency, we must:

1. Compare OGCMs on both global and regional bases, tailoring them to CO_2 storage and establishing a standard CO_2 sequestration scenario for comparison.
2. Involve the ocean community more widely in the concept of disposing CO_2 in the deep ocean.
3. Perform small scale experiments on CO_2 release to assess stability and environmental impacts.

Workshop 2: Environmental Impact – To ensure that the impact on the total environment will be less than continuing CO_2 emissions to the atmosphere, we must:

1. Confine the release to a small portion of the ocean, preferably where pelagic life is poor or distribute CO_2 widely so that pH is minimally affected.
2. Determine the CO_2 tolerance of both typical and important marine species by both pressurized laboratory and *in situ* field experiments to evaluate overall impact on pelagic, slope, and benthic communities.
3. Perform small pH change studies to assess the effect of sub-lethal amounts on geographic scales.
4. Assess the impact of a "Business-as-usual" impact on marine biology.
5. Use biogeographical mapping to interpret the impact on micro, meso, and global circulation scales.
6. Collaborate with researchers in marine biology more widely.
7. Develop guidelines for biological acceptability.

Workshop 3: International Links and Concerns – To enable a worldwide acceptance of ocean CO_2 sequestration we should:

1. Establish an strategic advisory group
2. Involve ongoing international science programs such as (a) the World Climate Research Program and (b) the Group of Experts on Scientific Aspects of Marine Environmental Protection
3. Define a process for legal and public acceptance
4. Identify and involve stakeholders
5. Provide mechanisms to incorporate past experience.

Workshop 4: Practical and Experimental Approaches – To provide demonstrated technology for ocean sequestration we must:

1. Obtain and apply basic data from physics, chemistry, and biology to show integrated technical feasibility
2. Initiate engineering design and costing calculations.
3. Improve models of global and regional ocean models to quantify ocean storage benefits and define he biological consequences, and
4. Find routes to public acceptance of ocean storage.

Results from the above models are sufficiently positive to justify further exploration of CO_2 sequestration. The best model for CO_2 ocean sequestration would be the actual large-scale sequestration itself, studied over a long period of time. Unfortunately, no such event has occurred, so in the Section D.3 the controlling principles physics and chemistry are presented.

Section III presents small-scale experiments of CO_2 injection in the ocean as the best evidence of the feasibility of CO_2 sequestration with hydrate interactions. The final section of this appendix (D.4) predicts the fate of CO_2 sequestration in the various scenarios, based upon field data.

D.3. Physical Phenomena for CO_2 Ocean Sequestration

Figure D-2 shows the phases which form when CO_2 contacts water as a function of pressure (P) and temperature (T). The lower boundary (lines I-H-V, L_W-H-V, L_W-H-L_{CO2}) marks the P-T region of CO_2 hydrate formation. At pressures and temperatures above and to the left of those lines, hydrates will form when CO_2 contacts water. At P-T conditions below and to the right of this boundary, hydrates cannot exist.

Two useful approximations relate to Figure D-2. First, as a general rule-of-thumb, 1 MPa is equivalent to 100 m of depth in the ocean. Second, Figure D-2 is for conditions of contact of CO_2 with fresh water. In sea water, the entire diagram is shifted to the left by 1.5K, so the diagram and accompanying discussion applies to sea water with an almost undetectable temperature shift.

The middle portion of the hydrate boundary (line L_W-H-V) gives the P-T conditions at which hydrates form when CO_2 vapor contacts water. The vertical portion of the hydrate boundary (line L_W-H-L_{CO2}) is due to three almost incompressible phases; at higher pressures (greater than 10MPa) it curves to the left due to CO_2 compressibility. The vertical L_W-H-L_{CO2} line intersects the L_W-H-V line at 4.45MPa and 283.3K, which are sometimes given as the upper temperature and lower pressure at which ocean CO_2 hydrates will form, although hydrates can form at lower pressures and temperatures.

In Figure D-2, the lower portion of the line (marked I-H-V) extends below the ice point (273K) and gives the conditions at which hydrates form when CO_2 vapor contacts ice. The region to the left of the ice point, marked by lines I-L_W-V and I-L_W-H are not of general concern to this study. Most conditions which concern ocean CO_2 sequestration deal with higher temperatures, such as those between 275K (the lowest typical sea floor temperature) and 283K (the upper hydrate formation temperature).

The line (H-V-L_{CO2}) slanting upward to the right gives P-T conditions at which CO_2 vapor liquefies in the hydrate region. At temperatures and pressures above this line hydrates will form when liquid water contacts liquid CO_2. Because most CO_2 ocean injection schemes occur at depths for which CO_2 is liquid, the H-V-L_{CO2} line is often

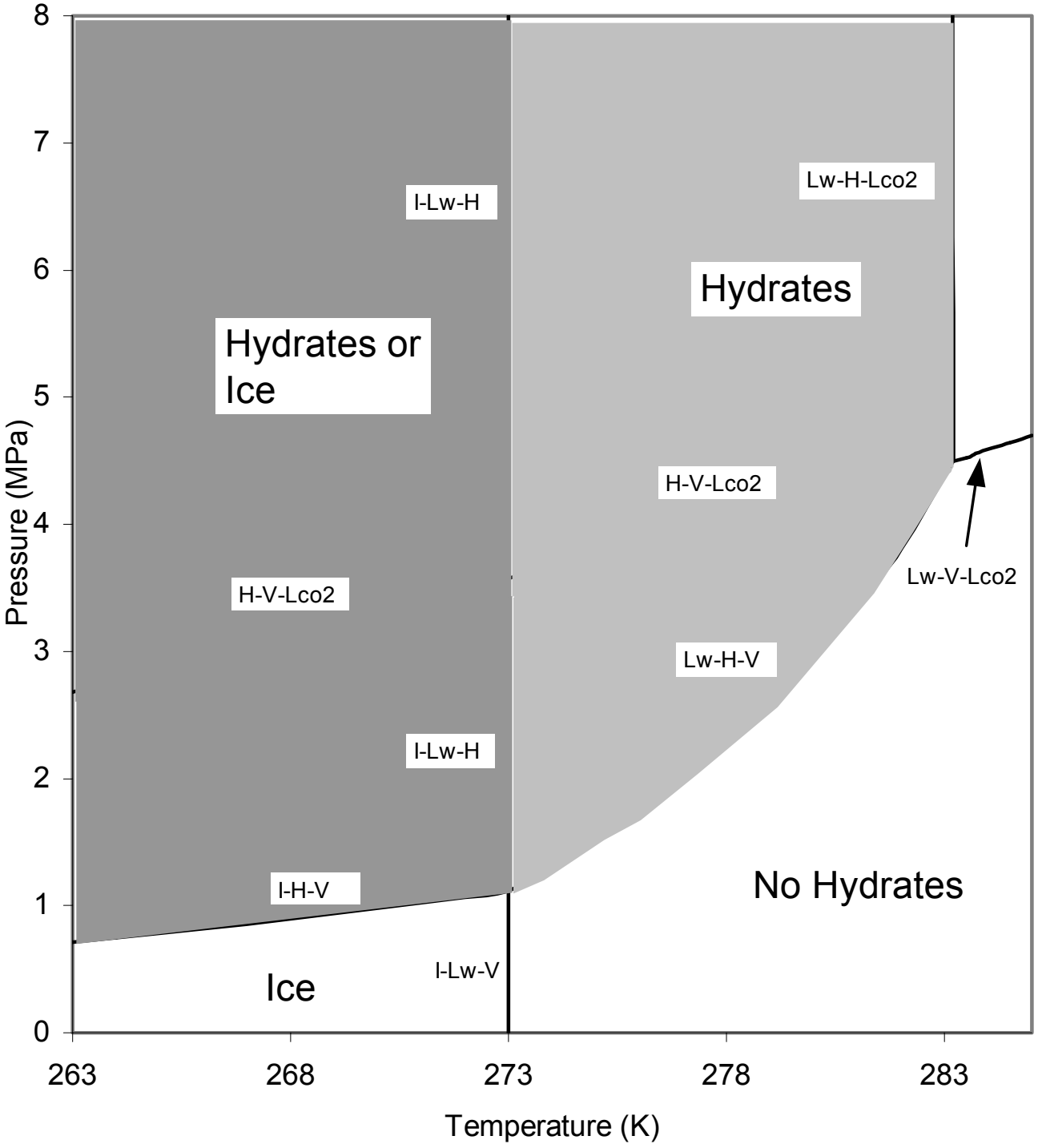

Figure D-2. Phase Diagram for CO_2 in H_2O

considered the lower boundary for hydrate formation, although hydrates can form from vapor at lower pressures (above the L_W-H-V line). Finally the vapor pressure line of CO_2 in water (L_W-V-L_{CO2}) extends to the rightmost boundary of Figure D-2; above this line CO_2 vapor liquefies in contact with water.

In summary, when injected into the ocean, pure CO_2 is a gas above 500m and a liquid below that depth. At pressures greater than 4.45 MPa (depths > 440m) and temperatures lower than 283.3K, CO_2 hydrates will form.

In addition to pressure and temperature, the relative density of the phases must be considered. For example hydrates have a density 8-10% greater than that of sea water. Below 2650 m in unsaturated sea water, the liquid CO_2 will sink, but in CO_2-saturated sea water, a depth of 3700 m is required before CO_2 sinks. Case Study D-1 provides a perspective on densities of CO_2 liquid and hydrate, which controls their buoyancy in sea water.

Case Study D-1. Density Differences Control Rise of Fall of CO_2 Droplets in Ocean

Figure D-3, modified from Aya et al. (1999) shows lines of constant density (isochores) of liquid CO_2 (light), and CO_2 hydrate (dark) sloping downward to the right with an increase in temperature and water depth, relative to sea water density. When the density ratio of either CO_2 liquid or hydrate is greater than 1.04, that phase will sink in the absence of an ocean current. Ocean currents can control the flow and dissolution of CO_2. Here we consider the simplest case of a stagnant ocean, without velocity fields.

Several lines in Figure D-3 provide a basis for a density perspective. First, a dashed vertical line is given at -1.5^oC, the ice formation point in sea water; second a horizontal dashed line is given at 2650m, the critical depth beyond which CO_2 liquid will sink in sea water. An almost vertical curve shows the temperature and pressure in a Pacific ocean location (30^oN West Pacific) approximating the ocean temperature around the world. A third dotted line sloping downward to the right gives the density ratio of sea water to that of water with temperature and depth, varying linearly between the surface (1.026) and 4000m (1.046).

The two almost horizontal curved lines serve as the starting conditions for CO_2 liquid and hydrate. The CO_2 liquid region in lines of constant density (called isochores) as a ratio with sea water is given below the lighter curved line; at depths less than the lighter horizontal curve marked “liquid boundary,” CO_2 will be a vapor. The CO_2 hydrate region begins at the darker horizontal curve marked “hydrate boundary”; at lesser depths hydrate will not form.

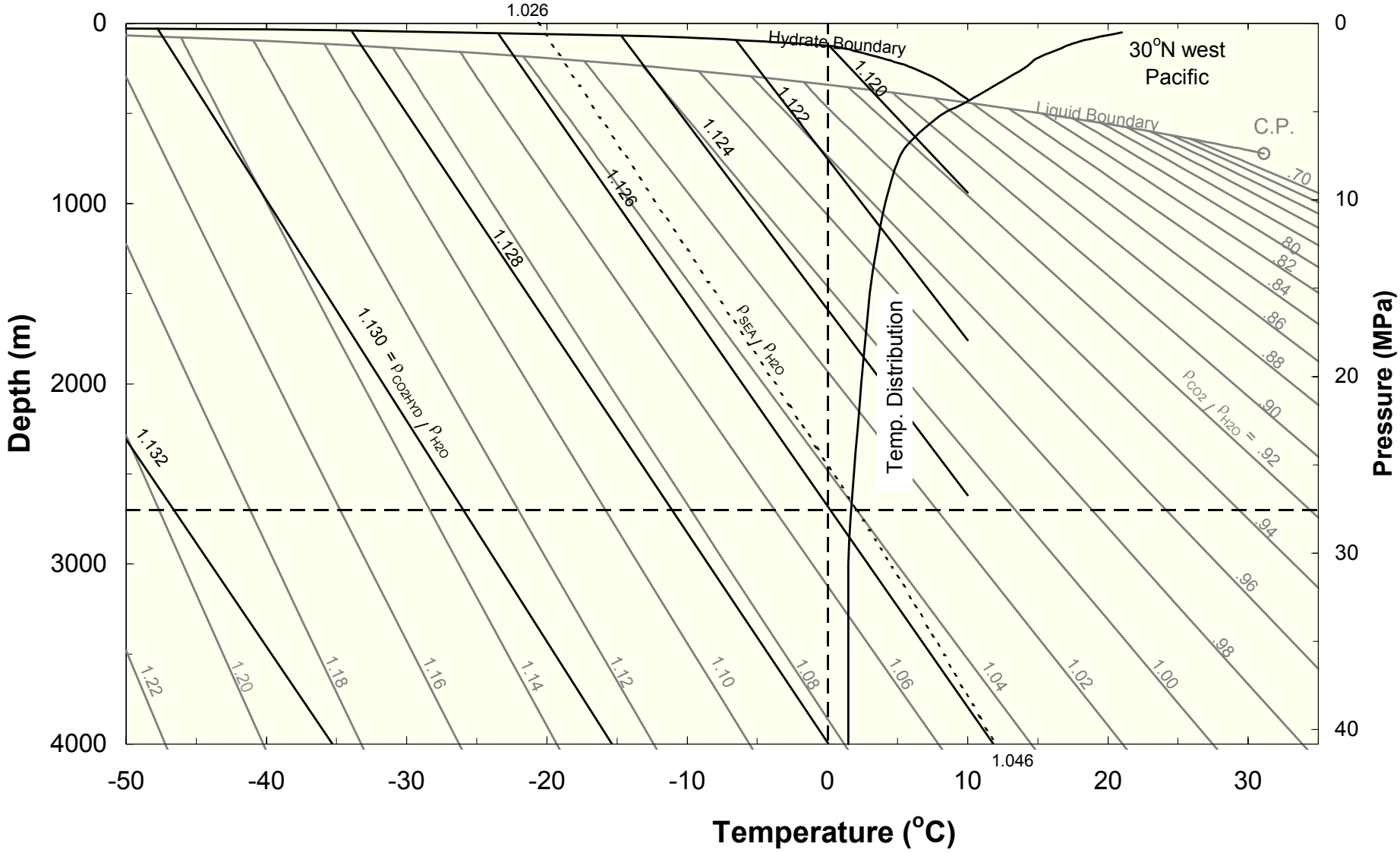

Figure D-3. Densities of CO_2 Liquid and Hydrate Relative to Water, as a Function of Temperature and Pressure, modified from Aya et al. (1999)

Density of CO_2 in the ocean and vertical temperature distributions

Several points are immediately obvious from Figure D-3. First, CO_2 is a very compressible liquid, compared to either sea water or to hydrates. Second, at typical deepwater temperatures of 2-5°C, CO_2 hydrates and CO_2 liquid form at similar depths from 200-500m. Third, the density of CO_2 hydrate is always greater than that of sea water, and hydrate density is greater than that of CO_2 unless the temperature is very low (<-25°C). Finally, at normal deepwater temperatures, CO_2 liquid droplets will be buoyant between 500 and 2650m, unless they are converted to hydrate, in which case they will sink.

A controlling factor in seafloor sequestration is a thin CO_2 hydrate film which will form around the CO_2 droplet in the water. Until that solid film dissolves (very slowly) in the surrounding sea water it will prevent further contact between CO_2 and sea water. The hydrate film will be the controlling factor in CO_2 liquid droplet dissolution in sea water.

The hydrate film will form very rapidly. Warzinski et al., (1997) measured the growth rate on 0.5-1 cm CO_2 drops to be 0.5-1.0 cm^2/s. For a water droplet in CO_2 liquid a linear film growth velocity (v_f) was measured relative to subcooling ΔT (= $T_{equilibrium}$ – T) by Uchida et al. (1999) as

$$v_f\left[\text{mms}^{-1}\right] = (1.73 \pm 0.16)\,\Delta T[\text{K}] \qquad \text{(D-1)}$$

Table D-3 gives the estimated thickness of hydrate films, including CO_2. For CO_2 hydrate, the thickness of the film ranges from 0.3-0.43 μm, increasing with time, but inversely proportional to subcooling and CO_2 concentration in the liquid water (Makogon et al., 1998; Mori, 1999; Uchida, 1999). A review of eight hydrate film models is presented by Mori (1998), who concluded additional experimental validation is required.

Table D-3. Thickness of Hydrate Films

Initial Thickness	Notes on Hydrate Film Measurement/Calculation	Reference
5μm	CH_4 measured by micrometer	Makogon et al., 1998
10-80 μm	CF_3CH_2F; interferometry; fn of ΔT	Ohmura et al., 1999a
< 200μm	CH_3CCl_2F; photographs	Ohmura et al., 1999a
1.3μm	CO_2 est. by Uchida &Kawabata(1997)	Aya et al. (1992)
10^{-2}–10^{-4}r	r = CO_2 radius; calcd. for unsatd. H_2O	Holder &Warzinski (1996)
6.2-17μm	CO_2 estimate from tensile strength	Uchida &Kawabata(1997)
0.43μm	CO_2 videocamera	Tabe et al., 1999
0.13μm	CO_2(calculated: heat diffusion model)	Uchida, et al., 1999
0.3μm	CO_2 (calculated)	Mori, 1999

In the batch experiments of Warzinski et al., (1999) hydrate film formation was a function of the CO_2 saturation. A 0.5 – 1.0 cm drop, was completely enveloped in 1-2s. When the dissolved concentration reached 51mg of CO_2/g seawater at 2°C and 17.5

MPa., the rate of hydrate-encrusted CO_2 droplet dissolution declined 2-3 orders of magnitude compared to that in the absence of hydrate. Because the surrounding sea water is not saturated with CO_2, the encrusted droplet will slowly dissolve as shown in Table D-4 for CO_2 droplets with and without hydrate shells.

In flow tunnel experiments Yamasaki et al., (1999) showed: (1) for particles from 0.5 to 1.5 cm ID a thin hydrate film formed almost immediately on the CO_2 droplet surface and was unaffected by hydrodynamics. In flow tunnel and mixed vessel experiments, for larger liquid CO_2 droplets (5-10cm) surface hydrate shedding occurred at Reynolds numbers between 3000 and 6000.

Tables D-3 and D-4 show that the hydrate film reduces the rate of mass transfer between the CO_2 and surrounding water by a factor between 1.6 and 3.2. However, heat transfer through the hydrate film can freely occur. As shown in the below Japanese Ship Research Institute study, heat transfer can control the sequestration of CO_2 ocean droplets.

Case Study D-2. CO_2 Injection Bouyancy Concepts: Large Drops Injected at Low Temperatures in 500 m Water Depth

For efficiency CO_2 will be transported to disposal sites as a liquid typically in a pipeline for distances less than 200-250km (Golomb, 1997; Fujioka et al., 1997) or in a tanker/injection platform system for greater distances from the shoreline. In a tanker, the CO_2 will likely be below 6 bar pressure for optimum vessel wall thickness, so the temperature is very low (-50^{o}C).

Table D-4. Small CO_2 Droplet Shrinkage Rates With and Without Hydrate Shells

Experimenter	P (MPa)	T(K)	Water Velocity (cm/s)	Initial Diam. (mm)	Final Diam. (mm)	Diameter Shrinkage Rate(m/s)	Hydrate Shell Formed?
Aya et al. (1992)	5.5	283-293	0	25-30	<10	0.39×10^{-6}	Yes
						0.85×10^{-6}	No
Fujioka et al., (1994)	28 & 35	280	0	13-15	3	0.5×10^{-6}	Yes
Aya et al. (1993)	30	274-285	2-3	6-8	0	$0.5\text{-}1.5\times10^{-6}$	Yes
						1.6×10^{-6}	No
Nishikawa et al. (1995)	30	275	3	12		0.8×10^{-6}	Yes
						1.6×10^{-6}	No
Saji et al., (1995)	4.2 – 8.3	277-279	3	15	NA	8.0×10^{-6}	Yes
Hirai et al. (1996)	9.8- 39.2	276-286	1.5-7	9	7	$0.4\text{-}1.9\times10^{-6}$	Yes
						$1.3\text{-}3\times10^{-6}$	No
Warzinski et al. (1997)	10-15	278	0	50-100	NA	$1.2\text{-}5.6\times10^{-8}$	Yes

The low CO_2 temperatures inside the injection pipe will cause sea water ice to form on the outside the pipe, which will insulate the pipe and provide low temperature (<-25°C) CO_2 liquid discharge into sea water at a pipe depth of 500m. In COSMOS, the Japanese Ship Research Institute's large droplet (> 20 cm) injection scheme, Aya et al. (1999) provide the following CO_2 injection conceptual picture, based upon the density (ρ) differences shown in Figure D-3:

1. Large CO_2 droplets will rapidly form a flexible, thin hydrate film ($\rho = 1.12$) which will prevent contact and mass transfer between the sea water ($\rho = 1.04$) and CO_2 liquid on either side of the film. As shown in Figure D-3, the liquid CO_2 density changes with depth and temperature.
2. Heat will be absorbed by the large droplet, so that an ice layer will form outside the hydrate film. The growing ice layer ($\rho = 0.9$) will cause the droplet to be buoyant.
3. The combined density of the CO_2 liquid droplet, thin hydrate film, and ice layer will determine whether the droplet rises or sinks. While the hydrate layer is stable, the ice layer will grow as long as the droplet temperature is below 0°C, and the CO_2 density changes with temperature and depth as indicated in Figure D-3. The combined particle density changes with time, due to two effects: (1) the growing ice layer, and (2) the temperature and pressure (depth) of the CO_2 droplet. Both are functions of the CO_2 droplet size, the injection temperature, and the depth of injection.
4. At high temperatures (>-25°C), low injection depths (<500m), and small droplet sizes (<1.2m diameter), an ice/hydrate-coated CO_2 droplet will rise to a shallow depth, where the ice/hydrate layer will decompose, and CO_2 will vaporize, soon finding its way back to the atmosphere.
5. At low temperatures (<-35°C), depths greater than 500m, and very large droplet sizes (>0.8m) the ice/hydrate-coated droplets will sink and be sequestered at very low depths for long times.
6. In order for CO_2 droplets to sink and be stabilized, heat transfer to the droplet plays a major role. Very large droplets and low temperatures are needed to maintain the high density required for sequestration of CO_2. Smaller, normal size droplets (< 2cm) will attain the temperature of the surrounding ocean (2-5°C) very rapidly and rise due to the absence of an ice layer and their lower CO_2 density. It should be noted that only CO_2 droplet sizes of less than 25 mm were considered likely by Teng et al.,(1997b) at depths greater than 500m. Aya et al.,(1999) have proposed a method to form large droplets.

With such a complex system, laboratory experiments alone will be insufficient to accurately predict behavior in the ocean. It will be necessary to use direct ocean CO_2 injection to assess the viability of models. Planned pilot CO_2 experiments will release 70 tonnes of CO_2 off the Hawaiian Kona Coast in the summer of 2000 (E. Adams et al., 1999; http://www.co2experiment.org). Unfortunately these experiments will be done after the completion of this report.

The best modern field CO_2 and CH_4 deepwater hydrate formation evidence was obtained at the Monterey Bay Aquarium Research Institute (MBARI), where deep ocean

injection experiments were made, beginning in January 1996. The MBARI results are summarized in Section III of this report.

D-4 Predictions for CO_2 Injections in the Ocean, Based Upon Field Data. The MBARI CO_2 injection data in Section III provide the best extant physical evidence of the fate of CO_2 injected into the oceans. Such deep sea experiments are closer to reality than laboratory experiments, and provide new insights. For example, the experiments call into serious question the widely-accepted concept of a hydrate film at the surface between sea water and liquid CO_2 (Fujioka, et al., 1995; Saji et al., 1995) at depths greater than 3700 m. Ultimately a long-term observation, with larger CO_2 injections will be very helpful to estimate the loss rate of CO_2 from a hydrate mass deep in the ocean.

However, one can make a preliminary prediction of the fate of CO_2 sequestration at various depths, using the above MBARI experiments of CO_2 injection into the deep ocean, in the absence of ocean currents. The CO_2 droplets are likely to be small (nominally 1cm) due to surface tension. The small drops will attain the temperature of the surroundings almost immediately; heat transfer effects, noted in Case Study D-2, will not play a significant role in determining the buoyancy.

The following prediction is for the case in which small CO_2 liquid droplets are injected into a quiescent ocean at shallow depths. Because large shallow injections are likely to be dispersed as many small (< 1cm) droplets in a vast ocean environment, the fate of a single droplet may be indicative of the fate of many injected droplets.

D.4.a. Prediction Based Upon Field Data: Shallow Injection of a Small CO_2 Droplet. Consider the fate of a single small ($\leq$ 1cm) CO_2 droplet injected at depths less than 2650 m. Upon injection into seawater the droplet will experience the following:

1. The droplet will rapidly attain the temperature of the surrounding sea water.
2. A thin, flexible hydrate shell will form within 2 seconds on the droplet surface, preventing further contact between seawater and CO_2.
3. As the hydrate-coated droplet rises, the diameter will slowly shrink at a rate of 5.0×10^{-7} m/s, due to CO_2 hydrate dissolution in sea water. This shrinkage is slower than that without the hydrate film by a factor of 1.6-3.2 as shown in Table D-4; the hydrate film will slow the dissolution rate for a considerable change in depth.
4. The droplet size will increase slightly due to reductions in density as the droplet rises, (ρ = 1.04 to 0.9 g/cc). The flexible hydrate film will grow and expand to accommodate these density changes.
5. The coated droplet will rise in the seawater at a rate of approximately 6 m/min.
6. When the droplet passes a depth between 350m, the hydrate coating will disappear and the droplet will vaporize.
7. The resulting vapor bubbles will rapidly dissolve in the sea water at low depths.
8. The dissolved CO_2 will be more dense than sea water. However this small density difference may cause the dissolved CO_2 to be strongly affected by ocean currents, and subject to similar concerns raised with Injection Scheme 4 (Drange and Haugen,

1992). For example, there is the possibility of acidification of shallow sea water, or the rapid return of CO_2 to the atmosphere.

In contrast to the above picture, consider the below prediction for injection of CO_2 at depths greater than 3700 m. These predictions are also based upon the MBARI experiments cited in Section III.B.

D.4.b Prediction Based Upon Field Data. Deep Injection of CO_2 Liquid Consider the fate of a large injection of CO_2 at depths greater than 3700 m. Upon injection into a deep ocean depression or trench the CO_2 will cause the following phenomena:

1. The CO_2 liquid will congeal as a deep ocean lake with a density about 8% greater than sea water. That difference will act as a stabilizing force to keep the lake in place, in the absence of ocean bottom currents.
2. The lake will attain the temperature of the ocean depression (2-5^{o}C).
3. The high surface tension will prevent CO_2 penetration into the sediments, but the CO_2 lake will deplete all life immediately below the lake.
4. At the interface, hydrates will rapidly form and sink to the bottom of the CO_2 lake before a film forms at the interface between the sea water and the lake.
5. The hydrate layer will continue to form at the interface and sink, growing to a hydrate layer beneath the CO_2 lake. Because the hydrates are of higher density and have a higher volume than CO_2 liquid, the entire CO_2 liquid and hydrate layer will expand
6. The entire CO_2 liquid lake will be converted to a CO_2 hydrate solid lake, starting from the bottom upwards.
7. The dissolution of the CO_2 hydrate into the surrounding quiescent seawater will be 1×10^{-8} m/s, a rate between 1.6-3.2 times slower than the dissolution of liquid CO_2 into seawater, without hydrate formation.
8. CO_2 hydrate will continue to dissolve until the hydrate lake is totally depleted, because the ocean will never be saturated with CO_2. However the dissolution rate of CO_2 hydrate, in the absence of ocean currents will be very long, decreasing 0.3 m/yr. The likelihood of a CO_2 return to the atmosphere is very small.

D.5. Economics of CO_2 Injection into the Ocean.

Two economic factors provide a baseline for evaluation of CO_2 injection, perhaps as bellweathers for the future: (1) Norway has imposed a tax of $US 50/tonne of CO_2 emitted, and (2) the cost estimation of CO_2 injection by Statoil (the state-owned Norwegian oil company) into the Sleipner West field aquifer is $15/ tonne of CO_2 avoided (Herzog, 1999). At Sleipner West, 20,000 tonnes/week of CO_2 (equivalent to the CO_2 produced from a 140MW coal fired plant) has been injected into an aquifer 1000m below the North Sea since September 1996.

The capture and concentration of CO_2 from stack gases represents the major cost in CO_2 ocean sequestration. Herzog (1999a) summarized 10 economic studies to account for the capture and compression (to 2000 psia) of CO_2 from stack gases from three types of power plants: (1) Pulverized Coal, (2) Integrated Gasification Combined Cycle, and (3) Natural Gas Combined Cycle, listed in order of common usage. For the most common pulverized coal process, three studies indicated the price of electricity would increase by an average of 96.3% for such CO_2 capture and compression.

To these costs should be added the cost of CO_2 liquefaction and transportation to determine a realistic cost estimate of sequestration. Process economics indicate that CO_2 should be transported and injected in the more dense form, as a liquid rather than a vapor or a slurry. Herzog (1999a) indicated a nominal cost of $10/tonne for sequestration schemes, compared with the CO_2 capture and compression cost average of $40/tonne.

Fujioka et al., (1997) performed the most comprehensive economic analysis for CO_2 capture and sequestration. They considered two 554 MW pulverized coal plants, which used monoethanolamine (MEA) to capture 93% of the CO_2, with a maximum handling CO_2 capacity of 20,400 tonnes/day. The five sequestration processes in Section D.1 shown in Figure D-1 are analyzed, with a slight modification of the Fujioka approach to account for Process 4 (dense CO_2–water solution injected into sea water).

For each of the five sequestration processes, Figure D-4 illustrates five components of the total cost: (1) power plant, (2) fuel, (3) separation, (4) liquefaction, and (5) transportation. From the figure two conclusions can be drawn:

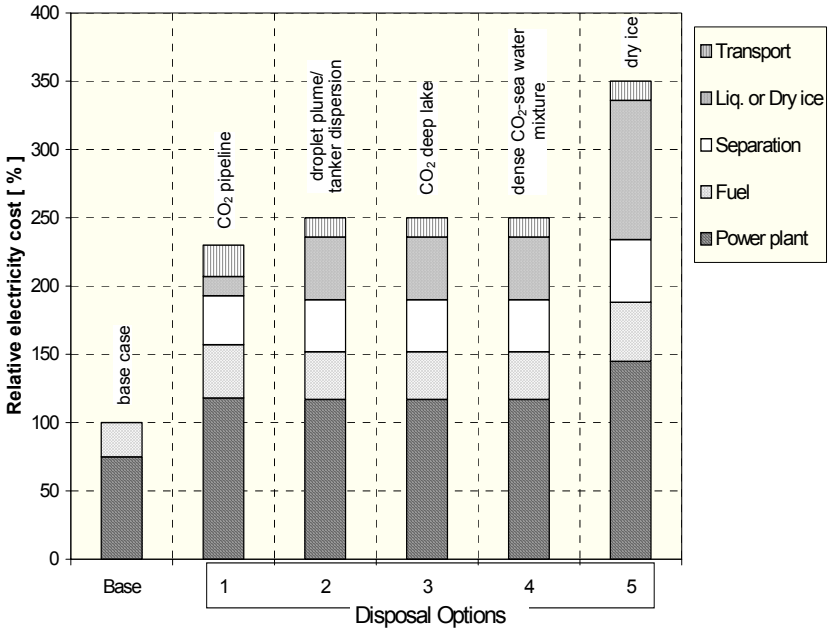

Figure D-4. Relative Costs of Components of the Sequestration Schemes in Figure D-1 (page 87), modified from Fujioka et al., (1997)

1. The cost of CO_2 disposal in the ocean will be \$90-180/tonne avoided CO_2. Ocean disposal increases the cost of electricity by a factor of 2 to 2.5.
2. The costs of four processes are comparable (pipeline disposal, CO_2 tanker dispersion, CO_2 deep lake and CO_2 dense mixture disposal). The solidification costs of dry ice production renders it infeasible.

An IEA Greenhouse Gas Programme study (Ormerod, 1995) summaried the transportation costs for CO_2 recovered from a 2GW coal-fired power station. In every case economics favored liquid CO_2 transportation. Pipeline costs are less than \$10/tonne CO_2/1000km; beyond 2000 km transport of liquid CO_2 via ocean tanker is more economical.

IX. References

Adams, D., Ormerod, W., Riemer, P., and Smith, A., "Carbon Dioxide Disposal from Power Stations", IEA Greenhouse Gas R&D Programme Report, ISBN 1898373 07 8 1994, available at http://www.ieagreen.org.uk

Adams, E.E., Golomb, D., Zhang, X.Y., Herzog, H.J., "Confined Research of CO_2 into Shallow Seawater", in Direct Ocean Disposal of Carbon Dioxide, N. Handa, and T. Ohsumi, eds., 153, Terrapub, Tokyo (1995)

Adams, E., Akai, M., Golmen, L., Haugan, P., Herzog, H., Masuda, S., Masutani, S., Ohsumi, T., and Wong, C.S., "An International Experiment on CO_2 Ocean Sequestration," in Greenhouse Gas Control Technologies, (Proc. Of 4th Intrntl. Conf. On Greehouse Gas Control Technologies 8/30 – 9/2/98 Interlaken, Switzerland) Eliasson, B., Riemer, P., Wokaun, A., eds., Pergamon, pg 293, (1999)

Ahlbrandt, T., U.S. Geological Survey World Gas Estimation, Personal Communication (July 9, 1999)Website http://energy.cr.usgs.gov/energy/WorldEnergy/WEnergy.html

Anderson, A.L., Sloan, E.D., Brooks, J.M. "Gas Hydrate Recoveries in the Gulf of Mexico: What is the Shallow Water Depth Limit for Hydrate Occurrence?"Proc. Offshore Tech Conf, OTC 6853, Houston, TX, May 4-7 (1992)

Arri, L. E., Yee, D., Morgan ,W.D., Jeansonne, M.W., "Modeling Coalbed – Methane Recovery with Binary Gas Sorption," Proc. SPE Rocky Mountain Regional Meeting, SPE 24363, page 459, May 18-21, (1992)

Aya, I., Yamane, K., Yamada, N., "Stability of Clathrate Hydrate of Carbon Dioxide in Highly Pressurized Sea Water" Proc. Winter Ann. Mtg of ASME, HTD, **215**, 17 (1992)

Aya, I., Yamane, K., Yamada, N., "Effect of CO_2 Concentration in Water on the Dissolution Rate of Its Clathrate" Proc. Int. Symp. on CO_2 Fixation & Efficient Utilization of Energy, 351 (1993)

Aya, I., Yamane, K., Shiozaki, K., "Proposal of Self Sinking CO_2 Sending System: COSMOS," in Greenhouse Gas Control Technologies, (Proc. Of 4th Intrntl. Conf. On Greehouse Gas Control Technologies 8/30 – 9/2/98 Interlaken, Switzerland) Eliasson, B., Riemer, P., Wokaun, A., eds., Pergamon, pg. 269, (1999)

Auerbach, D.I. Caulfield, J.A. Adams, E.E., Herzog, H.J., "Impacts of Ocean CO_2 Disposal on Marine Life: 1. Toxicological Assessment Integrating Constant Concentration Lab Assay," Environmental Modeling and Assessment, 2, 333 (1997)

Bains, S., Corfield, R.M., Norris, R.D., "Mechanisms of Climate Warming at the End of the Paleocene," Science, **285**, 724, July 30, 1999.

Bayles, G.A., Sawyer, W.K., Anada, H.R., Reddy, S., and Malone, R.D., "A Steam Cyclic Model for Gas Production from a Hydrate Reservoir," Chem. Eng. Commun., **47**, 225 (1986)

Bell, P. R., "Methane Hydrate and the Carbon Dioxide Question," in Carbon Dioxide Review, W. Clark, ed., Oxford Univ. Press, 1982.

Booth, J., Rowe, M., Fischer, K., "Offshore Gas Hydrate Sample Database," U.S. Geological Survey Open File Report, **96** (1996)

Brewer, P.G., "Gas Hydrates and Global Climate Change," Proc. 3rd International Conference on Natural Gas Hydrates, Salt Lake City, New York Academy of Sciences, July 19-23, 1999.

Brewer, P.G., Friederich, G., Peltzer, E.T., Orr, F.M., "Direct Experiments on the Ocean Disposal of Fossil Fuel Carbon Dioxide,"Science, **284**, 943 (1999)

Brewer, P.G., Orr, F.M., Friederich, G., Kvenvolden, K.A., , Orange, D.L., "Gas Hydrate Formation in the Deep Sea: In Situ Experiments with Controlled Release of Methane, Natural Gas and Carbon Dioxide," Energy and Fuels, **12**, 183 (1998)

Bugge, T., Benderson, R.H., Kenyon, N.H., "The Storegga Slide," Phil. Trans. R. Soc. London, A325, 357 (1988)

Burshears, M., O'Brien, T.J., and Malone, R.D., "A Multi-Phase Multi-Dimensional, Variable Composition Simulaton of Gas Production from a Conventional Gas Reservoir in Contact With Hydrates," Proc. SPE Unconventional Gas Technology Symposium, SPE 15246, May 1986.

Byrer, C.W., Guthrie, H.D., "Coal Deposits: Potential Geological Sink for Sequestering Carbon Dioxide Emissions from Power Plants," in Greenhouse Gas Control Technologies, (Proc. Of 4th Intrntl. Conf. on Greenhouse Gas Control Technologies 8/30 – 9/2/98 Interlaken, Switzerland) Eliasson, B., Riemer, P., Wokaun, A., eds., Pergamon, pg 181, (1999)

Campbell, K.J., "Deepwater Geohazards: An Engineering Challenge," Offshore, pg. 46, October (1991).

Caulfield, J.A., Adams, E.E., Auerbach, E.I., Herzog, H.J., "Impacts of Ocean CO2 Disposal on Marine Life: II. Probabilistic Plume Exposure Model Used With a Time-Varying Dose Response Analysis," Environmental Modeling and Assessment, 2, 345 (1992)

Chu, C., "Current In Situ Combustion Technology," J. Petroleum Technology, p 1412, 1983.

Clennell, M.B., Hovland, M., Booth, J.S., Henry, P., Winters, W.J., "Formation of Natural Gas Hydrates in Marine Sediments: 1. Conceptual Model of Gas Hydrate Growth Conditioned by Host Sediment Properties," J. Geophys. Res. **104, B10**, 22,985 (1999)

Cole, K.H., Stegen, G.R., Spencer, D., "The Capacity of the Deep Oceans to Absorb Carbon Dioxide," in Direct Ocean Disposal of Carbon Dioxide, N. Handa, and T. Ohsumi, eds., 143, Terrapub, Tokyo (1995)

Collett, T.S., "Gas Hydrates Resources of the United States," in National Assessment of United States Oil and Gas Resources – Results, Methodology, and Supporting Data, Gautier, D.L., Dolton, G.L., Takahashi, K.I., and K.L. Varnes, Eds., U.S. Geological Survey Digital Data Series 30. (1995)

Collett, T.S., Ginsburg, G.D., "Gas Hydrates in the Messoyakha Gas Field of the West Siberian Basin – A Re-Examination of the Geologic Evidence," Inter. J. of Offshore and Polar Eng., **8**, 22, (1998)

Cranston, R., "Marine Sediments as a Source of Atmospheric Methane," Bulletin of the Geological Society of Denmark, **41**, 101, (1994)

Dallimore, S.R., Uchida, T., and T.S. Collett, Eds., Scientific Results from JAPEX/JNOC/GSC Mallik 2L-38 gas Hydrate Research Well, MacKenzie Delta, Northwest Territories, Canada, Geological Survey of Canada Bulletin 544, 601 Booth St., Ottawa, Ontario, K1A 0E8 (1999)

Dickens, G.R., "Methane Oxidation During the Late Palaeocene Thermal Maximum" Bulletin de la Societe Geologique de France, (in press) (1999)

Dickens, G.R., Castillo, M.M., Walker, J.C.G., "A Blast of Gas in the Latest Paleocene: Simulating First-Order Effects of Massive Dissociation of Ocean Methane Hydrate," Geology, **25**, p, 259 (1997)

Dickens, G., O'Neil, J., Rea, D., and Owen, R., "Dissociation of Oceanic Methane Hydrates as a Cause of the Carbon Isotope Excursion at the End of the Paleocene," Paleoceanography, **10**, 965 (1995)

Dillon, W.P., "Gas Hydrate as a Potential Resource – What Do We Need to Know?" in Proceedings of the International Symposium of Japan National Oil Company, "Methane Hydrates,; Resources in the near Future? Chiba City, Japan, October 20-22, 1998. Page 13. Panel Discussion Proceedings.

Dobrynin, V.M., Korotajev, Yu.P., and Plyuschev, D.V., "Gas Hydrates – A Possible Energy Resource," in Meyer, R.F. and Olson J.C., eds. Long-Term Energy Resources, Pitman, Boston, 727 (1981)

Drange, H., Haugen, P.M., "Carbon Dioxide Sequestration in the Ocean: The Possibility of Injection in Shallow Water," Energy Convers. Mgmnt., **33(5-8)**, 697 (1992)

Drenth.A.J.J. and W.J.A.M. Swinkels, "A Thermal Reservoir Simulation Model of Natural Gas Hydrate Production," in Proceedings of the International Symposium of Japan National Oil Company, "Methane Hydrates,; Resources in the near Future? Chiba City, Japan, October 20-22, 1998. Page 187.

Ebinuma, T., "Carbon Dioxide Fixation and Exploitation of Methane Hydrate by CH_4-CO_2 Replacement," Research Institute of Innovative Technology for the Earth (RITE), Proc. 2nd Japanese Institute of Energy Meeting (1994)

Ebinuma, T., "Carbon Dioxide Fixation and Exploitation of Methane Hydrate by CH_4-CO_2 Replacement," Research Institute of Innovative Technology for the Earth (RITE), Proc. 3rd Japanese Institute of Energy Meeting (1995)

Ebinuma, T., Uchida, T., Narita, H., Yoshida, R., "Studies on Exploitation of Methane Hydrates Using Carbon Dioxide," Research Institute of Innovative Technology for the Earth (RITE), Proc. 6th Japanese Institute of Energy Meeting (1997)

Englezos, P., "Atmospheric Climate Changes and the Stability of the in situ Methane Hydrates in the Arctic," in Proc. 2nd Intnl Offshore & Polar Eng. Conf., San Francisco, CA, 644 (1992)

Fei, T., A Theoretical Study of the Effects of Sea Level and Climatic Change on Permafrost Temperatures and Gas Hydrates, M.S. Thesis, University of Alaska, Fairbanks, 1991

Fujioka, Y., Takeuchi, K., Shindo, Y., Komiyama, H., "Shrinkage of Liquid CO_2 Droplets in Water," Int. J. Energy Res., **18**, 765 (1994)

Fujioka, Y., Ozaki, M., Takeuchi, K., Shindo, Y., Yanagisawa, Y., Komiyama, H., Ocean CO_2 Sequestration at the Depths Larger than 3700m" Energy Convers. Mgmt., **36(6-9)**, 551 (1993)

Fujioka, Y., Ozaki, M., Takeuchi, K., Shindo, Y., Yanagisawa, Y., Komiyama, H., "Ocean CO_2 Sequestration at the Depths Larger than 3700m" Energy Convers. Mgmt., **36(6-9)**, 551 (1995)

Fujioka, Y., Ozaki, M., Takeuchi, K., Shindo, Y., Herzog, H., "Cost Comparison in Various CO2 Ocean Disposal Options," Energy Convers. Mgmt., **38S**, S273 (1997)

Gautier, D.L., Dolton, G.L., Takahashi, K.I., and K.L. Varnes, Eds., National Assessment of United States Oil and Gas Resources – Results, Methodology, and Supporting Data, U.S. Geological Survey Digital Data Series 30. (1995)

Ginsburg, G.D., and Soloviev, V.A., Submarine Gas Hydrates, Ivanov, V.I., ed., VNIIOkeangeologia, St. Petersburg, (1994) ISBN 5-8894-103-9

Ginsburg, G.D., and Soloviev, V.A., "Submarine Gas Hydrate Estimation: Theoretical and Empirical Approaches," Proc. 27th Annual Offshore Technology Conference, OTC 7693, p 513 (1995)

Godbole, S.P., Ehlig-Economides, C., "Natural Gas Hydrates in Alaska: Quantification and Economic Evaluation," Proc. SPE 1985 California Regional Meeting, SPE 13593, Bakersfield, CA, March 27-29, 1985.

Golomb, D., "Transport Systems for Ocean Disposal of CO_2 and Their Environmental Effects," Energy Convers. Mgmt., **38S**, S279 (1997)

Golomb, D.S., Zemba, S.G., Dacey, J.W.H., Michaels, A.F., "The Fate of CO2 Sequestered in the Deep Ocean," Energy Convers. Mgmt, **33(5-8)**, 675 (1992)

Gornitz, V., and Fung, I., "Potential Distribution of Methane Hydrates in the World's Oceans," Global Biogeochemical Cycles, **8(3),** 335 (1994)

Gunter, W.D., Gentzis, T., Rottenfusser, B.A., Richardson, R.J.H., "Deep Coalbed Methane in Alberta, Canada: A Fuel Resource with the Potential of Zero Greenhouse Gas Emissions," Energy Convers. Mgmt., **38S**, S217 (1997)

Harrison, W.J., Wendlandt, R.F., Sloan, E.D., "Geochemical Ineteractions Resulting from Carbon Dioxide Disposal on the Seafloor," Applied Geochemistry, **10**, 461 (1995)

Harvey, L.D., Huang, Z., "Evaluation of the Potential Impact of Methane Clathrate Destabilization on the Future Global Warming," J. Geophysical Research, **100 (D2)**, 2905 (1995)

Haq, B.U., "Methane in the Deep Blue Sea," Science, **283**, 543 , 23 July 1999.

Hatzirkiriakos, S.G., Englezos, P., "The Relationship Between Global Warming and Methane Gas Hydrates in the Earth," Chem. Eng. Sci., **48**, 3963 (1993)

Henriet, J.-P., and Mienert, Eds., Gas Hydrates: Relevance to World Margin Stability and Climatic Change, Geological Society Special Publication No. 137, page 303, London, (1998)

Herzog, H.J., "The Economics of CO_2 Capture," in Greenhouse Gas Control Technologies, (Proc. Of 4th Intrntl. Conf. On Greehouse Gas Control Technologies

8/30 – 9/2/98 Interlaken, Switzerland) Eliasson, B., Riemer, P., Wokaun, A., eds., Pergamon, pg 101 (1999a)

Herzog, H.J., "Ocean Sequestration of CO_2 – An Overview," in Greenhouse Gas Control Technologies, (Proc. Of 4th Intrntl. Conf. On Greehouse Gas Control Technologies 8/30 – 9/2/98 Interlaken, Switzerland) Eliasson, B., Riemer, P., Wokaun, A., eds., Pergamon, pg 237 (1999b)

Herzog, H., Drake, E., Adams, E., CO_2 Capture, Reuse, and Storage Technologies for Mitigating Global Climate Change; A White Paper Final Report, MIT Energy Laboratory, DOE Order No. DE-AF22-96PC01257 (1997)

Hinkel, R.M., Thibodeau, S.L., "Experience with Drillship Operations in the US Beaufort Sea," Proc. 20th Annual Offshore Tech Conf. , Houston, TX May 2-5, (1988)

Hinrichs, K.-U., Hayes, J.M., Sylva, S.P., Brewer, P.G., DeLong, E.F., "Methane-Consuming Archaea – Molecular Isotopic and Phylogenetic Evidence," Nature, (in press 1999).

Hirai, S., Okazaki, K., Araki, N., Yazawa, Y., Ito, H., Hijikata, K., "Transport Phenomena of Liquid CO2 in Pressurize Water Flow with Clathrate Hydrate at the Interface," Energy Convers. Mgmt., **36(6-8)**, 471 (1996)

Hirai, S., Okazaki, K., Tabe, Y., Hijikata, K., "Numerical Simulation for Dissolution of Liquid CO_2 Droplets Covered with Clathrate Film in Intermediate Depth of Ocean," Energy Convers. Mgmt., **38S**, S313, (1997)

Hirai, S., Tabe, S., Kuwano, K., Ogawa, K., Okazaki, K., "MRI Measurement of Hydrate Growth and Application to Advanced CO_2 Sequestration Technology," presented at 3rd International Hydrate Conference, Salt Lake City, Utah, July 18-22, 1999a

Hirai, S., Tabe, Y., Tanaka, G., Okazaki, K., "Advanced CO_2 Ocean Dissolution Technology for Longer Term Sequestration with Minimum Biological Impacts," in Greenhouse Gas Control Technologies, (Proc. Of 4th Intrntl. Conf. On Greehouse Gas Control Technologies 8/30 – 9/2/98 Interlaken, Switzerland) Eliasson, B., Riemer, P., Wokaun, A., eds., Pergamon, pg 317, (1999b)

Hirohama, S., Shimoyama, Y., Wakabayashi, A., Tatsuta, S., Nishida, N., "Conversion of CH_4-Hydrate to CO_2-Hydrate in Liquid CO_2," J. Chem. Eng. Japan, **29(6)**, 1014, (1996)

Hirohama, S., Shimoyama, Y., Wakabayashi, A., Tatsuta, S., Nishida, N., "Research on CO_2 Disposal/Displacement of Methane by CO_2 in Clathrate Hydrate," Chiyoda Chemical Company Annual Report, p 111, (1997-8)

Holbrook, W.S., Hoskins, H., Wood, W.T., Stephen, R.A., Lizarralde, D., and Leg 164 Science Party, "Methane Hydrate and Free Gas on the Blake Ridge from Vertical Seismic Profiling," Science, **273,** 1840 (1996)

Holder, G.D., Angert, P.F., Godbole, S.P., "Simulation of Gas Producton from a Reservoir Containing both Gas hydrates and Free natural Gas," SPE11105, Proceeding of Annual SPE Technical Conference, New Orleans, LA, Sept. 1982

Holder, G.D., Kamath, V., Godbole, S., "The Potential of Natural Gas Hydrates as an Energy Resource," Annu. Rev. Energy, **9**, 427 (1984)

Holder, G.D., Cugini, A.V., Warzinski, R.P., "Modeling Clathrate Hydrate Formation During Carbon Dioxide Injection into the Ocean, " Environ. Sci. Technol., 29, 276 (1995)

Holder, G.D., Warzinski, R.P., "Formation and Growth of CO2 Clathrate Hydrate Shells Around Gas Bubbles or Liquid Drops," Preprnt.Pap. – Amer. Chem. Soc., Div, Fuel Chem., **41(4)** 1452 (1996)

Hoffert, M.I., Wey,Y.-C., Callegari, A.J., Broecker, W.S., "Atmospheric Response to Deep-Sea Injections of Fossil-Fuel Carbon Dioxide," Climatic Change, **2** 53 (1979)

Houghton, J.T., Meira Fiolho, L.G., Callender. B.A. Harris, N., Kattenberg, A., Maskell, K. (Eds) Climate Change 1995. The Science of Climate Change, Cambridge University Press, 1996.

Hovland, M., "Are There Commercial Deposits of Methane Hydrates in Ocean Sediments?" in Proceedings of the International Symposium of Japan National Oil Company, "Methane Hydrates,; Resources in the near Future? Chiba City, Japan, October 20-22, 1998. Page 17. Panel Discussion Proceedings.

Hovland, M., Clennell, B., Gallagher, J.W., Lekvam, K., "Gas Hydrate and Free Gas Volumes in Marine Sediment: Example from the Niger Delta Front," Marine and Petroleum Geology, **14**, 245 (1997)

Iseux, J.C., "Gas Hydrate: Occurrence, Productionm, and Economics," Proc. SPE Prod Oper. Symp, page 467, Oklahoma City, Oklahoma, SPE 21682, April 7-9, 1990

Islam, M.R., "A New Recovery Technique for Gas Production from Alaskan Gas Hydrates," J. Petrol Sci & Eng., **11**. 267 (1994)

Jamaluddin, A.kl.,M., Kalogerakis, N., and Bishnoi, P.R., "Modeling Decomposition of Synthestic Core of Methane Gas Hydrate by Coupling Intrinsic Kinetics with Heat Transfer Rates," Can. J. Chem. Eng., **67**, 948 (1989)

Japan National Oil Corporation, Proc. of Intnl. Symp. on Methane Hydrates: Resources in the Near Future?, Chiba, City, Japan, October 20-22, 1998

Kaiho, K., Arinobu, T., Ishiwatari, R., Morgans, Hl., Okada, H., Takeda, N., Tazaki, N., Zhou, G., Kajiwara, Y., Matsumoto, R., Hirai, A., Niitsuma, N., Wada, H., "Latest Palaeocene Benthic Foramiferal Extinction and Environmental changes at Tawanui, New Zealand," Paleoceanography, **11**, 447 (1996)

Kamath, V.A., "A Perspective on Gas Production from Hydrates," in Proceedings of the International Symposium of Japan National Oil Company, "Methane Hydrates,; Resources in the near Future?" Chiba City, Japan, October 20-22, 1998. Page 173

Kamath, V.A., Godbole, S.P., "Evaluation of Hot Brine Stimulation Technique for Gas Production from Natural Gas Hydrates," Proc. 1985 SPE California Regional Meeting, Bakersfield, CA, SPE 13496, March 27-29, 1985.

Kamath, V.A., Mutalik, P.N., Sira, J.H., Patil, S.L., "Experimental Study of Brine Injection and Depressurization Methods for Dissociation of Gas Hydrates," SPE 19810, Proc. of 64th Annual Technical Converence of SPE, San Antonio, TX, October 1989.

Khairkhah, D., Pooladi-Darvish, M., Bishnoi, P.R., Collett, T.S., Dallimore, S.R., "Produciton Potential and Viability of Gas Production, Mallik Field Reservoir," Scientific Results from JAPEX/JNOC/GSC Mallik 2L-38 gas Hydrate Research Well, MacKenzie Delta, Northwest Territories, Canada, Dallimore, S.R., Uchida, T., and T.S. Collett, Eds., Geological Survey of Canada Bulletin 544, p. 377, 601 Booth St., Ottawa, Ontario, K1A 0E8 (1999)

Kim, H.C., Bishnoi, P.R., Heidemann, R.A., and Rizvi, S.S.H., "Kinetics of Methane Hydrate Decomposition," Chem. Eng. Sci., **42(7)**, 1645 (1987)

Komai, T., Yamamoto, Y., Ohga, K., "Dynamic Process of Reformation and Replacement of CO_2 and CH_4 Gas Hydrates," Proc. 3rd International Conference on Natural Gas Hydrates, Salt Lake City, New York Academy of Sciences, July 19-23, 1999.

Krason, J., Ciesnik, M., "Geological Evolution and Analysis of Confirmed or Suspected Gas Hydrate Localities Volume 5; Russian Literature," DOE/MC/21181-1950.V5 (DE86006635), 164 pages, October (1985)

Kvenvolden, K.A., "Methane Hydrates – a Major Reservoir of Carbon in the Shallow Geosphere?" Chemical Geology, **71**, p 41 (1988a)

Kvenvolden, K.A., "Methane Hydrates and Global Climate," Global Biogeochemical Cycles, 2(3), 221 (1988b)

Kvenvolden, K.A., "Gas Hydrates and Geological Perspectives and Global Change," Reviews of Geophysics, **31**, 173 (1993a)

Kvenvolden, KA., "Estimates of the Methane Content of Worldwise Gas-Hydrate Deposits" in Proceedings of the International Symposium of Japan National Oil Company, "Methane Hydrates,; Resources in the near Future? Chiba City, Japan, October 20-22, 1998. Page 1. Panel Discussion Proceedings.

Kvenvolden, K.A., Collett, T., Lorenson, T., "Studies of Permafrost and Gas Hydrates as Possible Sources of Atmospheric Methane at High Latitudes," in Biogeochemistry of Global Change, Orenland, R., ed., Chapman & Hall, New York, (1993b)

Kvenvolden, K. A., McMenamin, M., "Hydrates of Natural Gas: A Review of Their Geologic Occurrence," U.S. Geological Survey Circular 825 (1980)

Lachenbruch, A.H., and Marshall, B.V., "Changing Climate: Geothermal Evidence from Permafrost in the Alaskan Arctic," Science, **234**, 689 (1986)

Larsen, R., Wessel-Berg, D., Borthne, G., Nakamura, A., "Simple Modelling of Hydrate Dissociation in Reservoirs Caused by Pressure Drawdown," in Proceedings of the International Symposium of Japan National Oil Company, "Methane Hydrates,; Resources in the near Future? Chiba City, Japan, October 20-22, 1998. Page 175.

Leggett, J., "The Nature of the Greenhouse Threat," in Global Warming: The Greenhouse Report, Oxford Univ. Press, p. 30,40, and 41, 1990.

Liro, C.R., Adams, E.E., Herzog, H.J., "Modeling the Release of $C0_2$ in the Deep Ocean," Energy Convers. Mgmt, **33(5-8)**, 667 (1992)

MacDonald, G. J., "Role of Methane Clathrate in Past and Future Climates," Climactic Change, 16 247 (1990a)

MacDonald, G. J., "The Future of Methane as an Energy Resource," Annual Review of Energy, 15, 53 (1990b)

MacDonald, I.R., Guinasso, N., Sassen, R., et al., "Gas Hydrate that Breaches the Sea Floor on the Continental Slope of the Gulf of Mexico,"Geology, **22**, 699 (1994)

Makogon, Yu. F., Hydrates of Natural Gas, Moscow, Nedra, Izadatelstro, p.208 (1974 in Russian) Translated by W.J. Cieslewicz, PennWell Books, Tulsa, OK, p237 (1981 in English).

Makogon, Yu. F., Personal Communication, January 3, 1988a.

Makogon, Yu. F., "Natural Gas Hydrates: The State of Study in the USSR and Perspectives on its Use," Paper Presented at the Third Chemical Congress of North America, Toronto, Canada, June 5-10, 1988b, with no published abstract.

Makogon, Yu.F., "Hydrates of Hydrocarbons," PenWell Books, 482pp, (1997)

Makogon, Y.F., Makogon, T. Y., Holditch, S.A., "Several Aspects of the Kinetics and Morphology of Gas Hydrates," in Proceedings of the International Symposium of Japan National Oil Company, "Methane Hydrates,; Resources in the near Future? Chiba City, Japan, pg. 259, October 20-22, 1998

Masters, C.D., Toor, D.H., Attanasi, E.D., "Resource Constraints in Petroleum Production Potential," Science, **352**, 146 (1991)

Masters, C.D., Attanasi, E.D., Root, D.H., "World Petroleum Assessment and Analysis," Proc. of 4th World Petroleum Congress, Chichester, England, John Wiley & Sons, Vol 5, p529 (1994)

Masuda, Y., Fujita, K., Fuhinaga, Y., Naganawa, S., Kodaira, H., Hayashi, Y., Sato, K., Ichikawa, M., "Development of a Numerical Model for Predicting Hydrate-Decomposition Behavior in Reservoirs," in Proceedings of the International Symposium of Japan National Oil Company, "Methane Hydrates,; Resources in the near Future? Chiba City, Japan, October 20-22, 1998. Page 185.

McGuire, P.L., "Methane Hydrate Gas Production: An Assessment of Conventional Production Technology as Applied to Hydrate Gas Recovery," Los Alamos National Laboratory Report LA-91-MS, Los Alamos, NM, 1981.

McIver, R.D., "Gas Hydrates," in Meyer, R.F. and Olson J.C., eds. Long-Term Energy Resources, Pitman, Boston, p713 (1981)

Meredith, Roger, Engineers' Handbook of Industrial Microwave Heating, The Institution of Electrical Engineers, London, (1998)

Meyer, R.F., "Speculations in Oil and Gas Resources in Small Fields and Unconventional Deposits," in Meyer, R.F. and Olson J.C., eds. Long-Term Energy Resources, Pitman, Boston, p. 49 (1981)

Milgram, H., Erb, P.R., "How Floaters Respond to Subsea Blowouts," Petroleum Engineer International, 64, June (1984)

Monfort, J.P., ed, Proc. 2nd Intnl. Conf. on Natural Gas Hydrates, F. Foucaud, Secretariat, 18 Chemin de la Loge, 31078 Toulouse Cedex, France 2-6 June, 1996

Mori, Y.H., "Clathrate Hydrate Formation at the Interface Between Liquid CO_2 and Water Phases – A Review of Rival Models Characterizing Hydrate Films," Energy Convers. Mgmt, **39(15)**, 1537 (1998)

Mori, Y.H., Personal Communication, 28 July 1999.

Moridis, G., Apps, J., Pruess, K., and L. Myer, "EOSHYDR: A TOUGH2 Module for CH_4-Hydrate Release and Flow in the Subsurface," in Proceedings of the International Symposium of Japan National Oil Company, "Methane Hydrates,; Resources in the near Future? Chiba City, Japan, October 20-22, 1998. Page 183.

Nakano, S., Moritoki, M., Ohgaki, K., "High-Pressure Phase Equilibrium and Raman Microprobe Spectroscopic Studies on the CO_2 Hydrate System," J. Chem Eng. Data, **43(5)**, 807 (1998)

Nakano, S., Moritoki, M., Ohgaki, K., "High-Pressure Phase Equilibrium and Raman Microprobe Spectroscopic Studies on the Methane Hydrate System," J. Chem Eng. Data, **44(2)**, 254 (1999)

Nakashiki, N., Ohsumi, T., Katano, N., "Technical View on CO_2 Transportation onto the Deep Ocean Floor and Dispersion at Intermediate Depths," in Direct Ocean Disposal of Carbon Dioxide, N. Handa, and T. Ohsumi, eds., 183, Terrapub, Tokyo (1995)

National Academic of Science (U.S.), Changing Climate, Report of the Carbon Dioxide Assessment Committee, National Academy Press, Washington, D.C., 1983.

National Academic of Science (U.S.), Global Change in the Geosphere-biosphere: Initial Priorities for an IGBP, National Academy Press, Washington, D.C., 1984.

Neurater, T.W., Mud Mounds on the Continental Slope Northwestern Gulf of Mexico and Their Relation to Hydrates and Seafloor Instability, Ph.D. Dissertation, Texas A&M University, May (1988)

Nisbet, E.G., "Some Northern Sources of Atmospheric Methane: Production, History, and Future Implications," Canadian J. of Earth Sciences, **26**, 1603 (1989)

Nishikawa, H., Ishibashi, M., Ohta, H., Akutsu, N., Tajika, M., Sugitani, T., Hiraoka, R., Kimuro, H., Shiota, T., "Stability of Liquid CO_2 Spheres Covered with Clathrate Film When Exposed to Environment Simulating the Deep Sea," Energy Convers. Mgmt., **36(6-9)**, 489 (1995)

Ohgaki, K., et al., Proc. Chem. Eng. Soc. of Japan, Spring 1995, pg A212 (in Japanese)

Ohgaki, K., Nakano, S., Matsubara, T., Yamanaka, S., "Decomposition of CO_2, CH_4, and CO_2-CH_4 Mixed Gas Hydrates, J. Chem. Eng. Japan, **30**, 310 (1997)

Ohgaki, K., Sugahara, T., Nakano, S., "Hysteresis in Dissociation and Reformation on Methane Hydrate Crystal," J. Chem. Eng. Japan, **32(2)**, 235 (1999)

Ohgaki, K., Takano, T., Moritoki, M., "Exploitation of CH_4 Hydrates Under the Nankai Trough in Combination with CO_2 Storage," Kagaku Kogaku Ronbunshu, **20**, 121 (1994)

Ohgaki, K., Takano, K., Sangawa, H., Matsubara, T., Nakano, S. "Methane Exploitation by Carbon Dioxide from Gas Hydrates – Phase Equilibria for CO2-CH4 Mixed hydrate System, J. Chem. Eng. Japan, 29, 478 (1996)

Ohmura, R., Kashiwazaki, S., Fukumoto, K., Mori, Y.H., "Measurement of Clathrate Hydrate Film Thickness by Means of Laser Interferometry," Proc. 36th National Heat Transfer Symposium of Japan, (in Japanese) May 1999a

Ohmura, R., Mori, Y.H., "Critical Conditions for CO_2 Hydrate Films to Rest on Submarine CO_2 Pond Surfaces: A Mechanistic Study," Environmental Science & Technology, **32(8)**, 1120, (1998)

Ohmura, R., Shigetomi, T., Mori, Y.H., "Formation, Growth and dissociation of Clathrate Hydrate Crystals in Liquid Water in Contact with a Hydrophobic Hydrate-Forming Liquid," J. Crystal Growth, **196**, 64 (1999b)

Ohsumi, T., "Predictions of Solution Carbon Dioxide Behavior around a Liquid Carbon Dioxide Pool on Deep Ocean Basins," Energy Convers. Mgmnt., **34 (9-11)** 1059, (1993)

Omenihu, S.D., Feasibility Study of Gas Production from Gas Hydrate Resources of Alaska North Slope, M.S. Thesis, University of Alaska, Fairbanks, May (1995)

Ormerod, W., The Disposal of Carbon Dioxide from Fossil Fuel Fired Power Stations, IEAGHG/SR3, IEA Greenhouse Gas R&D Programme, Cheltenham, UK (1994)

Ormerod, W., Transport & Environmental Aspects of Carbon Dioxide Sequestration, IEAGHG/SR5, IEA Greenhouse Gas R&D Programme, Cheltenham, UK (1995)

Ormerod, B., Ocean Storage of Carbon Dioxide, Workshop 1 – Ocean Circulation, IEA Greenhouse Gas R&D Programme, Cheltenham, UK, (http://www.ieagreen.org.uk/) 1996a.

Ormerod, B., Ocean Storage of Carbon Dioxide, Workshop 3 –International Links and Concerns, IEA Greenhouse Gas R&D Programme, Cheltenham, UK, (http://www.ieagreen.org.uk/) 1996b.

Ormerod, B., Ocean Storage of Carbon Dioxide, Workshop 4 –Practical and Experimental Approaches, IEA Greenhouse Gas R&D Programme, Cheltenham, UK, (http://www.ieagreen.org.uk/) 1997.

Ormerod, B., Angel, M., Ocean Storage of Carbon Dioxide, Workshop 2 – Environmental Impact, IEA Greenhouse Gas R&D Programme, Cheltenham, UK, (http://www.ieagreen.org.uk/) 1996.

Ormerod, B., Angel, M., Ocean Fertilization as a CO_2 Sequestration Option, IEA Greenhouse Gas R&D Programme, Cheltenham, UK, (http://www.ieagreen.org.uk/) 1998.

Ozaki, M., Sonoda, K., Fujioka, Y., Tsukamoto, O., and Komatsu, M. "Co2 Discharge from Vertical Pipes on a Moving Ship," Energy Convers. Mgmt, **36** 475(1995)

Paull, C.K., Matsumoto, R., Wallace, P., and Shipboard Scientific Party, "Gas Hydrates Sampling on the Blake Ridge and Carolina Rise," Proceedings of the Ocean Drilling Program, Volume 164, Ocean Drilling Program, College Station Texas (1996)

Paull, C.K., Ussler, W., Dillon, W.P., "Is the Extent of Glaciation Limited by Marine Gas Hydrates?" Geophys. Rsch. Lttrs., **18(3)**,432, (1991)

Peters, D.J., Hydrate Dissociation in Pipelines by Two-Sided Depressurization: Experiment and Model, M.S. Thesis, Colorado School of Mines, Golden, (1999)

Petroleum Consultants, Inc., CO_2 Database Personal Communication to E. D. Sloan, December 1, 1999 by IHS Inc.

Poettmann, F.H., Personal Communication, July 20, 1988.

Puri, R., Yee, D., "Enhanced Coalbed Methane Recovery," Proc. 65th Annl SPE Tech Conf., New Orleans, LA, SPE 20732, page 193, September 23-26, (1990)

Reznik, A.A., Singh, P.K., Foley, W.L., "An Analysis of the Effect of CO_2 Injection on the Recovery of In-Situ Methane from Bituminous Coal: An Experimental Simulation, Soc. Petrol. Eng. J., p 521, October 1984.

Riemer, P.W.F., "Greenhouse Gas Mitigation Technologies. An Overview of the CO_2 Capture, Storage, and Future Activities of the IEA Greenhouse Gas R&D Programme," IEA Greenhouse Gas Report, (1995) available at http://www.ieagreen.org.uk

Riemer, P.W.F., The Abatement of Methane Emissions, (Volumes 1 and 2) IEAGHG/SR7, Restricted Circulation, IEA Greenhouse Gas R&D Programme, Cheltenham, UK, February 1999.

Rodger, P.M., "Issues Underlying the Feasibility of Storing CO_2 as Hydrate Deposits," IEA GHG Report PH3/25, February 2000.

Rogner, H.-H., " An Assessment of World Hydrocarbon Resources," Annu. Rev. Energy Environ., 22, 217 (1997)

Romanovskii, N.N., Tipenko, G.S., "Regularities of Permafrost Interactions with Gas and Gas Hydrate Deposits," Proc. 7th Intnl Conf on Permafrost, Yellowknife, Canada, June 1998

Saji, A., Noda, H., Takamura, Y., Tanii, T., Takata, T, Kitamura, H., Kamata, T., "Dissolution and Sedimentation Behavior of Carbon Dioxide Clathrate," Energy Convers. Mgmt, **36(6-9)**, 493 (1995)

Sasaki, K., Akibayashi, S., "A Calculation Model for Liquid CO_2 Injection into Shallow Sub-Seabed Aquifer," Proc. 3rd International Conference on Natural Gas Hydrates, Salt Lake City, New York Academy of Sciences, July 19-23, 1999.

Selim, M.S., Sloan, E.D., "Heat and Mass Transfer During Dissociation of Hydrates in Porous Media," AIChE J., **35(6)**, 1049 (1989)

Selim, M.S., Sloan, E.D., "Hydrate Dissociation in Sediment, Reservoir Engineering - Society of Petroleum Engineers, 245, May 1990.

Sheshukov, N.L., "Occurrence of Gas In the Hydrate State in Messoyahka Field," Gazovoe Delo., **6**:8 (1972) (in Russian)

Shindo, Y., Fujioka, Y., Yamagisawa, Y., Hakuta, T., Komiyama, H., "Formation and Stability of CO_2 Hydrate," in Direct Ocean Disposal of Carbon Dioxide, N. Handa, and T. Ohsumi, eds., 217, Terrapub, Tokyo (1995)

Sira, J.H., Patil, S.L., and V.A. Kamath, "Study of Hydrate Dissociation by Methanol and Glycol Injection," Proc. SPE Annual Tech. Conf. And Exhib., New Orleans, LA, Sept 1990.

Sloan, E.D., Jr., Clathrate Hydrates of Natural Gases, Marcel Dekker, Inc., New York, 705 pp and software, (1998)

Sloan, E.D., Happel, J., Hnatow, M.A., Eds., International Conference on Natural Gas Hydrates, Annals of the New York Academy of Sciences, vol. 715, (1994)

Sloan, E.D., Brewer, P.G., T.S. Collett, W.P. Dillon, W.S. Holbrook, K.A. Kvenvolden, C.K. Paull, "Future of Gas Hydrate Research," EOS, **80(22)**, American Geophysical Union, p 247, June 1, 1999

Smith, J.M., Van Ness, H.C., Introduction to Chemical Engineering Thermodynamics, (4th Ed.) McGraw-Hill Book Co., New York (1987)

Sresty, G.C., Dev, H., Snow, R.H., Bridges, J.E., "Recovery of Bitumen from Tar Sand Deposits with the Radio Frequency Process," SPE Reservoir Engineering, 85, January 1986.

Stevens, S.H., Kuuskraa, V.A., Schraufnagel, R.A., "Technology Spurs Growth of U.S. Coalbed Methane," Oil and Gas Journal, January 1, 1999c

Stevens, S.H., Kuuskraa, V.A., Spector, D., Riemer, P., "CO_2 Sequestration in Deep Coal Seams: Pilot Results and Worldwide Potential," in Greenhouse Gas Control Technologies, (Proc. Of 4th Intrntl. Conf. On Greehouse Gas Control Technologies 8/30 – 9/2/98 Interlaken, Switzerland) Eliasson, B., Riemer, P., Wokaun, A., eds., Pergamon, pg 175, (1999a)

Stevens, S.H., L. Schoeling, Pekot, L., "CO_2 Injection for Enhanced Coalbed Methane Recovery: Project Screening and Design," Proc. Intnl. Coalbed Methane Symp., Tuscaloosa, Alabama, May 3-7, (1999b)

Stevenson, M.D., Pinczewski, W.V., Downey, R.A., "Economic Evaluation of Nitrogen Injection for Coalseam Gas Recovery," SPE 26199, p. 627, SPE Gas Tech. Symp., Calgary, Canada, 28-30 June 1993.

Sumetz, V.I., "Prevention of Hydrate Formation in Well Bottom Zone," Gaz. Prom, **2**, 24 (in Russian) (1974)

Tabe, Y. Hirai, S., Okazaki, K., "Measurement of Clathrate Hydrate Film Thickness at the Interface Between Liquid CO_2 and Water," in Greenhouse Gas Control Technologies, (Proc. Of 4th Intrntl. Conf. On Greehouse Gas Control Technologies 8/30 – 9/2/98 Interlaken, Switzerland) Eliasson, B., Riemer, P., Wokaun, A., eds., Pergamon, pg. 311 (1999)

Taber, J.J., Martin, F.D., Seright, R.S., "EOR Screening Criteria Revisited – Part 1: Introduction to Screening Criteria and Enhanced Recovery Field Projects, SPE Reservoir Engineering, page 189, August (1997)

Tamburri, M.N., Peltzer, E.M., Friederich, G.E., Aya, I., Yamane, K., Brewer, P.G., "A Field Study of the Effects of CO2 Ocean Disposal on Mobile Deep –Sea Animals," Submitted to Marine Chemistry, (1999)

Teng, H., Masutani, S.M., Kinoshita, C.M., "Dispoersion of CO_2 Droplets in the Deep Ocean," Energy Convers. Mgmt., **38S**, S319 (1997a)

Teng, H., Yamasaki, A., Shindo, Y., "Influence of Disposal Depth on the Size of CO_2 Droplets Produced from a Circular Orifice," Energy Convers. Mgmt., **38S**, S325 (1997b)

Thomas,E., Shackleton, N.J., "The Paleocene-Eocene Benthic Foraminiferal Extinction and Stable isotope anomalies," in R.O. Knox et al., eds., Correlations of the Early Paleogene in Northwest Europe, Geological Society Special Publications, 101,London, UK, p. 401 (1996)

Trofimuk, A.A., Cherskiy, N.V., and Tsarev, V/.P., "The Role of Continental Glaciation and Hydrate Formation on Petroleum Occurrences," in Meyer, R.F., ed. Future Supply of Nature-made Petroleum and Gas, Pergamon Press, p 919, New York (1977).

Uchida, T., Personal Communication on CO_2 Hydrate Film Thickness, 11 August 1999.

Uchida, T., Matsumoto, R., Waseda, A., Okui, T., Yamada, K., Uchida, T., Okada, S., Takano, O., "Summary of Physicocemical Proeprties of Natural Gas Hydrate and Associated Gas-Hydrate-Bearing Sediments, JAPEX/JNOC/GSC Mallike 2L-38 Gas Hydrate Research Well, by the Japanese Research Consortium," Scientific Results from JAPEX/JNOC/GSC Mallik 2L-38 gas Hydrate Research Well, MacKenzie Delta, Northwest Territories, Canada, Dallimore, S.R., Uchida, T., and T.S. Collett, Eds., Geological Survey of Canada Bulletin 544, p 205, 601 Booth St., Ottawa, Ontario, K1A 0E8 (1999)

Uchida, T., Ebinuma, T., Kawabata, J., and Narita, H., "Microscopic Observations of Formation Processes of Clathrate-Hydrate Films at an Interface Between Water and Carbon Dioxide," J. Crystal Growth, 204(3), 348 (1999)

Ullerich, J.W., Selim, M.S., Sloan, E.D., "Theory and Measurement of Hydrate Dissociation," AIChE J, **33(5)**, 747 (1987)

U.S. Department of Energy, A Strategy for Methane Hydrate Research &Development, Office of Fossil Energy, Federal Energy Technology Center, August 1998, DOE/FE-0378, 54 pages

U.S. Department of Energy, National Methane Hydrate Multi-year R&D Program Plan, Office of Fossil Energy, Federal Energy Technology Center, June 1999a. 33 pages

U.S. Department of Energy, Working Paper on Carbon Sequestration Science and Technology, Office of Science and Office of Fossil Energy, http://www/fe/doe/gov/sequestration February 1999b,149 pages

Warzinski, R.P., Bergman, P.D., Masutani, S.P., Holder, G.D., "The Effect of CO2 Clathrate Hydrates on the Ocean Disposal of CO_2: A Review of DOE-Sponsored Research," Preprnt.Pap. – Amer. Chem. Soc., Div, Fuel Chem., **42(2)** 578 (1997)

Warzinski, R.P., Lynn, R.J., Holder, G.D., "The Impact of CO2 Clathrate Hydrate on Deep Ocean Sequestration of CO2: Experimental Observations and Modeling Results," Proc. 3rd International Conference on Natural Gas Hydrates, Salt Lake City, New York Academy of Sciences, July 19-23, 1999.

Wong, C.S., Hirai, S., Ocean Storage of Crbon Dioxide: A Review of Oceanic Carbonate and CO_2 Hydrate Chemistry, IEA Greenhouse Gas R&D Programme, Sept. 1997

Wong, S., Foy, C., Gunter, B., Jack, T., "Injection of CO_2 for Enhanced Energy Recovery: Coalbed Methane Versus Oil Recovery," in Greenhouse Gas Control Technologies, (Proc. Of 4th Intrntl. Conf. On Greehouse Gas Control Technologies 8/30 – 9/2/98 Interlaken, Switzerland) Eliasson, B., Riemer, P., Wokaun, A., eds., Pergamon, pg 189, (1999)

Yakushev, V., "Some Environmental Problems of Gas Recovery Related to Permafrost and Natural Gas Hydrates," in Proc. of 19th World Gas Conference, Intnl. Gas Union, Milan, (1994)

Yamasaki, A., Teng, H., Wakatsuki, M., Yanagisawa, Y., Yamada, K., "CO_2 Hydrate Formation in Various Hydrodynamic Conditions," Proc. 3rd International Conference on Natural Gas Hydrates, Salt Lake City, New York Academy of Sciences, July 19-23, 1999.

Yousif, M.H., Abass, H.H., Selim, M.S., and E.D. Sloan, "Experimental and Theoretical Investigation of Methane Gas Hydrate Dissociaiton in Porous Media," SPE Reservoir Engineering, 69 (February 1991)

Yousif, M.H., Li, P.M., Selim, M.S., and E.D. Sloan, "Depressurization of natural Gas Hydrates in Berea Sandstone Cores," J. Inclus. Phenomen., D.W. Davidson Memorial Volume, **8**, pg 71,(1990)